Chapter 4

FORMULATION, OPTIMIZATION AND CHARACTERIZATION OF NANOPARTICULATE FORMULATIONS

4.1 Introduction

Breast cancer is the leading cause of death among women, with one million new cases in the world each year [McPherson et al. 2000], out of which one-third are reported to be hormone-dependent [Henderson and Canellos 1980; Theobald 2000]. Growth of breast cancer cells is often estrogen-dependent. Continuous estrogen suppression in patients with hormone sensitive breast cancer prevents proliferation of tumor. Aromatase is the key enzyme that converts androgens to estrogens both in pre- and post-menopausal women [Lonning 1998; Strassmer-Weippl and Goss 2003]. Treatment of breast cancer has included efforts to decrease estrogen levels by the use of antiestrogen and progestational agents [Chowdhury and Ellis 2005]. Anastrozole (ATZ) is a nonsteroidal aromatase inhibitor. The problems associated with oral delivery of ATZ are low aqueous solubility, short half-life and uncontrolled release [Sarkar and Yang 2008]. Exemestane (EXE) is a third generation, potent irreversible Type I steroidal aromatase inhibitor approved by the Food and Drug Administration (FDA) for the treatment of breast cancer [Johannessen et al. 1997]. It acts as a false substrate for the aromatase enzyme, and is processed to an intermediate that binds irreversibly to the active site of the enzyme causing its inactivation, an effect also known as suicide inhibition [Dowsett 1998]. Although treatment with orally administered EXE has been shown to be well tolerated by patients, the most common adverse events consist of hot flashes, nausea, fatigue, dizziness, increased sweating, headache, body weight change, vaginal dryness, arthralgias, and myalgias [Clemett and Lamb 2000; Scott and Wiseman 1999]. The problem with the oral delivery of EXE is its inability to target the tumor site. This problem can be overcome by employing delivery systems capable of providing targeted drug delivery.

One of the technological resources to improve the availability of drugs at the site of action is by colloidal carriers like nanoparticles (NPs) prepared using biodegradable polymers like poly(d,l-lactic-co-glycolic acid) (PLGA) and poly caprolactone (PCL) [De Jong and Borm 2008]. PLGA has been studied extensively as a polymeric carrier for NPs. PLGA nanoparticles (NPs) are already reported to provide passive targeting of anticancer drugs to tumor site [Fonseca et al. 2002; Yallapu et al. 2010]. A wide variety of drugs ranging from small molecular-weight therapeutic agents to peptide hormones, antibiotics, and chemotherapeutic drugs have been formulated using PLGA [Tuncay et

al. 2000]. PLGA NPs have proven to be successful targeted drug delivery systems for different classes of drugs, such as anticancer drugs like etoposide [Snehalatha et al. 2008] and rapamycin [Acharya et al. 2009], proteins and peptides like insulin [Shi et al. 2009] and steroidal hormones like estrogen [Kwon et al. 2001]. PCL is biodegradable polyester and is prepared by ring opening polymerization of ε-caprolactone. PCL is degraded by hydrolysis of its ester linkages in physiological conditions and has therefore received a great deal of attention for use as a biomaterial for sustained release drug delivery systems [Aberturas et al. 2011; Lam et al. 2008]. Different methods reported for preparing NPs using biodegradable polymers include monomer polymerization, interfacial deposition, salting out, nanoprecipitation, emulsification solvent evaporation, etc. [Quintanar-Guerrero et al. 1998]. Interfacial deposition of preformed polymer technique is based upon interfacial deposition of a polymer followed by diffusion of a semi polar and miscible solvent in aqueous medium containing surfactant [Barichello et al. 1999; Fessi et al. 1989]. Moraes et al. used this method for preparation of PLGA nanocapsules with particle size of 123 nm and 69% drug loading [Moraes et al. 2009]. Formulation of NPs by this method involves many important factors which contribute to the outcome of experiment in terms of drug entrapment and particle size. Different process variables include stirring speed, temperature, rate of addition of organic phase to aqueous phase, etc. Different formulation variables include drug:polymer ratio, concentration of polymer in organic phase, surfactants, surfactant concentration, volume of aqueous and organic phase, organic solvents, etc.

Optimization of any pharmaceutical process begins with the objectives to find out and evaluate independent variables that affect formulation response, determine them and establish their best response values. However, considering the cost of the drugs and polymers, it is desirable to optimize the formulation development with minimum batches with maximum desired characteristics. While developing formulations, various formulations as well as process variables related to effectiveness, safety and usefulness should be simultaneously optimized. Polynomial non-linear regression analysis are widely used for establishing approximate mathematical models in which the variables are screened by stepwise selection method according to statistical significance [Miller 1984; Wagner and Shimshak 2007] and final model would be used to predict the

relationship between different variables and their levels. But such predictions are often limited to low levels, resulting in poor estimation of optimum formulation [Levison et al. 1994; Shirakura et al. 1991]. Therefore, it is important to understand the complexity of pharmaceutical formulations by using established statistical tools such as multiple regression analysis (MRA), Box Behnken design (BBD), etc. Optimization by changing one-variable-at-a-time is a complex method to evaluate the effects of different variables on an experimental outcome. This approach assesses one variable at a time instead of all simultaneously. The method is time-consuming, expensive and often leads to misinterpretation of results when interactions between different components are present. Another approach is to accurately evaluate the impact of the independent variables on the dependent variables by varying all the important factors simultaneously in a systematic manner. This approach is known as response surface methodology (RSM). RSM is a statistical technique which can address the present scenario and can be used to establish relationships between several independent variables and one or more dependent variables [Myer and Montogomery 2002; Ray et al. 2009]. RSM optimizes multiple variables by systematic variation of all variables in a well-designed experiment with a minimum number of experiments. The RSM optimization process involves the following steps: performing statistically designed experiments; estimating the coefficients of a mathematical model using regression analysis technique; and predicting the response and checking the adequacy of the model. Among the available statistical design methods, a full factorial design (FFD) involves a large number of experiments for accurately predicting the response. At the same time, it is often considered unpractical due to its requirement of more number of experiment as compared to other designs [Box et al. 1978; Myer et al. 1989]. Fractional factorial design lacks the ability to accurately predict all positions of the factor space that are equidistant from the centre (rotatability). Based upon the desirable features of orthogonality and rotatability, Central Composite design (CCD) and BBD are commonly chosen for the purpose of response optimization [Bae and Shoda 2005; Ray 2006]. BBD is successfully used by Rahman et al. for optimization of risperidone loaded solid lipid nanoparticles [Rahman et al. 2010]. The BBD requires fewer runs than 3-factor, 3-level FFD and CCD when three or more variables are involved. This cubic design is characterized by a set of points lying at the midpoint of each edge and a replicate centre

point of the multidimensional cube [George Box 1960]. The BBD technique is a three-level design based upon the combination of two-level factorial designs and incomplete block designs. BBD is a spherical design with excellent predictability within the spherical design space. Compared to the CCD method, the BBD technique is considered as the most suitable for evaluating quadratic response surfaces particularly in cases when prediction of response at the extreme level is not the goal of the model. In addition, the BBD technique is rotatable or nearly rotatable regardless of the number of factors under consideration [Bae and Shoda 2005; Myer and Montogomery 2002; Ray 2006]. Also, it is very time consuming method. Hence, deriving a quantitative mathematical relationship between the variables to evaluate its effect on dependent variables is of utmost importance [Mehta et al. 2007; Seth and Misra 2002].

The number of formulations required for such studies is dependent on the number of independent variables selected after preliminary experiments. The dependent response is measured for each trial and then either simple linear equation (equation 1), or interactive equation (equation 2) or quadratic model (equation 3) is fitted by carrying out MRA and F-statistic to identify statistically significant terms.

$$Y = b_0 + b_1X_1 + b_2X_2 + b_3X_3 \quad (1)$$

$$Y = b_0 + b_1X_1 + b_2X_2 + b_3X_3 + b_{12}X_1X_2 + b_{13}X_1X_3 + b_{23}X_2X_3 + b_{123}X_1X_2X_3 \quad (2)$$

$$Y = b_0 + b_1X_1 + b_2X_2 + b_3X_3 + b_{12}X_1X_2 + b_{13}X_1X_3 + b_{23}X_2X_3 + b_1^2X_{11} + b_2^2X_{22} + b_3^2X_{33} + b_{123}X_1X_2X_3 \quad (3)$$

where, Y is estimated response; b_0 is constant; b_1, b_2, b_3 are linear coefficients; b_{12}, b_{23}, b_{13} are interaction coefficients; and b_1^2, b_2^2, b_3^2 are quadratic coefficients.

Based on the results obtained in preliminary experiments, variables which are found to be influencing majorly to dependent variables were selected to find the optimized condition required for higher PDE and lower PS using MRA. In developing the regression equation, the test factors were coded according to the equation 4.

$$x_i = (X_i - X_i^X) / \Delta X_i \quad (4)$$

where, x_i is the coded value of the i^{th} independent variable, X_i is the natural value of the i^{th} independent variable, X_i^X is the natural value of the i^{th} independent variable at the center point and ΔX_i is the step change value.

Equation for quadratic model (equation 3) can be summarized as,

$$Y = b_0 + \sum_i b_iX_i + \sum_i \sum_j b_{ij}X_iX_j + \sum b_{ii}X_i^2 \quad (5)$$

where Y is the measured response, b_0 is the intercept term, b_i, b_{ij} and b_{ii} are, respectively the measures of the variables X_i, X_iX_j and X_i^2. The variable X_iX_j represents the first order interactions between X_i and X_j ($i < j$). A full model (FM) was established after putting the values of regression coefficients in equation 5.

4.2 Materials

Anastrozole and Exemestane were received as gift sample from Sun Pharma Advanced Research Centre, Vadodara, India. Poly (D, L Lactide-co-Glycolide) (PLGA 50:50, inherent viscosity 0.2 dl/g) was received as gift sample from PURAC Biomaterials, Gorinchem, Netherlands. Poloxamer 188 was obtained as gift sample from BASF, Ludwigshafen, Germany. Capric/caprylic triglyceride (Capmul MCM, C8) was obtained as gift sample from Abitec Corporation, Janesville, USA. Caprolactone monomer and Sulpho-NHS were purchased from Sigma-Aldrich, Mumbai, India. All other chemicals were of analytical reagent grade and obtained commercially.

4.3 Synthesis of polymer and conjugates

4.3.1 Synthesis of PLGA-PEG conjugate

PLGA-PEG conjugate was synthesized using N-Hydroxysuccinimide (NHS) and 1-ethyl-3-(3-dimethylaminopropyl) carbodiimide hydrochloride (EDC) as an activator [Chaudhari et al. 2012]. Carboxylic group of PLGA (1.7 g) was activated by addition of NHS (240 mg) and EDC (384 mg) in dichloromethane (DCM) (free from moisture) to form PLGA-NHS. The reaction mixture was stirred in tightly closed flask under nitrogen blanket for 12 h. PLGA-NHS was then precipitated with addition of ice cold methanol. Reaction mixture was centrifuged at 50,000×g for 5 min to collect activated PLGA. Precipitation process was repeated again to remove excess EDC and NHS by dissolving it in small quantity of acetone and again precipitated in ice cold methanol. Residual methanol was then evaporated using rotary flask evaporator. Activated PLGA was dissolved in DCM followed by addition of amine-PEG-carboxylic acid (600 mg) which was allowed to react for 12 h. Reaction mixture was precipitated in double distilled water and centrifuged at 50,000×g for 5 min to collect PLGA-PEG. Precipitation process was repeated twice to remove un-reacted PEG and the product was lyophilized (Heto Drywinner, Allerod, Denmark). Lyophilized product was stored under refrigeration till

further use. Each reaction step as well as purification step were monitored by TLC using 100% ethyl acetate as a mobile phase and iodine as a spotting reagent. Characterization of conjugate was done by FTIR, NMR and GPC.

4.3.2 Synthesis of cPCL

Synthesis of carboxylated PCL was carried out by ring opening polymerization of caprolactone monomer in presence of succinic acid as reported by Zhang et al. with some modifications [Zhang et al. 1994]. Reaction was carried out at room temperature in presence of tertiary butoxide (4 g) for 24 h instead of heating reaction mixture at 225 °C for 3 h. Polymerization was carried out in a flask sealed with a ball filled with nitrogen. The reactant mixture of succinic acid (23.5 mg) and caprolactone (3.65 g) was added to about 15 ml of dichloromethane in the flask for initiation of polymerization reaction. The reaction was catalyzed using tertiary butoxide (4 g). The reaction was allowed to continue for 24 h. The reaction mixture was precipitated in ice cold water and precipitates were dissolved in acetone for re-precipitation and purification to remove excess succinic acid. Each reaction step as well as purification step was monitored by TLC using 100% ethyl acetate as a mobile phase and iodine as a spotting reagent. The reaction was considered to be complete when there was absence of spots for caprolactone monomer and succinic acid from the reaction mixture.

4.3.3 Synthesis of PCL-PEG conjugate

Caprolactone containing carboxylic acid groups was polymerized as per previous reported method [Kumar and Sawant 2013]. PCL-PEG conjugate was synthesized using NHS and EDC as an activator [Chaudhari et al. 2012]. Carboxylic group of PCL (1.75 g) was activated by addition of NHS (240 mg) and EDC (384 mg) in DCM (free from moisture) to form PCL-NHS. The reaction mixture was stirred in tightly closed flask under nitrogen blanket for 12 h. PCL-NHS was then precipitated with addition of ice cold methanol. Reaction mixture was centrifuged at 50,000×g for 5 min to collect activated PCL. Precipitation process was repeated again to remove excess EDC and NHS by dissolving it in small quantity of acetone and again precipitated in ice cold methanol. Residual methanol was then evaporated using rotary flask evaporator. Activated PCL was dissolved in DCM followed by addition of amine-PEG-carboxylic acid (600 mg) which was allowed to react for 12 h. Reaction mixture was precipitated in double distilled water and centrifuged at 50,000×g for 5 min to collect PCL-PEG. Precipitation

process was repeated twice to remove un-reacted PEG and the product was lyophilized (HetoDry, Germany). Lyophilized product was stored under refrigeration till further use. Each reaction step as well as purification step were monitored by TLC using 100% ethyl acetate as a mobile phase and iodine as a spotting reagent. Characterization of PCL and PCL-PEG conjugate was done by FTIR, NMR and GPC.

4.4 Characterization of polymer and conjugates

4.4.1 FTIR spectroscopy

The sample (2 mg) was finely grounded with purified potassium bromide (200 mg) (to remove scattering effects from large crystals). This powder mixture was then pressed in a mechanical die press to form a pellet. These pellets were scanned and spectra were recorded on FTIR (Bruker Corporation, USA). The scanning range was 400 - 4000 cm^{-1} with the resolution of 2 cm^{-1}.

4.4.2 NMR spectroscopy

The proton NMR spectrum of the conjugate was recorded to confirm formation of amide bond. Sample was dissolved in DMSO (deuterated, Merck Germany) and transferred to a 5 mm NMR tube. NMR tube containing sample was placed in 5 mm broad band probe head and pulse programming was performed using Brucker 300MHz (Switzerland) and the NMR spectra was recorded.

4.4.3 Molecular weight determination

Gel permeation chromatography (GPC) was carried out to determine the molecular weight of the formed polymer [Behan et al. 2001]. The molecular weight of PCL-PEG polymer was determined by GPC equipped with a Waters 510 pump, 50, 10–3, and 10–4 ºA Phenogel columns serially set (Phenomenex, USA) and a Waters 410 differential refractometer. The mobile phase was tetrahydrofuran at a flow rate of 1.0 ml/min. 50 µl of a 2% polymer solution in THF was injected into the system, and size exclusion chromatogram was recorded.

4.5 Formulation and optimization of ATZ loaded PLGA NPs

4.5.1 Preparation of ATZ loaded PLGA NPs

ATZ loaded PLGA NPs were prepared using solvent diffusion (nanoprecipitation) method [Fessi et al. 1989; Seju et al. 2011]. The optimized formulation was prepared by

dissolving PLGA (100 mg) and ATZ (5 mg) in 5 ml of acetone. This organic phase was added at the rate of 0.5 ml/min into 10 ml of aqueous phase containing 0.25% w/v Poloxamer 188 with continuous stirring on magnetic stirrer at room temperature. Stirring was continued for 3-4 h to allow complete evaporation of organic solvent. The NPs suspension was centrifuged at 50,000×g for 30 min at 4 °C (3K30, Sigma Centrifuge, Osterode, Germany), supernatant was alienated and free drug present in supernatant was measured using HPLC [Mendes et al. 2007]. Based on preliminary experiments, variables like drug:polymer ratio (X_1), polymer concentration in organic phase (X_2) and surfactant concentration in aqueous phase (X_3) were selected as independent variables and percentage drug entrapment (PDE) and particle size (PS) were taken as dependent variables. Effect of independent variables on dependent variables was studied using 3^3 factorial design.

4.5.2 Drug content and percentage drug entrapment

The drug content in the NPs was determined by dissolving 10 mg of lyophilized NPs in 10 ml of acetonitrile. The solution was then filtered through 0.22 μ, appropriately diluted with mobile phase and drug content in the NPs was determined by HPLC.

Drug loading was calculated as follows,

Percentage drug loading = A/B × 100

Where A is the drug content in the NPs and B is the weight of NPs.

PDE was estimated by calculating amount of drug entrapped in NPs with respect to total drug added during preparation of formulation.

The PDE was calculated according to following formula:

PDE (%) = (TD-FD/TD) × 100

where, TD is total amount of drug added and FD is amount of drug in supernatant

4.5.3 Particle size

The PS and polydispersity index (PDI) of the NPs were determined using a Malvern Zetasizer (Nano ZS, Malvern Instrument, Worcestershire, UK). Each sample was diluted ten times with filtered distilled water to avoid multi-scattering phenomena and placed in disposable sizing cuvette. PDI was studied to determine the narrowness of the particle size distribution. The size analysis of a sample consisted of 3 measurements, and the results are expressed as mean size ± SD.

4.5.4 Preliminary optimization of ATZ loaded PLGA NPs

Different formulation parameters were optimized based on their effect on response parameters like PDE and PS. Some of the formulation parameters like organic solvent, volume of organic solvent and type of surfactant were optimized in preliminary stages, while drug:polymer ratio, polymer concentration in organic phase and surfactant concentration in aqueous phase were optimized by 3^3 full factorial design. All the experiments were performed in triplicate. Formulation parameters optimized in preliminary stages were selection of organic solvent, volume of organic solvent and type of surfactant.

4.5.4.1 Selection of organic solvent

Three different organic solvents (acetone, acetonitrile and tetrahydrofuran) were used for preparation of PLGA NPs. Volume of organic phase (4 ml) and ratio of organic phase and aqueous phase (1:2.5) were kept constant. All other parameters were also kept constant in all three experiments.

4.5.4.2 Selection of volume of organic solvent

Acetone was used as organic solvent. Three different volumes of organic phase were selected (3, 4 and 5 ml) and their effect of different volume of organic phase was observed on PDE and PS. Volume of aqueous phase (10 ml) was kept constant along with other formulation and process variables.

4.5.4.3 Selection of surfactant

Three different surfactants were initially used for formulation development, namely Pluronic F-68®, Pluronic F-127® and Poly vinyl alcohol (PVA). Out of these, better one was selected based on resultant PDE and PS. Concentration of surfactants were kept constant (0.5%) for all three surfactants. All other parameters were also kept constant in all three formulations.

4.5.5 Optimization

4.5.5.1 Experimental design for optimization of key formulation variables

Twenty seven batches of different combinations were prepared using 3^3 factorial design by taking values of X_1, X_2 and X_3 at different levels and evaluated for PDE and PS. Mathematical modeling was carried out by using equation 3 to obtain a second order polynomial equation [Armstrong and James 1996]. A FM equation was established after putting the values of regression coefficients of PDE and PS in equation 3. The predicted

values were calculated by using the mathematical model based on the coefficients of the model and the predicted values along with their observed values were recorded along with percentage of error obtained when predicted value and observed values were compared. Neglecting non-significant ($p<0.05$) terms from the FM, a reduced model (RM) was established to facilitate the optimization technique by plotting contour plots and response surface plots by keeping least significant independent variable constant and varying other two independent variables, to establish the relationship between independent and dependent variables. F-Statistic was applied on the results of analysis of variance (ANOVA) of FM and RM to check whether the non-significant terms can be omitted or not from the FM [Bolton 1997]. Design Expert 8.0.3 and Microsoft Excel 2007 were used for the statistical optimization.

4.5.5.2 Contour plots

Contour plots are diagrammatic representation of the values of the responses that help in explaining the relationship between independent and dependent variables. Two dimensional contour plots were established between X_1 and X_2 at different levels (-1, 0, 1) of X_3 for PDE and PS.

4.5.5.3 Response surface plots

To understand the main and the interaction effects of two variables, response surface plots were used as a function of two factors at a time maintaining all other factors at fixed levels [Box 1951; Mak 1995]. These plots were obtained by calculating the values taken by one factor where the second varies (from -1 to 1 for instance) with constraint of a given Y value. The yield values for different levels of variables can also be predicted from the respective response surface plots.

4.5.5.4 Check point analysis

A check point analysis was performed to confirm the utility of the established contour plots and reduced polynomial equation in the preparation of NPs. Values of independent variables (X_1 and X_2) were taken from three check points on contour plots plotted at fixed levels of -1, 0 and 1 of X_3 and the values of PDE (Y_1) and PS (Y_2) were calculated by substituting the values in the reduced polynomial equation. ATZ loaded NPs were prepared experimentally by taking the amounts of the independent variables (X_1 and X_2). Each batch was prepared three times and mean values were determined. Difference

in the predicted and mean values of experimentally obtained PDE and PS was compared by using student's 't' test.

4.5.5.5 Desirability criteria

For simultaneous optimization of PDE and PS, desirability function (multi-response optimization technique) was applied and total desirability was calculated using Design Expert software (version 8.0.3). The desirability lies between 0 and 1 and it represents the closeness of a response to its ideal value (equation 6). The total desirability is defined as a geometric mean of the individual desirability for PDE and PS [Derringer and Suich 1980].

$$D = (d_{PDE} \times d_{PS})^{1/2} \quad (6)$$

Where, D is the total desirability, d_{PDE} and d_{PS} are individual desirability for PDE and PS. If both the quality characteristics reach their ideal values, the individual desirability is 1 for both. Consequently, the total desirability is also 1. Our optimization criteria included maximum PDE and PS of less than 200 nm.

4.5.5.6 Normalized error determination

The quantitative relationship established by MRA was confirmed by evaluating experimentally prepared ATZ loaded NPs. PDE and PS predicted from the MRA were compared with those generated from prepared batches of check point analysis using normalized error (NE). The equation of NE (equation 7) is expressed as follows:

$$NE = [\Sigma\{(Pre - Obs)/Obs\}^2]^{1/2} \quad (7)$$

where, Pre and Obs represents predicted and observed response, respectively.

4.5.6 Lyophilization and optimization of cryoprotectant

In the present study, trehalose, sucrose and mannitol were investigated in different ratios and change in particle size upon re-dispersion was observed. Nanoparticulate suspension (2 ml) was dispensed in 10 ml semi-stoppered vials with rubber closures and frozen for 24 h at -60 °C. Thereafter, the vials are lyophilized (Heto Drywinner, Allerod, Denmark) using different cryoprotectants like trehalose, sucrose and mannitol in different concentrations (1:1, 1:2, 1:3 and 1:4). Finally, glass vials were sealed under anhydrous conditions and stored until being re-hydrated. Lyophilized NPs were re-dispersed in exactly the same volume of distilled water as before lyophilization. NP suspension was subjected to particle size measurement as described earlier. Ratio of

final particle size (S_f) and initial particle size (S_i) was calculated to finalize the suitable cryoprotectant based upon lowest S_f/S_i ratio.

4.6 Formulation and optimization of ATZ loaded cPCL NPs

4.6.1 Preparation of ATZ loaded cPCL NPs

ATZ loaded cPCL NPs were prepared using solvent diffusion (nanoprecipitation) method [Fessi et al. 1989; Seju et al. 2011]. The optimized formulation was prepared by dissolving cPCL (100 mg) and ATZ (5 mg) in 5 ml of acetone. This organic phase was added at the rate of 0.5 ml/min into 10 ml of aqueous phase containing 0.25% w/v Poloxamer 188 with continuous stirring on magnetic stirrer at room temperature. Stirring was continued for 3-4 h to allow complete evaporation of organic solvent. The NPs suspension was centrifuged at 50,000×g for 30 min at 4 °C (3K30, Sigma Centrifuge, Osterode, Germany), supernatant was alienated and free drug present in supernatant was measured using HPLC [Mendes et al. 2007]. Based on preliminary experiments, variables like drug:polymer ratio (X_1), polymer concentration in organic phase (X_2) and surfactant concentration in aqueous phase (X_3) were selected as independent variables and percentage drug entrapment (PDE) and particle size (PS) were taken as dependent variables. Effect of independent variables on dependent variables was studied using 3^3 factorial design.

4.6.2 Drug content and percentage drug entrapment

The drug content in the NPs was determined by dissolving 10 mg of lyophilized NPs in 10 ml of acetonitrile. The solution was then filtered through 0.22 μ, appropriately diluted with mobile phase and drug content in the NPs was determined by HPLC.

Drug loading was calculated as follows,

Percentage drug loading = A/B × 100

Where A is the drug content in the NPs and B is the weight of NPs.

PDE was estimated by calculating amount of drug entrapped in NPs with respect to total drug added during preparation of formulation.

The PDE was calculated according to following formula:

PDE (%) = (TD-FD/TD) × 100

where, TD is total amount of drug added and FD is amount of drug in supernatant

4.6.3 Particle size

The PS and PDI of the NPs were determined using a Malvern Zetasizer (Nano ZS, Malvern Instrument, Worcestershire, UK). Each sample was diluted ten times with filtered distilled water to avoid multi-scattering phenomena and placed in disposable sizing cuvette. PDI was studied to determine the narrowness of the particle size distribution. The size analysis of a sample consisted of 3 measurements, and the results are expressed as mean size ± SD.

4.6.4 Preliminary optimization of ATZ loaded cPCL NPs

Different formulation parameters were optimized based on their effect on response parameters like PDE and PS. Some of the formulation parameters like organic solvent, volume of organic solvent and type of surfactant were optimized in preliminary stages, while drug:polymer ratio, polymer concentration in organic phase and surfactant concentration in aqueous phase were optimized by 3^3 full factorial design. All the experiments were performed in triplicate. Formulation parameters optimized in preliminary stages were selection of organic solvent, volume of organic solvent and type of surfactant.

4.6.4.1 Selection of organic solvent

Three different organic solvents (acetone, acetonitrile and tetrahydrofuran) were used for preparation of cPCL NPs. Volume of organic phase (4 ml) and ratio of organic phase and aqueous phase (1:2.5) were kept constant. All other parameters were also kept constant in all three experiments.

4.6.4.2 Selection of volume of organic solvent

Acetone was used as organic solvent. Three different volumes of organic phase were selected (3, 4 and 5 ml) and the effect of different volume of organic phase was observed on PDE and PS. Volume of aqueous phase (10 ml) was kept constant along with other formulation and process variables.

4.6.4.3 Selection of surfactant

Three different surfactants were initially used for formulation development namely Pluronic F-68®, Pluronic F-127® and Poly vinyl alcohol (PVA). Out of these, better one is selected based on resultant PDE and PS. Concentration of surfactants were kept constant (0.5%) for all three surfactants. All other parameters were also kept constant in all three formulations.

4.6.5 Optimization

4.6.5.1 Experimental design for optimization of key formulation variables

Twenty seven batches of different combinations were prepared using 3^3 factorial design by taking values of X_1, X_2 and X_3 at different levels as shown in table 1 and evaluated for PDE and PS. Mathematical modeling was carried out by using equation 3 to obtain a second order polynomial equation [Armstrong and James 1996]. A FM equation was established after putting the values of regression coefficients of PDE and PS in equation 3. The predicted values were calculated by using the mathematical model based on the coefficients of the model and the predicted values along with their observed values were recorded along with percentage of error obtained when predicted value and observed values were compared. Neglecting non-significant ($p<0.05$) terms from the FM, RM was established to facilitate the optimization technique by plotting contour plots and response surface plots by keeping least significant independent variable constant and varying other two independent variables, to establish the relationship between independent and dependent variables. F-Statistic was applied on the results of analysis of variance (ANOVA) of FM and RM to check whether the non-significant terms can be omitted or not from the FM [Bolton 1997]. Design Expert 8.0.3 and Microsoft Excel 2007 were used for the statistical optimization.

4.6.5.2 Contour plots

Contour plots are diagrammatic representation of the values of the responses that help in explaining the relationship between independent and dependent variables. Two dimensional contour plots were established between X_1 and X_2 at different levels (-1, 0, 1) of X_3 for PDE and PS.

4.6.5.3 Response surface plots

To understand the main and the interaction effects of two variables, response surface plots were used as a function of two factors at a time maintaining all other factors at fixed levels [Box 1951; Mak 1995]. These plots were obtained by calculating the values taken by one factor where the second varies (from -1 to 1 for instance) with constraint of a given Y value. The yield values for different levels of variables can also be predicted from the respective response surface plots.

4.6.5.4 Check point analysis

A check point analysis was performed to confirm the utility of the established contour plots and reduced polynomial equation in the preparation of NPs. Values of independent variables (X_1 and X_2) were taken from three check points on contour plots plotted at fixed levels of -1, 0 and 1 of X_3 and the values of PDE (Y_1) and PS (Y_2) were calculated by substituting the values in the reduced polynomial equation. ATZ loaded NPs were prepared experimentally by taking the amounts of the independent variables (X_1 and X_2). Each batch was prepared three times and mean values were determined. Difference in the predicted and mean values of experimentally obtained PDE and PS was compared by using student's 't' test.

4.6.5.5 Desirability criteria

For simultaneous optimization of PDE and PS, desirability function (multi-response optimization technique) was applied and total desirability was calculated using Design Expert software (version 8.0.3). The desirability lies between 0 and 1 and it represents the closeness of a response to its ideal value (equation 6). The total desirability is defined as a geometric mean of the individual desirability for PDE and PS [Derringer and Suich 1980].

$$D = (d_{PDE} \times d_{PS})^{1/2} \quad (6)$$

Where, D is the total desirability, d_{PDE} and d_{PS} are individual desirability for PDE and PS. If both the quality characteristics reach their ideal values, the individual desirability is 1 for both. Consequently, the total desirability is also 1. Our optimization criteria included maximum PDE and PS of less than 200 nm.

4.6.5.6 Normalized error determination

The quantitative relationship established by MRA was confirmed by evaluating experimentally prepared ATZ loaded NPs. PDE and PS predicted from the MRA were compared with those generated from prepared batches of check point analysis using normalized error (NE). The equation of NE (equation 7) is expressed as follows:

$$NE = [\Sigma\{(Pre - Obs)/Obs\}^2]^{1/2} \quad (7)$$

where, Pre and Obs represents predicted and observed response, respectively.

4.6.6 Lyophilization and optimization of cryoprotectant

In the present study, trehalose, sucrose and mannitol were investigated in different ratios and change in particle size upon re-dispersion was observed. Nanoparticulate

suspension (2 ml) was dispensed in 10 ml semi-stoppered vials with rubber closures and frozen for 24 h at -60 °C. Thereafter, the vials are lyophilized (Heto Drywinner, Allerod, Denmark) using different cryoprotectants like trehalose, sucrose and mannitol in different concentrations (1:1, 1:2, 1:3 and 1:4). Finally, glass vials were sealed under anhydrous conditions and stored until being re-hydrated. Lyophilized NPs were re-dispersed in exactly the same volume of distilled water as before lyophilization. NP suspension was subjected to particle size measurement as described earlier. Ratio of final particle size (S_f) and initial particle size (S_i) was calculated to finalize the suitable cryoprotectant based upon lowest S_f/S_i ratio.

4.7 Formulation and optimization of EXE loaded PLGA NPs

4.7.1 Preparation of EXE loaded PLGA NPs

PLGA NPs loaded with EXE were prepared by interfacial deposition of preformed polymer [Fessi et al. 1989]. EXE (5 mg) was dissolved in oil (400 µl capric/caprylic triglyceride mixture) and added to acetone (8 ml) in which PLGA (100 mg) was dissolved along with sorbitan monooleate (Span 60, 0.05 ml), under moderate magnetic stirring. This solution was then added to an aqueous phase (40 ml distilled water) containing Poloxamer 188 (0.5%) with continuous stirring on magnetic stirrer at room temperature. Stirring was continued for 3-4 h to allow complete evaporation of organic solvent. The NPs suspension was centrifuged at 50,000×g for 30 min at 4 °C (3K30, Sigma Centrifuge, Osterode, Germany), supernatant was alienated and free drug present in supernatant was measured using modified HPLC method [Breda et al. 1993]. Nanoparticulate pellet was redispersed in water (10 ml) and lyophilized (Heto Drywinner, Allerod, Denmark) using sucrose as cryoprotectant [NPs (1 part) and cryoprotectant (2 parts)]. Empty NPs were prepared by the method described above with the exception of adding EXE. Based on preliminary experiments, variables like drug:polymer ratio (X_1), amount of polymer (X_2) and volume of organic phase (X_3) were selected as independent variables and PDE and PS were taken as dependent variables. Effect of independent variables on dependent variables was studied using 3×3 BBD.

4.7.2 Drug content and percentage drug entrapment

The drug content in the NPs was determined by dissolving 10 mg of lyophilized NPs in 10 ml of acetonitrile. The solution was then measured by HPLC after filtration through

0.22 μ and appropriate dilution with mobile phase and the amount of drug entrapped in the NPs was determined.

Drug loading was calculated as follows,

Percentage drug loading = A/B × 100

Where A is the drug content in the NPs and B is the weight of NPs.

PDE was estimated by calculating amount of drug entrapped in NPs with respect to total drug added during preparation of formulation.

The PDE was calculated according to following formula:

PDE (%) = (TD-FD/TD) × 100

where, TD is total amount of drug added and FD is amount of drug in supernatant

4.7.3 Particle size

The PS and PDI of the NPs were determined using a Malvern Zetasizer Nano ZS (Malvern Instrument, Worcestershire, UK). Each sample was diluted ten times with filtered distilled water to avoid multi-scattering phenomena and placed in disposable sizing cuvette. Polydispersity index was noted to determine the narrowness of the particle size distribution. The size analysis was performed in triplicate and the results were expressed as mean size ± SD.

4.7.4 Preliminary optimization of EXE loaded PLGA NPs

Different formulation parameters were optimized based on their effect on response parameters like PDE and PS. Some of the formulation parameters like type of organic solvent, type of surfactant and concentration of surfactant were optimized in preliminary stages, while drug:polymer ratio, amount of polymer in organic phase and volume of organic phase were optimized using 3×3 BBD. All the experiments were performed in triplicate.

4.7.4.1 Type of organic solvent

Three different organic solvents (acetone, acetonitrile and tetrahydrofuran) were used for preparation of EXE loaded PLGA NPs. Volume of organic phase (10 ml) and ratio of organic phase and aqueous phase (1:4) were kept constant. All other parameters were also kept constant in all three experiments.

4.7.4.2 Selection of surfactant

Three different surfactants were initially used for formulation development namely Pluronic F-68®, Pluronic F-127® and Poly vinyl alcohol (PVA). Out of these, better one is

selected based on resultant PDE and PS. Concentration of surfactants were kept constant (0.5%) for all three surfactants. All other parameters were also kept constant in all three formulations.

4.7.4.3 Concentration of surfactant

Different concentration (0.5, 1.0 and 1.5%) of surfactant (Pluronic F-68®) were used for the preparation of EXE loaded PLGA NPs. Others parameters were kept constant in all the three formulations.

4.7.5 Optimization

4.7.5.1 Experimental design for optimization of key formulation variables

A 3-factor, 3-level Box-Behnken statistical design was employed to optimize the process and formulation parameters in preparation of EXE loaded PLGA NPs and evaluate main effects, interaction effects and quadratic effects of the process parameters on the percentage drug entrapment (PDE) and particle size (PS). The independent variables selected were ratio of drug:polymer ratio (X_1), amount of PLGA (X_2), and volume of organic phase (X_3). A design matrix comprising of 13 experimental runs was constructed. The design was used to explore quadratic response surfaces and constructing second order polynomial models and construct contour plots to predict responses with Design Expert (Version 8.0.3, Stat-Ease Inc., Minneapolis, MN, USA).

4.7.5.2 Contour plots

Contour plots are diagrammatic representation of the values of the response. They are helpful in explaining the relationship between independent and dependent variables. The reduced models were used to plot two dimension contour plots. Two contour plots for PDE and PS were established between X_2 and X_3 at fixed levels (-1, 0 and 1) of X_1.

4.7.5.3 Response surface plots

To understand the main and the interaction effects of two variables, response surface plots were used as a function of two factors at a time, maintaining the third factor at fixed level [Mak et al. 1995]. These plots were obtained by calculating the values obtained by one factor where the second varied (from -1 to 1 for instance) with constraint of a given Y value.

4.7.5.4 Check point analysis

A check point analysis was performed to confirm the utility of the established contour plots and reduced polynomial equation in the preparation of NPs. Values of independent

variables (X_2 and X_3) were taken from three check points on contour plots plotted at fixed levels of -1, 0 and 1 of X_1 and the values of PDE (Y_1) and PS (Y_2) were calculated by substituting the values in the reduced polynomial equation. EXE loaded NPs were prepared experimentally by taking the amounts of the independent variables (X_1 and X_2). Each batch was prepared three times and mean values were determined. Difference in the predicted and mean values of experimentally obtained PDE and PS was compared by using student's 't' test.

4.7.5.5 Desirability Criteria

For simultaneous optimization of PDE and PS, desirability function (multi-response optimization technique) was applied and total desirability was calculated using Design Expert software. The desirability lies between 0 and 1 and it represents the closeness of a response to its ideal value. The total desirability is defined as a geometric mean of the individual desirability for PDE and PS [Derringer and Suich 1980].

$$D = (d_{PDE} X d_{PS})^{1/2} \quad (6)$$

where, D is the total desirability, d_{PDE} and d_{PS} are individual desirability for PDE and PS. If both the quality characteristics reach their ideal values, the individual desirability is 1 for both. Consequently, the total desirability is also 1. Our criteria included highest possible PDE and PS of less than 200 nm.

4.7.5.6 Normalized error determination

The quantitative relationship established by BBD was confirmed by evaluating experimentally prepared EXE loaded NPs. PDE and PS predicted from the BBD were compared with those generated from prepared batches of check point analysis using normalized error (NE). The equation of NE (equation 7) is expressed as follows:

$$NE = [\Sigma\{(Pre - Obs)/Obs\}^2]^{1/2} \quad (7)$$

where, Pre and Obs represents predicted and observed response, respectively.

4.7.6 Lyophilization and optimization of cryoprotectant

Lyophilization is the process in which freeze-drying is done to remove solvent from the formulation and therefore improve its stability upon storage. The process of freeze drying is stressful and hence a cryoprotectant is added in the process, which also helps in re-dispersibility of the freeze-dried NPs in a suitable solvent [Chacon et al. 1999]. One of the main challenges during the freeze-drying process is preserving or rather increasing the re-dispersibility of the NPs upon reconstitution with distilled water or

buffered saline. Cryoprotectants are generally added to the NPs prior to the drying step and also act as re-dispersants. Cryoprotectants such as trehalose, sucrose, mannitol can be used to increase the physical stability of NPs during freeze-drying [Paolicelli et al. 2010]. In the present study, trehalose, sucrose and mannitol were investigated in different ratios (1:1, 1:2, 1:3 and 1:4) and change in particle size upon re-dispersion was observed. Nanoparticulate suspension (2 ml) was dispensed in 10 ml semi-stoppered glass vials with rubber closures and frozen for 24 h at -60 °C. Thereafter, the vials were lyophilized (Heto Drywinner, Allerod, Denmark) using different cryoprotectants like trehalose, sucrose and mannitol in different concentrations. Finally, vials were sealed under anhydrous conditions and stored until being re-hydrated. Lyophilized NPs were re-dispersed in exactly the same volume of distilled water as before lyophilization. NP suspension was subjected to particle size measurement as described earlier. Ratio of final particle size (S_f) and initial particle size (S_i) was calculated to finalize the suitable cryoprotectant based on lowest S_f/S_i ratio [Kashi et al. 2012].

4.8 Formulation and optimization of EXE loaded cPCL NPs

4.8.1 Preparation of EXE loaded cPCL NPs

cPCL NPs loaded with EXE were prepared by interfacial deposition of preformed polymer [Fessi et al. 1989]. EXE (5 mg) was dissolved in oil (400 µl capric/caprylic triglyceride mixture) and added to acetone (8 ml) in which PCL (100 mg) was dissolved along with sorbitan monooleate (Span 60, 0.05 ml), under moderate magnetic stirring. This solution was then added to an aqueous phase (40 ml distilled water) containing Poloxamer 188 (0.5%) with continuous stirring on magnetic stirrer at room temperature. Stirring was continued for 3-4 h to allow complete evaporation of organic solvent. The NPs suspension was centrifuged at 50,000×g for 30 min at 4 °C (3K30, Sigma Centrifuge, Osterode, Germany), supernatant was alienated and nanoparticulate pellet was re-dispersed in water (10 ml) and lyophilized (Heto Drywinner, Allerod, Denmark) using sucrose as cryoprotectant [NPs (1 part) and cryoprotectant (2 parts)]. Empty NPs were prepared by the method described above with the exception of adding EXE. Based on preliminary experiments, variables like drug:polymer ratio (X_1), amount of polymer (X_2) and volume of organic phase (X_3) were selected as independent

variables and PDE and PS were taken as dependent variables. Effect of independent variables on dependent variables was studied using 3×3 BBD.

4.8.2 Drug content and percentage drug entrapment

The drug content in the NPs was determined by dissolving 10 mg of lyophilized NPs in 10 ml of acetonitrile analyzing by HPLC after filtration through 0.22 μ and appropriate dilution with mobile phase. Drug loading was calculated as follows,

Percentage drug loading = A/B × 100

Where A is the drug content in the NPs and B is the weight of NPs.

PDE was estimated by calculating amount of drug entrapped in NPs with respect to total drug added during preparation of formulation.

The PDE was calculated according to following formula:

PDE (%) = (TD-FD/TD) × 100

where, TD is total amount of drug added and FD is amount of drug in supernatant

4.8.3 Particle size

The size analysis and polydispersity index of the NPs were determined using a Malvern Zetasizer Nano ZS (Malvern Instrument, Worcestershire, UK). Each sample was diluted ten times with filtered distilled water to avoid multi-scattering phenomena and placed in disposable sizing cuvette. Polydispersity index was noted to determine the narrowness of the particle size distribution. The size analysis was performed in triplicate and the results were expressed as mean size ± SD.

4.8.4 Preliminary optimization of EXE loaded cPCL NPs

Different formulation parameters were optimized based on their effect on response parameters like PDE and PS. Some of the formulation parameters like type of organic solvent, type of surfactant and concentration of surfactant were optimized in preliminary stages, while drug:polymer ratio, amount of polymer in organic phase and volume of organic phase were optimized using 3×3 BBD. All the experiments were performed in triplicate.

4.8.4.1 Type of organic solvent

Three different organic solvents (acetone, acetonitrile and tetrahydrofuran) were used for preparation of EXE loaded cPCL NPs. Volume of organic phase (10 ml) and ratio of organic phase and aqueous phase (1:4) were kept constant. All other parameters were also kept constant in all three experiments.

4.8.4.2 Selection of surfactant

Three different surfactants were initially used for formulation development namely Pluronic F-68®, Pluronic F-127® and Poly vinyl alcohol (PVA). Out of these, better one is selected based on resultant PDE and PS. Concentration of surfactants were kept constant (0.5%) for all three surfactants. All other parameters were also kept constant in all three formulations.

4.8.4.3 Concentration of surfactant

Different concentration (0.5, 1.0 and 1.5%) of surfactant (Pluronic F-68®) were used for the preparation of EXE loaded cPCL NPs. Others parameters were kept constant in all the three formulations.

4.8.5 Optimization

4.8.5.1 Experimental design for optimization of key formulation variables

A 3-factor, 3-level Box-Behnken statistical design was employed to optimize the process and formulation parameters in preparation of EXE loaded cPCL NPs and evaluate main effects, interaction effects and quadratic effects of the process parameters on the percentage drug entrapment (PDE) and particle size (PS). The independent variables selected were ratio of drug:polymer ratio (X_1), amount of cPCL (X_2), and volume of organic phase (X_3). A design matrix comprising of 13 experimental runs was constructed. The design was used to explore quadratic response surfaces and constructing second order polynomial models and construct contour plots to predict responses with Design Expert (Version 8.0.3, Stat-Ease Inc., Minneapolis, MN, USA).

4.8.5.2 Contour plots

Contour plots are diagrammatic representation of the values of the response. They are helpful in explaining the relationship between independent and dependent variables. The reduced models were used to plot two dimension contour plots. Two contour plots for PDE and PS were established between X_2 and X_3 at fixed levels (-1, 0 and 1) of X_1.

4.8.5.3 Response surface plots

To understand the main and the interaction effects of two variables, response surface plots were used as a function of two factors at a time, maintaining the third factor at fixed level [Mak et al. 1995]. These plots were obtained by calculating the values obtained by one factor where the second varied (from -1 to 1 for instance) with constraint of a given Y value.

4.8.5.4 Check point analysis

A check point analysis was performed to confirm the utility of the established contour plots and reduced polynomial equation in the preparation of NPs. Values of independent variables (X_2 and X_3) were taken from three check points on contour plots plotted at fixed levels of -1, 0 and 1 of X_1 and the values of PDE (Y_1) and PS (Y_2) were calculated by substituting the values in the reduced polynomial equation. EXE loaded NPs were prepared experimentally by taking the amounts of the independent variables (X_1 and X_2). Each batch was prepared three times and mean values were determined. Difference in the predicted and mean values of experimentally obtained PDE and PS was compared by using student's 't' test.

4.8.5.5 Desirability criteria

For simultaneous optimization of PDE and PS, desirability function (multi-response optimization technique) was applied and total desirability was calculated using Design Expert software. The desirability lies between 0 and 1 and it represents the closeness of a response to its ideal value. The total desirability is defined as a geometric mean of the individual desirability for PDE and PS [Derringer and Suich 1980].

$$D = (d_{PDE} X d_{PS})^{1/2} \quad (6)$$

where, D is the total desirability, d_{PDE} and d_{PS} are individual desirability for PDE and PS. If both the quality characteristics reach their ideal values, the individual desirability is 1 for both. Consequently, the total desirability is also 1. Our criteria included highest possible PDE and PS of less than 200 nm.

4.8.5.6 Normalized error determination

The quantitative relationship established by BBD was confirmed by evaluating experimentally prepared EXE loaded NPs. PDE and PS predicted from the BBD were compared with those generated from prepared batches of check point analysis using normalized error (NE). The equation of NE (equation 1) is expressed as follows:

$$NE = [\Sigma\{(Pre - Obs)/Obs\}^2]^{1/2} \quad (7)$$

where, Pre and Obs represents predicted and observed response, respectively.

4.8.6 Lyophilization and optimization of cryoprotectant

Lyophilization is the process in which freeze-drying is done to remove solvent from the formulation and therefore improve its stability upon storage. The process of freeze drying is stressful and hence a cryoprotectant is added in the process, which also helps

in re-dispersibility of the freeze-dried NPs in a suitable solvent [Chacon et al. 1999]. One of the main challenges during the freeze-drying process is preserving or rather increasing the re-dispersibility of the NPs upon reconstitution with distilled water or buffered saline. Cryoprotectants are generally added to the NPs prior to the drying step and also act as re-dispersants. Cryoprotectants such as trehalose, sucrose, mannitol can be used to increase the physical stability of NPs during freeze-drying [Paolicelli et al. 2010]. In the present study, trehalose, sucrose and mannitol were investigated in different ratios (1:1, 1:2, 1:3 and 1:4) and change in particle size upon re-dispersion was observed. Nanoparticulate suspension (2 ml) was dispensed in 10 ml semi-stoppered glass vials with rubber closures and frozen for 24 h at -60 °C. Thereafter, the vials were lyophilized (Heto Drywinner, Allerod, Denmark) using different cryoprotectants like trehalose, sucrose and mannitol in different concentrations. Finally, vials were sealed under anhydrous conditions and stored until being re-hydrated. Lyophilized NPs were re-dispersed in exactly the same volume of distilled water as before lyophilization. NP suspension was subjected to particle size measurement as described earlier. Ratio of final particle size (S_f) and initial particle size (S_i) was calculated to finalize the suitable cryoprotectant based on lowest S_f/S_i ratio.

4.9 Characterization of optimized nanoparticulate formulation

4.9.1 Zeta potential

Zeta potential distribution was also measured using a Zetasizer (Nano ZS, Malvern instrument, Worcestershire, UK). Each sample was suitably diluted 10 times with filtered distilled water and placed in a disposable zeta cell. Zeta limits ranged from -200 to +200 mV. The electrophoretic mobility (μm/sec) was converted to zeta potential by in-built software using Helmholtz-Smoluchowski equation. Average of 3 measurements of each sample was used to derive average zeta potential.

4.9.2 Transmission electron microscope (TEM) studies

A sample of NPs (0.5 mg/ml) was suspended in water and bath sonicated for 30 s. 2 μl of this suspension was placed over a formvar coated copper TEM grid (150 mesh) and negatively stained with 2 μl uranyl acetate (1%) for 10 min, allowed to dry and the images were visualized at 80 kV under TEM (FEI Tecnai G2 Spirit Twin, Czech Republic) and captured using Gatan Digital Micrograph software.

4.9.3 Differential scanning calorimetric (DSC) studies

All the samples were dried in desiccators for 24 h before thermal analysis. DSC studies on pure drug, polymer, physical mixtures of drug and polymer and drug loaded NPs were performed in order to characterize the physical state of drug in the NPs. Thermograms were obtained using DSC model 2910 (TA Instruments, New Castle, USA). Dry nitrogen gas was used as the purge gas through the DSC cell at a flow rate of 40 ml/min. Samples (4 - 8 mg) were sealed in standard aluminum pans with lids and heated at a rate of 10 °C /min from 20 to 300 °C. Data was analyzed using TA Universal Analysis 2000 software (TA Instruments, New Castle, USA).

4.9.4 In vitro drug release studies

In vitro release of drug from non-pegylated NPs and pegylated NPs were evaluated by the dialysis bag diffusion technique in phosphate buffered saline (PBS) (pH 7.4) [Yang et al. 1999]. The aqueous nanoparticulate dispersion equivalent to 2 mg of drug was placed in a dialysis bag (cut-off 12,000 Da; Himedia, Mumbai, India), which was previously soaked overnight in water, cleaned next morning and sealed at both ends. The dialysis bag was immersed in the receptor compartment containing 50 ml of PBS (pH 7.4), which was stirred at 100 rpm and maintained at 37 ± 2 °C. The receptor compartment was covered to prevent the evaporation of release medium. Samples (2 ml) were withdrawn at regular time intervals, the same volume was replaced by fresh release medium and measured for amount of drug released using previously described HPLC method [Breda et al. 1993; Mendes et al. 2007]. All the experiments were performed in triplicate, and the average values were taken. Drug suspension prepared in PBS (pH 7.4) was used as a control. The kinetic analysis of the release data was done using Korsmeyer and Peppas equation or the Power law equation [Peppas 1985]:

$M_t/M_\infty = kt^n$

$\text{Log } (M_t/M_\infty) = \log k + n \log t$ (8)

Where, M_t/M_∞ is the fractional amount of drug released, k is the release constant, n is the release exponent and t is the time of release.

4.9.5 Stability studies

Stability studies were conducted using the optimized batch of lyophilized NPs. The NPs were stored at ambient temperature and at refrigerated temperature (2-8 °C). At

different time points, samples were withdrawn and subjected to drug content and particle size analysis as described previously.

4.10 Results and discussion

4.10.1 Characterization of PLGA-PEG conjugate

The infra red spectra of polymers are presented in figure 4.1 (A: PLGA; B: PEG and C: PLGA-PEG). The peak at 1760 cm^{-1} was observed corresponding to amide bond formation between PLGA and PEG. Peak due to N-H stretching observed in PEG at 3450 cm^{-1} was retained in PLGA-PEG. PLGA-PEG also retained all other peaks present in PEG confirming conjugation of PEG with PLGA. The NMR spectrum (figure 4.2) showed some distinct peaks confirming successful conjugation of PEG with PLGA as reported by other authors [Song et al. 2011]. The major peaks present at δ values 1.55 and 5.21 ppm showed presence of methyl (CH_3) and methine (CH) protons of lactic acid. The peaks of methene protons in CH_2 group of PEG and in terminal CH_2 group of PEG were around 3.65 and 4.32 ppm, respectively. The peak at 4.81 corresponds to methane in glycolic acid. Peak at 7.2 ppm is due to protons in amide linkage. Hence, we could conclude the successful formation of PLGA-PEG from the combined results of FTIR and NMR. The

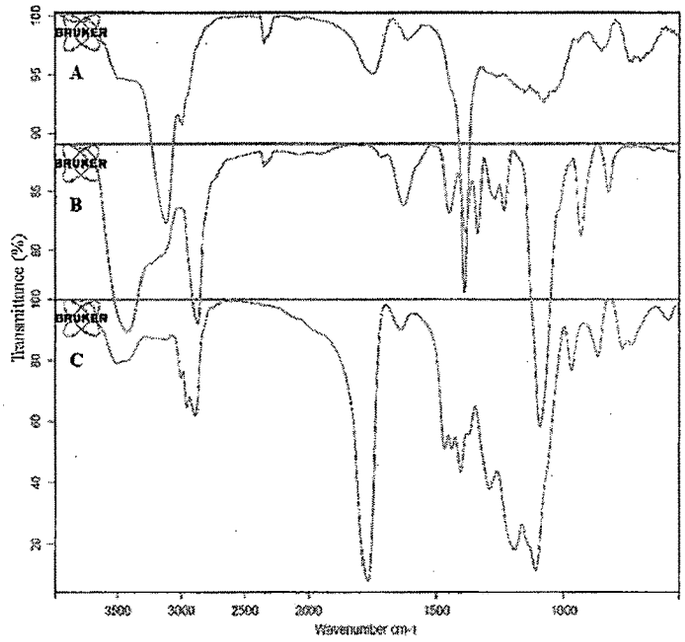

Figure 4.1 FTIR spectra of polymers, A: PLGA; B: PEG and C: PLGA-PEG.

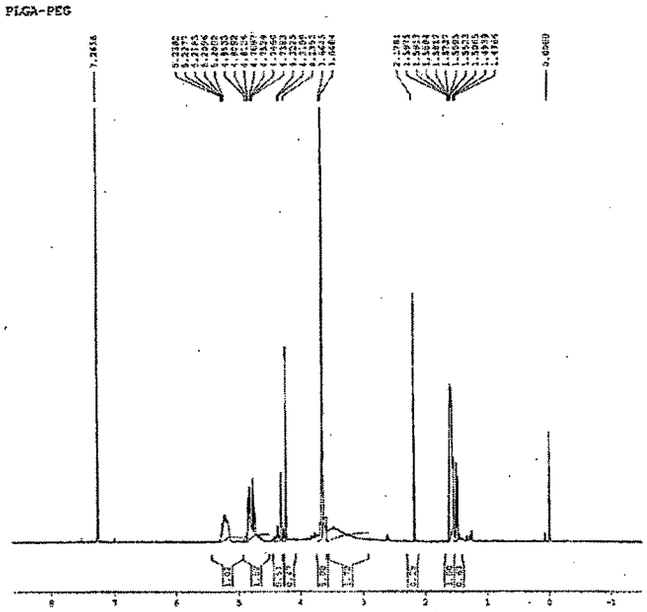

Figure 4.2 NMR spectra of pegylated PLGA.

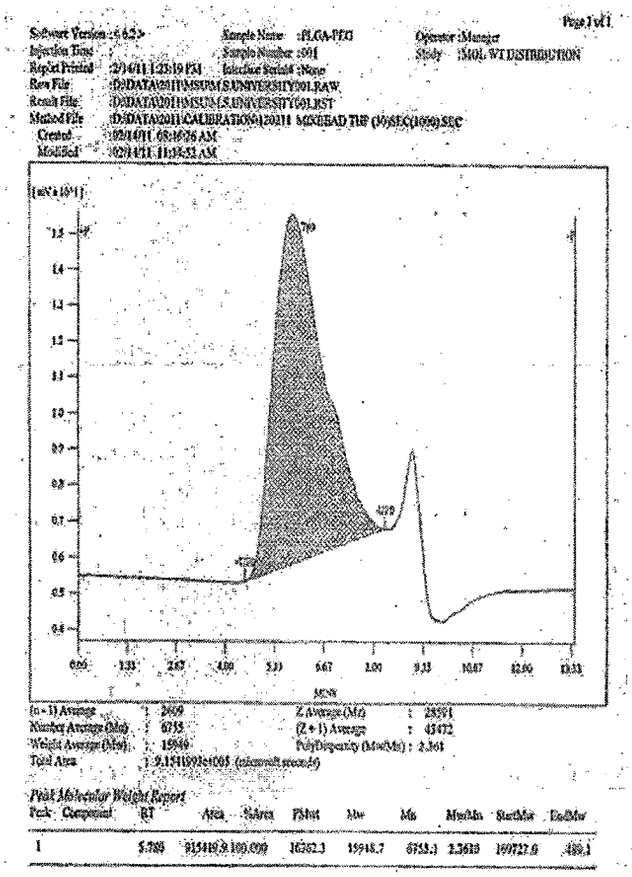

Figure 4.3 Gel permeation chromatogram of pegylated PLGA.

molecular weight of pegylated PLGA was determined using GPC. Chromatogram of copolymer is shown in figure 4.3. The Mw (Weight-average molecular weight) of PLGA-PEG was 15949 ± 683 Da) which was found to be close to theoretically predicted molecular weight (17000 Da). These results confirmed that PEG reacted with PLGA and as a result, PLGA-PEG was produced.

4.10.2 Characterization of cPCL

Successful polymerization of caprolactone to cPCL was confirmed by FTIR spectra of polymer (figure 4.4). The peak at 1727.81 cm^{-1} corresponding to carboxylic group and 3441 cm^{-1} for OH stretching of COOH group confirmed the conversion of caprolactone to cPCL [Zhang et al. 1994]. Molecular weight of cPCL was found to be 17487 ± 276 Da using GPC (figure 4.5) which was found to be close to theoretically predicted molecular weight (17814 Da).

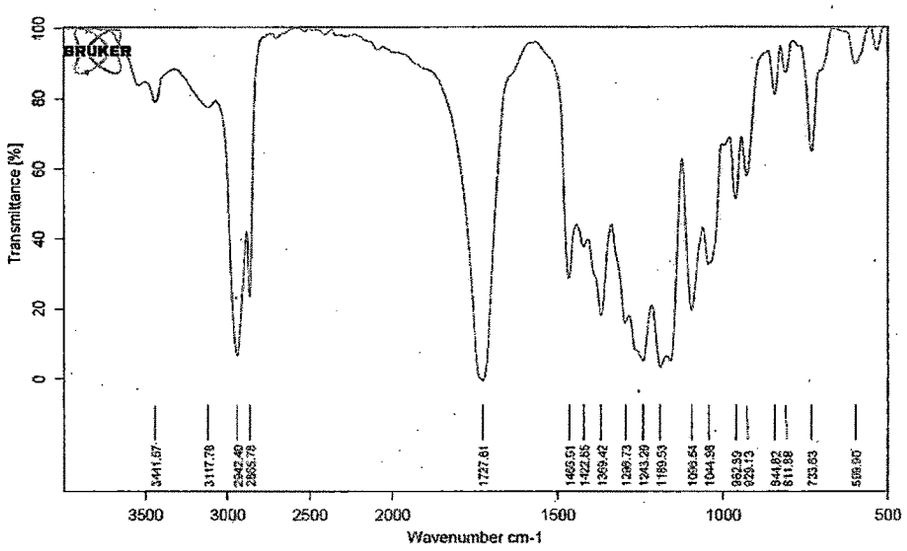

Figure 4.4 FTIR spectra of cPCL

4.10.3 Characterization of PCL-PEG conjugate

FTIR, NMR and GPC

The infra red spectra of polymers were presented in figure 4.6 (A: PCL; B: PEG and C: PCL-PEG). The peak at 1642 cm^{-1} was observed corresponding to C=O str. of amide bond between PCL and PEG. Peak at 3444 cm^{-1} due to N-H str. observed in PEG is retained in PCL-PEG. PCL-PEG also retained all other peaks present in PEG. These results confirmed

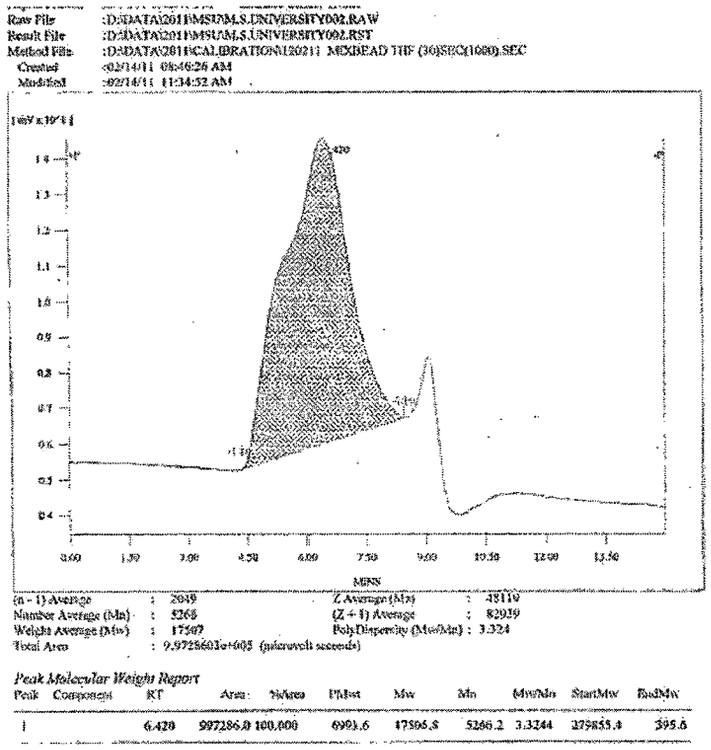

Figure 4.5 Gel permeation chromatogram of cPCL.

that PEG reacted with PCL and as a result, PCL-PEG was produced. The NMR spectrum (figure 4.7) showed some distinct peaks in PCL-PEG as reported by other researchers [Darbandy et al. 2011]. The major peaks are at δ values 1.3 and 1.6 ppm showed presence of methene (CH_2) protons of caprolactone. The peak of methene protons in terminal CH_2 group of caprolactone polymer chain was around 2.3 ppm. The peaks of methene protons in CH_2 group of PEG and in terminal CH_2 group of PEG were around 3.65 and 4.1 ppm, respectively. Peak at 7.2 ppm corresponds to protons in amide linkage. The molecular weight of pegylated PCL was determined using GPC method. Chromatogram of copolymer was shown in figure 4.8. The Mw (Weight-average molecular weight) of PCL-PEG was 22374 ± 779 Da which was found to be close to theoretically predicted molecular weight (22500 Da).

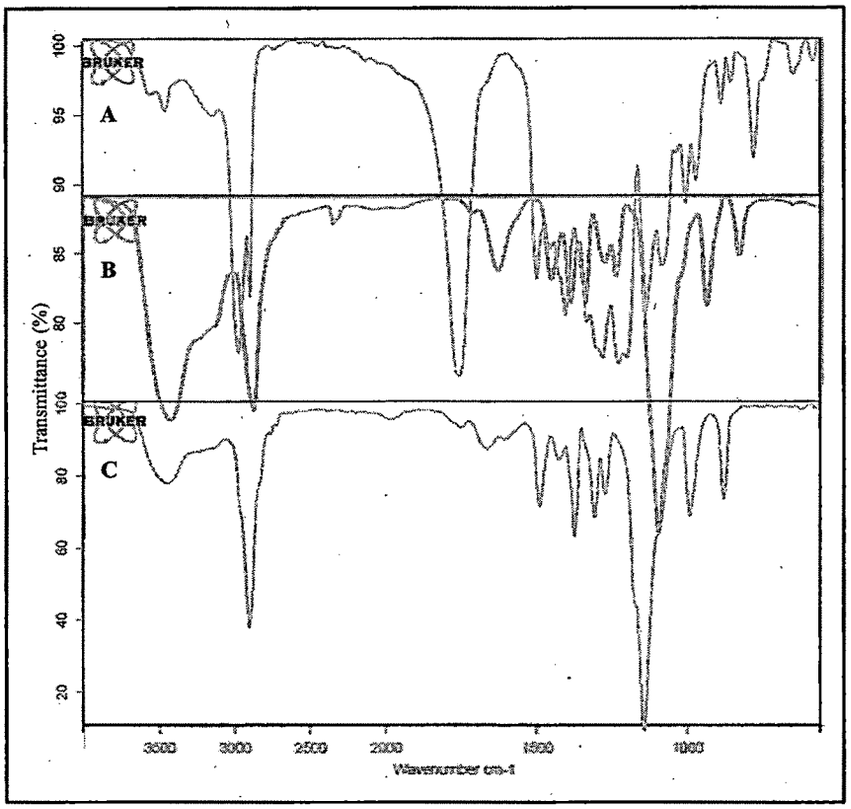

Figure 4.6 FTIR spectra of polymers, A: cPCL; B: PEG and C: PCL-PEG.

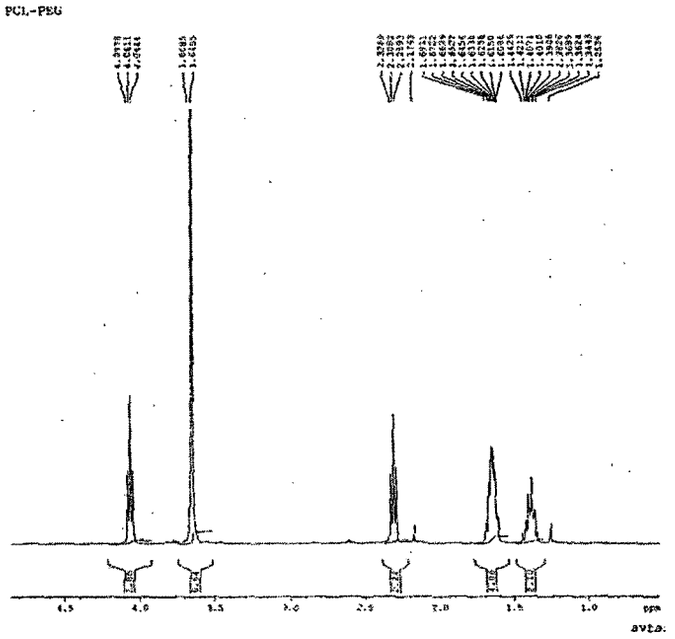

Figure 4.7 NMR spectra of pegylated PCL.

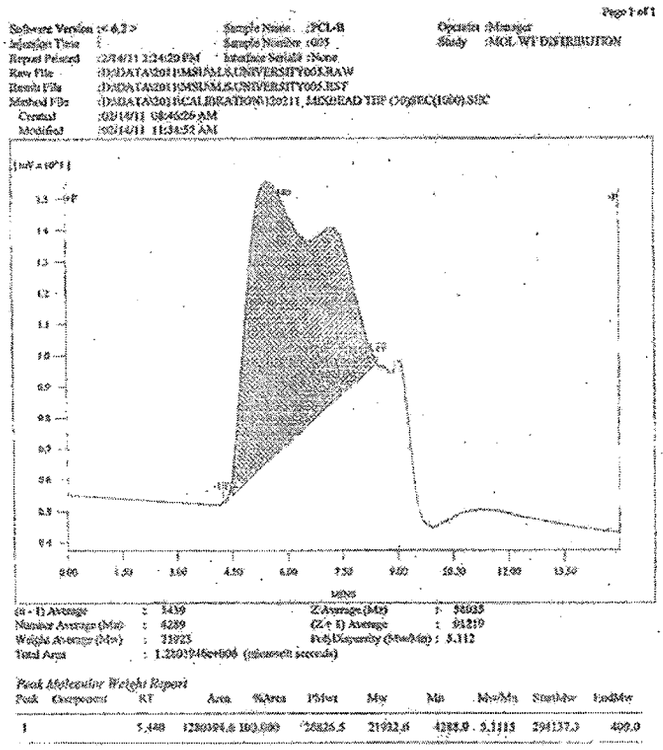

Figure 4.8 Gel permeation chromatogram of pegylated PCL.

4.11Formulation and optimization of ATZ loaded PLGA NPs

4.11.1 Preliminary optimization of ATZ loaded PLGA NPs

4.11.1.1 Selection of organic solvent

Three different organic solvents (acetone, acetonitrile and tetrahydrofuran) were used for preparation of PLGA NPs (table 4.1). NPs formulated using acetone showed PDE of 41.21 ± 0.85% with PS of 136.2 ± 5.3 nm while NPs formulated using acetonitrile were of low PDE and PS. PDE was again decreased when tetrahydrofuran was used as solvent with no significant change in PS. Hence, acetone was selected for further studies.

Table 4.1 Selection of organic phase in preliminary optimization of ATZ loaded PLGA NPs

Solvents	PDE (%)	PS (nm)
Acetone	41.21 ± 0.85	136.2 ± 5.3
Acetonitrile	35.79 ± 1.16	125.3 ± 3.9
Tetra hydro furan	33.61 ± 0.91	131.2 ± 4.1

4.11.1.2 Selection of volume of organic solvent

Different volumes of organic solvent (acetone) were used to dissolve polymer (50 mg) and results are represented in table 4.2. It was observed that as the volume of organic solvent was increased, PS decreases significantly with no major change in PDE. This was possibly due to decreased viscosity of organic phase with increase in volume of organic solvent which can easily dispersed in aqueous phase containing surfactant. Hence, 5 ml of acetone was selected as organic phase.

Table 4.2 Selection of volume of organic solvent in preliminary optimization of ATZ loaded PLGA NPs

Volume of organic solvent	PDE (%)	PS (nm)
3 ml	55.63 ± 0.91	230.1 ± 5.5
4 ml	53.32 ± 0.64	202.5 ± 7.2
5 ml	54.32 ± 1.81	180.1 ± 6.8

4.11.1.3 Selection of surfactant

Three different surfactants were initially used for formulation development namely Pluronic F-68® (P188), Pluronic F-127® (P127) and Poly vinyl alcohol (PVA) (table 4.3). Out of these, better one is selected based on resultant PDE and PS. With constant level of surfactant concentration (0.5%) for all three surfactants, PDE was found to be highest when PVA was used, but at the same time PS was found to be of larger size (332.4 ± 7.6 nm). No significant difference in PS was observed when P188 or P127 was used, but PDE was higher when P188 was used as surfactant. Hence, P188 was used in further studies.

Table 4.3 Selection of surfactant in preliminary optimization of ATZ loaded PLGA NPs

Surfactant	PDE (%)	PS (nm)
P188	45.99 ± 1.07	154.6 ± 6.8
P127	42.37 ± 0.89	148.2 ± 3.6
PVA	47.37 ± 1.07	332.4 ± 7.6

4.11.2 Optimization of ATZ loaded PLGA NPs using 3^3 factorial design

Twenty seven batches of ATZ loaded PLGA NPs were prepared by using 3^3 factorial design varying three independent variables, drug:polymer ratio (X_1), polymer

concentration in organic phase (X_2) and surfactant concentration in aqueous phase (X_3) (table 4.4). The PDE and PS were taken as dependent variables and the results were recorded (table 4.5). The main effects of X_1, X_2 and X_3 represent the average result of changing one variable at a time from its low to high value. The interactions (X_1X_2, X_1X_3, X_2X_3 and $X_1X_2X_3$) show how the PDE and PS changes when two or more variables were simultaneously changed. The values for the twenty seven batches showed a wide variation from 36.66 to 61.65% and 117.8 to 180.15 nm for PDE and PS respectively (table 4.5). This is reflected by the wide range of coefficients of the terms of equation 3 representing the individual and combined variables.

Table 4.4 Coded values of the formulation parameters of ATZ loaded PLGA NPs

Coded values	Actual values of dependent variables		
	X_1	X_2	X_3
-1	1 : 10	0.50 %	0.25 %
0	1 : 15	0.75 %	0.50 %
1	1 : 20	1.0 %	0.75 %

X_1 Drug:polymer ratio
X_2 Polymer concentration (% w/v)
X_3 Surfactant concentration (% w/v)

$$Y_1 = 51.08 + 0.69 X_1 + 8.12 X_2 - 0.87 X_3 + 0.64 X_1X_2 - 0.32 X_1X_3 - 0.67 X_2X_3 - 2.32 X_1^2 - 0.86 X_2^2 + 0.444 X_3^2 - 1.51 X_1X_2X_3 \quad (9)$$

$$Y_2 = 137.62 + 1.53 X_1 + 10.22 X_2 + 10.41 X_3 - 1.46 X_1X_2 + 2.05 X_1X_3 + 1.05 X_2X_3 + 15.37 X_1^2 + 3.91 X_2^2 - 0.74 X_3^2 + 1.01 X_1X_2X_3 \quad (10)$$

$$Y_1 = 50.8011 + 8.115 X_2 - 2.3188 X_1^2 \quad (11)$$

$$Y_2 = 137.1293 + 10.2183 X_2 + 10.41 X_3 + 15.3727 X_1^2 + 3.906 X_2^2 \quad (12)$$

The significance of each coefficient of equation 9 and 10 were determined by student's 't' test and p-value, which are listed in table 4.6 and 4.7 respectively. The larger the magnitude of the 't' value and the smaller the p-value, the more significant is the corresponding coefficient [Adinarayana and Ellaiah 2002; Akhnazarova 1982]. Small values of the coefficients of the terms X_1, X_3, X_2^2, X_3^2, X_1X_2, X_2X_3, X_1X_3, and $X_1X_2X_3$ in equation 9 and X_1, X_3^2, X_1X_2, X_2X_3, X_1X_3, and $X_1X_2X_3$ in equation 10 for PDE and PS respectively implied that all these terms were least contributing in the preparation of

Table 4.5 Layout of 3^3 full factorial design for ATZ loaded PLGA NPs

Sr. No.	X_1	X_2	X_3	Y_1* (PDE, in %)	Y_2* (PS, in nm)
1	-1	-1	-1	41.21 ± 0.8	136.3 ± 5.3
2	-1	-1	0	37.61 ± 0.6	145.2 ± 3.8
3	-1	-1	1	39.55 ± 0.9	153.3 ± 4.9
4	-1	0	-1	50.53 ± 0.9	139.5 ± 5.5
5	-1	0	0	45.99 ± 1.1	154.6 ± 6.8
6	-1	0	1	47.87 ± 0.9	158.1 ± 4.7
7	-1	1	-1	56.75 ± 1.9	158.7 ± 6.3
8	-1	1	0	53.26 ± 1.2	161.7 ± 4.4
9	-1	1	1	57.38 ±1.8	174.9 ± 6.6
10	0	-1	-1	43.29 ± 0.9	117.8 ± 3.3
11	0	-1	0	44.66 ± 1.2	129.2 ± 5.4
12	0	-1	1	42.42 ± 1.3	131.4 ± 5.2
13	0	0	-1	54.82 ± 0.9	127.0 ± 3.3
14	0	0	0	48.66 ± 1.3	140.7 ± 4.1
15	0	0	1	52.66 ± 1.8	152.7 ± 4.0
16	0	1	-1	58.52 ± 2.0	141.4 ± 3.3
17	0	1	0	55.04 ± 1.3	156.3 ± 3.7
18	0	1	1	57.14 ± 2.2	161.2 ± 7.0
19	1	-1	-1	36.66 ± 1.2	143.7 ± 3.8
20	1	-1	0	43.18 ± 1.0	149.4 ± 4.1
21	1	-1	1	39.11 ± 1.1	163.4 ± 5.2
22	1	0	-1	49.03 ± 2.7	136.4 ± 3.5
23	1	0	0	52.53 ± 2.3	151.5 ± 4.1
24	1	0	1	46.35 ± 1.0	166.3 ± 6.1
25	1	1	-1	61.65 ± 2.6	153.7 ± 4.4
26	1	1	0	59.7 ± 1.7	165.9 ± 3.5
27	1	1	1	54.32 ± 1.8	180.1 ± 6.8

*values are represented as mean ± s.d.

equations (equation 11 and 12, for PDE and PS respectively) were obtained following MRA of PDE and PS. Based on their p-value, it implied that the quadratic main effects of

Table 4.6 Model coefficients estimated by multiple regression analysis for PDE of ATZ loaded PLGA NPs

Factor	Coefficients	t Stat	p-value
Intercept	51.08	38.9531	< 0.0001*
X_1	0.69	1.1331	0.2731
X_2	8.11	13.3695	< 0.0001*
X_3	-0.87	-1.4716	0.1703
X_1X_2	0.64	0.8632	0.4000
X_1X_3	-0.32	-0.3639	0.6697
X_2X_3	-0.67	-0.8968	0.3823
X_1^2	-2.32	-2.2057	0.0421*
X_2^2	-0.86	-0.8154	0.4260
X_3^2	0.44	0.4227	0.6776
$X_1X_2X_3$	-1.51	-1.6571	0.1164

* Significant at $p < 0.05$

Table 4.7 Model coefficients estimated by multiple regression analysis for PS of ATZ loaded PLGA NPs

Factor	Coefficients	t Stat	p-value
Intercept	137.62	60.5771	< 0.0001*
X_1	1.53	1.4585	0.1477
X_2	10.22	9.7162	< 0.0001*
X_3	10.41	9.9540	< 0.0001*
X_1X_2	-1.46	-1.1367	0.2530
X_1X_3	2.05	1.1145	0.1159
X_2X_3	1.05	0.8120	0.4095
X_1^2	15.37	8.4394	< 0.0001*
X_2^2	3.91	2.1444	0.0399*
X_3^2	-0.74	-0.4075	0.6765
$X_1X_2X_3$	1.01	0.6379	0.5153

* Significant at $p < 0.05$

the ATZ loaded PLGA NPs by nanoprecipitation method. The small values of coefficients were not-significant ($p>0.05$) and hence neglected from the FM. Reduced polynomial

polymer concentration in organic phase (X_2) was significant for both PDE and PS, and surfactant concentration in aqueous phase (X_3) for PS only. The second order main effects of drug:polymer ratio (X_1) for PDE, and drug:polymer ratio (X_1) and polymer concentration in organic phase (X_2) for PS were found to be significant, as is evident from their p-values. The interactions between X_1X_2, X_2X_3, X_1X_3 and $X_1X_2X_3$ were not found to be significant for both PDE and PS from their p-values (table 4.6 and 4.7). The results of ANOVA of the second order polynomial equation of PDE and PS are given in table 4.8 and 4.9 respectively. Since the calculated F value was less than the tabulated F value for PDE and for PS [Bolton 1997], it was concluded that the neglected terms did not significantly contribute in the prediction of PDE and PS. Hence, F-Statistic of the results of ANOVA of full and reduced model justified the omission of non-significant terms of equation 9 and 10.

Table 4.8 ANOVA of full and reduced models for PDE of ATZ loaded PLGA NPs

		df	SS	MS	F	R	R^2	Adjusted R^2
Regression	FM	10	1274.7	127.5	19.22	0.9608	0.9231	0.8751
	RM	2	1217.6	608.8	89.53	0.9390	0.8818	0.8719
Residual	FM	16	106.1	6.6				
	RM	24	163.2	6.8				

SSE2 - SSE1 =163.201 - 106.106 = 57.0958

No. of parameters omitted = 8

MS of error (full model) = 6.6316

F calculated = (SSE2 - SSE1 / No. of parameters omitted) / MS of error (FM)

= (57.0958 / 8) / 6.6318 = 1.0761

F tabulated = 2.59

Table 4.9 ANOVA of full and reduced models for PS of ATZ loaded PLGA NPs

		df	SS	MS	F	R	R^2	Adjusted R^2
Regression	FM	10	5456.9	545.7	27.41	0.9720	0.9448	0.9104
	RM	4	5339.6	1334.9	67.38	0.9615	0.9245	0.9108
Residual	FM	16	318.5	19.9				
	RM	22	435.9	19.8				

SSE2 - SSE1 = 435.872 - 318.535 = 117.337

No. of parameters omitted = 6

MS of error (full model) = 19.908

F calculated = (SSE2 - SSE1 / No. of parameters omitted) / MS of error (FM)

= (117.337 / 6) / 19.908 = 0.9823

F tabulated = 2.74

When the coefficients of the three independent variables in equation 9 and 10 were compared, the value for the variable X_2 (b_1 = 8.12 for PDE and b_1 = 10.22 for PS) was found to be maximum and hence X_2 was considered to be a major contributing variable affecting the PDE and PS of the NPs. The Fisher F test with a very low probability value ($P_{model} > F = 0.000001$) demonstrated a very high significance for the regression model. The goodness of fit of the model was checked by the determination coefficient (R^2). In this case, the values of the determination coefficients (R^2 = 0.9232 and 0.9448 for FM and 0.8818 and 0.9245 for RM for PDE and PS respectively) indicated that over 88% of the total variations were explained by the model. High R^2 values of FM as compared to RM were due to the large number of factors included. More the number of factors more is the R^2 value [Montgomery 2004]. The values of adjusted R^2 (0.8751 and 0.9104 for FM and 0.8719 and 0.9108 for RM for PDE and PS respectively) were similar for FM and RM for both PDE and PS, indicating the suitability of reducing the model. Moreover, the high values of correlation coefficients (R = 0.9608 and 0.9720 for FM and 0.9390 and 0.9615 for RM for PDE and PS respectively) signifies an excellent correlation between the independent variables [Box et al. 1978]. All the above considerations indicated an excellent adequacy of the developed regression model [Adinarayana and Ellaiah 2002; Akhnazarova 1982; Box et al. 1978; Yee and Blanch 1993].

4.11.2.1 Contour plots

Contour plots were established between X_1 vs X_2, X_1 vs X_3 and X_2 vs X_3 at fixed level (- 1) of third variable as shown in figure 4.9 and 4.10 for each PDE and PS respectively. The plots showed that PDE was greatly dependent on drug:polymer ratio and polymer concentration (figure 4.9A). When both these variables were at their maximum levels, PDE was found to be maximum. However, the contour of drug:polymer ratio vs surfactant concentration (figure 4.9B) showed PDE between 40 to 42.5% in the whole range (-1 to 1) of both variables indicating negligible interaction between them. PDE was found to increase linearly with increase in polymer concentration (figure 4.9C). Also, the parallel lines of the contour plot with respect to X_1 implies that the surfactant

concentration in aqueous phase has negligible influence on PDE at constant levels of X_2 and X_3.Lowest PS of about 120 nm was observed at -1 level of polymer and surfactant concentration and 0 level of drug:polymer ratio (figure 4.10A). Relationship between drug:polymer ratio vs surfactant concentration was found to be non-linear (figure 4.10B). PS was found to show maximum variation at low level (-1) of drug:polymer ratio. It increased from 135 to 175 nm linearly with increase in both the variables i.e., polymer and surfactant concentration (figure 4.10C). It was concluded from the contours that low concentration of surfactant but high concentration of PLGA and high drug:polymer ratio was required for highest PDE and lowest PS in preparation of ATZ loaded PLGA NPs.

4.11.2.2 Response surface plots

Response surface plots, which are very helpful in learning about both the main and interaction effects of the independent variables, were plotted between X_1 vs X_2, X_1 vs X_3 and X_2 vs X_3 at fixed level (- 1) of third variable as shown in figure 4.11 and 4.12 for each PDE and PS respectively. PDE was not significantly affected when drug:polymer ratio was varied alone, but was increased upon simultaneous increase in drug:polymer ratio with polymer concentration (figure 4.11A). However, PDE was unaffected by simultaneous variation of X_1 and X_3. This may be because, increase in PDE due to increase in drug:polymer ratio was negated by increase in surfactant concentration (figure 4.11B). PDE was found to increase linearly with increase in polymer concentration, but no significant change was observed when surfactant concentration was varied. When both the variables were increased from -1 to 1 level, PDE increased linearly (figure 4.11C).

Response surface plot of drug:polymer ratio vs polymer concentration showed non-linear behaviour (figure 4.12A). With decrease in drug:polymer ratio from 1 to 0 level, PS first decreased and then increased. Response surface plot between drug:polymer ratio and surfactant concentration showed almost similar trends as observed in surface plot between drug:polymer ratio vs polymer concentration (figure 4.12B). Plot between polymer concentration and surfactant concentration showed linear relationship, with both the variables showing positive effect on PS, as simultaneous increase in levels of both the variables resulted into increase in PS (figure 4.12C).

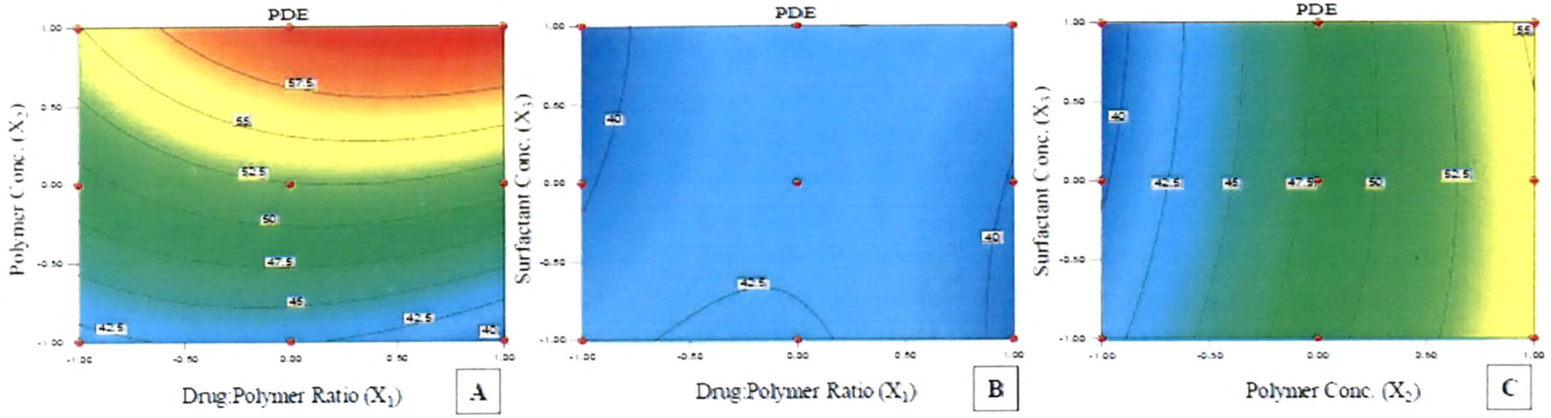

Figure 4.9 Contour plots showing effect of (A) X_1 vs X_2 (at -1 level of X_3), (B) X_1 vs X_3 (at -1 level of X_2) and (C) X_2 vs X_3 (at -1 level of X_1) on PDE of ATZ loaded PLGA NPs.

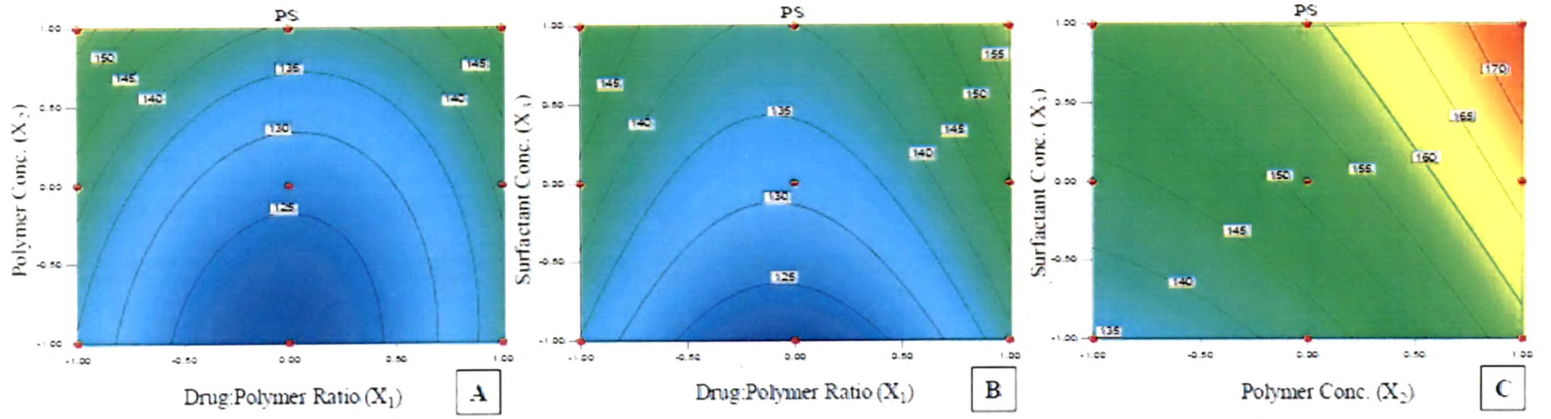

Figure 4.10 Contour plots showing effect of (A) X_1 vs X_2 (at -1 level of X_3), (B) X_1 vs X_3 (at -1 level of X_2) and (C) X_2 vs X_3 (at -1 level of X_1) on PS of ATZ loaded PLGA NPs.

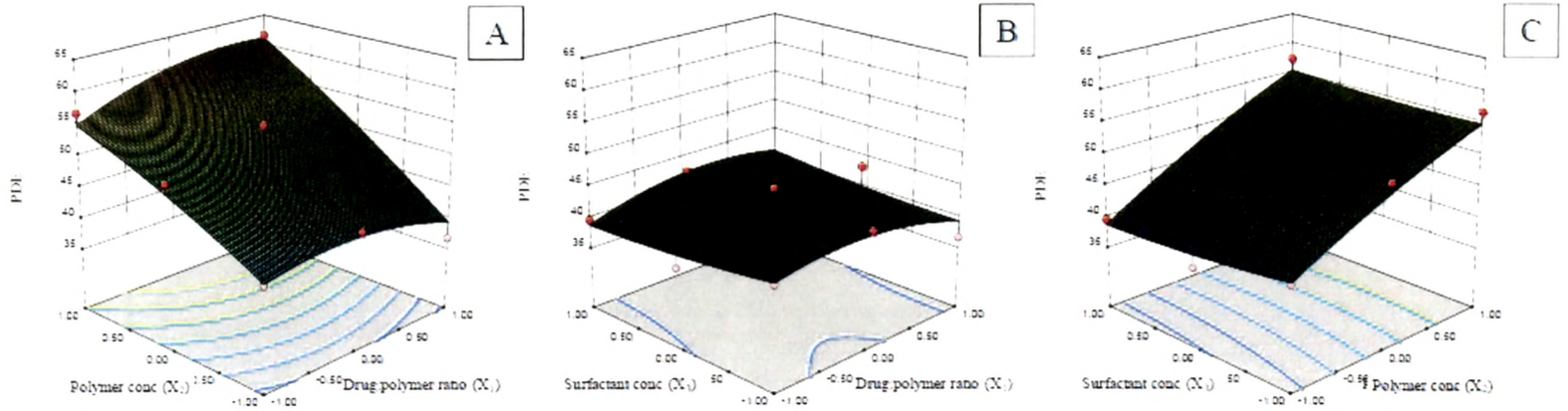

Figure 4.11 Response surface plot showing effect of (A) X_1 vs X_2 (at -1 level of X_3), (B) X_1 vs X_3 (at -1 level of X_2) and (C) X_2 vs X_3 (at -1 level of X_1) on PDE of ATZ loaded PLGA NPs.

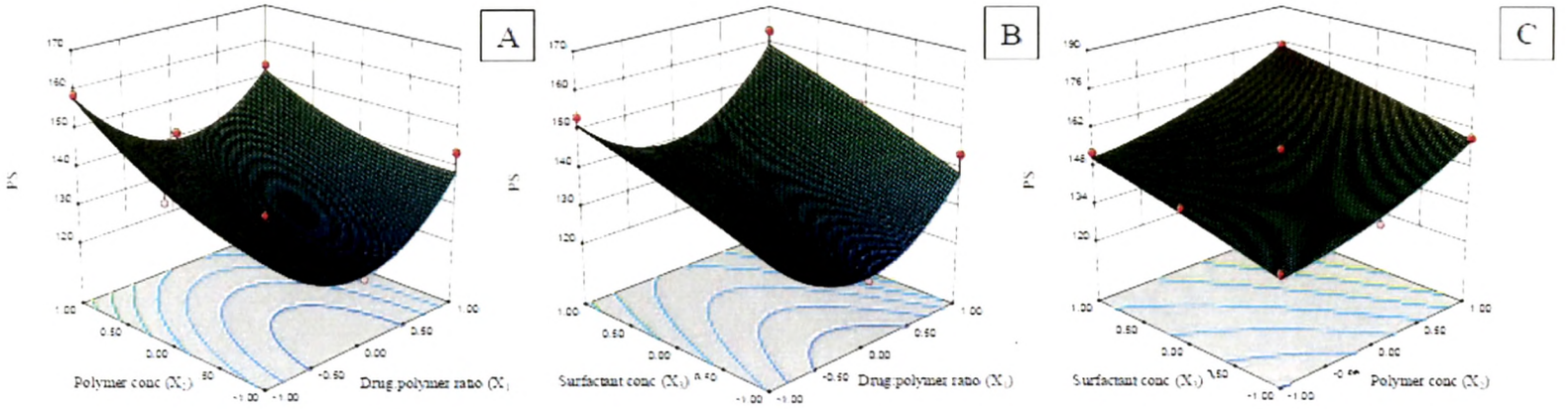

Figure 4.12 Response surface plot showing effect of (A) X_1 vs X_2 (at -1 level of X_3), (B) X_1 vs X_3 (at -1 level of X_2) and (C) X_2 vs X_3 (at -1 level of X_1) on PS of ATZ loaded PLGA NPs.

4.11.2.3 Desirability criteria

From the results, the optimum levels of independent variables were screened by multiple regression analysis. Since PDE and PS were taken into consideration simultaneously, the batch with smallest PS of 120 nm exhibited only 42.5% PDE (at X_1 = 0, X_2 = -0.6 to -1.0, X_3 = -0.6 to -1.0) while that with highest PDE of 60% produced particle size of 155 nm (at X_1 = 1, X_2 = 0.6 to 1.0, X_3 = -0.4 to -1.0). Hence, desirability criteria obtained using Design Expert software (version 8.0.3) was used to find out optimized formulation parameters. Our criteria included maximum PDE and PS not more than 200 nm. The optimum formulation offered by the software based on desirability was found at 0.68, 1, and -1 level of X_1, X_2 and X_3 respectively. The results of dependent variables from the software were found to be 61.39% for PDE and 144.68 nm for PS (figure 4.13) at these levels which is as per our desired criteria. The calculated desirability factor for offered formulations was 0.990, which was near to 1 and indicates suitability of the designed factorial model.

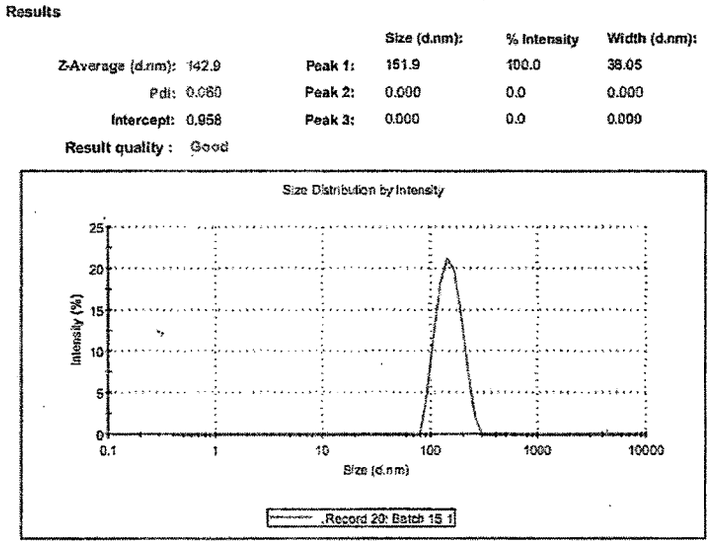

Figure 4.13 Particle size distribution of ATZ loaded PLGA NPs

4.11.2.4 Checkpoint analysis and normalized error

Three batches were prepared for check point analysis and results of both PDE and PS (table 4.10) indicated that the measured response was more accurately predicted by regression analysis which was proven by lower NE value of regression analysis (0.07022 for PDE and 0.04754 for PS). Data analysis using student's t test revealed that

there was no statistically significant difference ($p<0.05$) between experimentally obtained values and predicted values by MRA.

Table 4.10 Check point analysis, t test analysis and normalized error determination

Checkpoint batches with their predicted and measured values of PDE and PS							
Batch No.	X_1	X_2	X_3	PDE		PS	
				Observed	Predicted	Observed	Predicted
1	-1 (1:10)	0.7 (92.5 mg)	0.1 (52.5 mg)	52.74	54.163	161.4	162.609
2	0 (1:15)	-0.8 (55 mg)	0.8 (70 mg)	42.88	44.309	134.6	139.782
3	1 (1:20)	-0.3 (67.5 mg)	-0.5 (37.5 mg)	48.76	46.048	140.8	144.583
$t_{calculated}$				0.97608		0.10031	
$t_{tabulated}$				2.9199		2.9199	
Normalized Error				0.070229		0.04754	

4.11.3 Lyophilization and optimization of cryoprotectants

In this study, different cryoprotectants (trehalose, sucrose and mannitol) were used in different ratios (1:1, 1:2, 1:3, 1:4) and PS was recorded as shown in table 4.11. Initial PS

Table 4.11 Effect of cryoprotectants and their concentration on PS of lyophilized NPs after re-dispersion in distilled water

Cryoprotectant	Ratio	Final Avg. PS (nm)	S_f/S_i
Trehalose	1:1	252.8	1.57*
	1:2	243.3	1.51*
	1:3	260.1	1.62*
	1:4	355.7	2.21
Sucrose	1:1	216.8	1.35*
	1:2	213.9	1.33*
	1:3	233.3	1.45*
	1:4	250.3	1.56
Mannitol	1:1	239.1	1.49
	1:2	304.7	1.89
	1:3	278	1.73
	1:4	277.1	1.72

*indicates good re-dispersibility

of NPs was found to be 160.9 nm. The ratio of PS (after lyophilization, S_f and before lyophilization, S_i) was found to be lowest (1.33) for sucrose in 1:2 ratio. Trehalose also showed less increase in PS after re-dispersion (S_f/S_i ratio of 1.51). Batches prepared with trehalose and sucrose at 1:1, 1:2 and 1:3 ratio showed good re-dispersibility with PDI less than 0.2. PDI is a measure of dispersion homogeneity and usually ranges from 0 to 1. Values close to 0 indicate a homogeneous dispersion while those greater than 0.3 indicate high heterogeneity [Ahlin et al. 2002].

4.12Formulation and optimization of ATZ loaded cPCL NPs

4.12.1 Preliminary optimization of ATZ loaded cPCL NPs

4.12.1.1 Selection of organic solvent

Three different organic solvents (acetone, acetonitrile and tetrahydrofuran) were used for preparation of cPCL NPs (table 4.12). NPs formulated using acetone showed PDE of 49.63 ± 1.15% with PS of 138.2 ± 4.9 nm while NPs formulated using acetonitrile were of low PDE and PS. PDE was again decreased when tetrahydrofuran was used as solvent with no significant change in PS. Hence, acetone was selected for further studies.

Table 4.12 Selection of organic phase in preliminary optimization of ATZ loaded cPCL NPs

Solvents	PDE (%)	PS (nm)
Acetone	49.63 ± 1.15	138.2 ± 4.9
Acetonitrile	43.45 ± 1.64	130.6 ± 4.6
Tetra hydro furan	44.67 ± 1.12	150.6 ± 6.7

4.12.1.2 Selection of volume of organic solvent

Different volumes of organic solvent (acetone) were used to dissolve polymer (50 mg) and results are represented in table 4.13. It was observed that as the volume of organic

Table 4.13 Selection of volume of organic solvent in preliminary optimization of ATZ loaded cPCL NPs

Volume of organic solvent	PDE (%)	PS (nm)
3 ml	56.35 ± 1.82	235.2 ± 7.1
4 ml	53.68 ± 1.12	205.4 ± 4.7
5 ml	55.38 ± 2.23	190.6 ± 5.1

solvent was increased, PS decreases significantly with no major change in PDE. This was possibly due to decreased viscosity of organic phase with increase in volume of organic solvent which can easily dispersed in aqueous phase containing surfactant. Hence, 5 ml of acetone was selected as organic phase.

4.12.1.3 Selection of surfactant

Three different surfactants were initially used for formulation development namely Pluronic F-68® (P188), Pluronic F-127® (P127) and Poly vinyl alcohol (PVA) (table 4.14). Out of these, better one is selected based on resultant PDE and PS. With constant level of surfactant concentration (0.5%) for all three surfactants, PDE was found to be highest when PVA was used, but at the same time PS was found to be of larger size (332.4 ± 7.6 nm). No significant difference in PS was observed when P188 or P127 was used, but PDE was higher when P188 was used. Hence, P188 was used in further studies.

Table 4.14 Selection of surfactant in preliminary optimization of ATZ loaded cPCL NPs

Surfactant	PDE (%)	PS (nm)
P188	52.45 ± 0.42	175.9 ± 2.4
P127	50.6 ± 0.96	170.1 ± 3.9
PVA	54.36 ± 1.05	404.1 ± 8.63

4.12.2 Optimization of ATZ loaded cPCL NPs using 3^3 factorial design

Twenty seven batches of ATZ loaded cPCL NPs were prepared by using 3^3 factorial design varying three independent variables, drug:polymer ratio (X_1), polymer concentration in organic phase (X_2) and surfactant concentration in aqueous phase (X_3) (Table 4.15). The PDE and PS were taken as dependent variables and the results were recorded (Table 4.16). The main effects of X_1, X_2 and X_3 represent the average result of changing one variable at a time from its low to high value. The interactions (X_1X_2, X_1X_3, X_2X_3 and $X_1X_2X_3$) show how the PDE and PS changes when two or more variables were simultaneously changed. The values for the twenty seven batches showed a wide variation from 39.4 ± 1.9 to 72.5 ± 1.7% and 138.2 ± 4.9 to 241.6 ± 3.1 nm for PDE and PS respectively (Table 4.16). This is reflected by the wide range of coefficients of the terms of equation 3 representing the individual and combined variables.

Table 4.15 Coded values of the formulation parameters of ATZ loaded cPCL NPs

Coded Values	Actual values of dependent variables		
	X_1	X_2	X_3
-1	1 : 10	0.50 %	0.25 %
0	1 : 15	0.75 %	0.50 %
1	1 : 20	1.0 %	0.75 %

X_1 Drug:polymer ratio
X_2 Polymer concentration (% w/v)
X_3 Surfactant concentration (% w/v)

$$Y_1 = 55.92 + 6.23\ X_1 + 4.34\ X_2 - 4.33\ X_3 - 0.53\ X_1X_2 + 0.04\ X_1X_3 - 0.34\ X_2X_3 + 0.70\ X_1^2 - 0.32\ X_2^2 + 0.25\ X_3^2 - 0.44\ X_1X_2X_3 \quad (13)$$

$$Y_2 = 192.82 + 17.29\ X_1 + 16.31\ X_2 + 17.69\ X_3 - 0.7\ X_1X_2 + 0.32\ X_1X_3 + 0.50\ X_2X_3 + 1.03\ X_1^2 + 2.02\ X_2^2 - 4.19\ X_3^2 + 1.11\ X_1X_2X_3 \quad (14)$$

$$Y_1 = 56.34 + 6.23\ X_1 + 4.34\ X_2 - 4.33\ X_3 \quad (15)$$

$$Y_2 = 194.86 + 17.29\ X_1 + 16.31\ X_2 + 17.65\ X_3 - 4.19\ X_3^2 \quad (16)$$

The significance of each coefficient of equation 13 and 14 were determined by student's 't' test and p-value, which are listed in table 4.17 and 4.18 respectively. The larger the magnitude of the 't' value and the smaller the p-value, the more significant is the corresponding coefficient [Adinarayana and Ellaiah 2002; Akhnazarova 1982]. Small values of the coefficients of the terms X_1^2, X_2^2, X_3^2, X_1X_2, X_2X_3, X_1X_3, and $X_1X_2X_3$ in equation 13 and X_1^2, X_2^2, X_1X_2, X_2X_3, X_1X_3, and $X_1X_2X_3$ in equation 14 for PDE and PS respectively implied that all these terms were least contributing in the preparation of the ATZ loaded cPCL NPs.

The small values of coefficients were not-significant ($p>0.05$) and hence neglected from the FM. Reduced polynomial equations (equation 15 and 16, for PDE and PS resp.) were obtained following MRA of PDE and PS. Based on their p-value, it implied that the second order effects of drug:polymer ratio (X_1) and polymer concentration in organic phase (X_2) were not found to be significant for both PDE and PS. The interactions between X_1X_2, X_2X_3, X_1X_3 and $X_1X_2X_3$ were also not found to be significant for both PDE and PS as evident from their p-values (p-values>0.05 in all cases) (table 4.17 and 4.18).

Table 4.16 Layout of 3^3 full factorial design for ATZ loaded cPCL NPs

Sr. No.	X_1	X_2	X_3	Y_1* (PDE, in %)	Y_2* (PS, in nm)
1	-1	-1	-1	49.6 ± 1.15	138.2 ± 4.9
2	-1	-1	0	44.2 ± 1.87	164.6 ± 6.6
3	-1	-1	1	39.4 ± 1.89	178.0 ± 3.6
4	-1	0	-1	55.3 ± 1.18	157.1 ± 1.9
5	-1	0	0	52.5 ± 0.42	175.9 ± 2.4
6	-1	0	1	47.7 ± 1.76	187.9 ± 2.5
7	-1	1	-1	59.4 ± 0.6	174.8 ± 2.5
8	-1	1	0	54.3 ± 1.43	191.7 ± 4.7
9	-1	1	1	50.8 ± 0.96	207.8 ± 2.9
10	0	-1	-1	56.2 ± 2.35	156.3 ± 4.6
11	0	-1	0	51.9 ± 1.8	175.1 ± 4.3
12	0	-1	1	48.34 ± 1.72	188.6 ± 4.5
13	0	0	-1	60.7 ± 0.92	170.3 ± 1.2
14	0	0	0	5.1.4 ± 2.2	190.6 ± 5.1
15	0	0	1	52. ± 2.3	206.3 ± 5.7
16	0	1	-1	65.63 ± 2.08	188.5 ± 2.8
17	0	1	0	58.82 ± 0.79	215.2 ± 3.6
18	0	1	1	53.99 ± 1.28	231.5 ± 3.8
19	1	-1	-1	62.94 ± 2.10	175.9 ± 2.9
20	1	-1	0	59.3 ± 1.68	200.3 ± 5.9
21	1	-1	1	55.17 ± 1.78	210.7 ± 3.9
22	1	0	-1	64.72 ± 3.10	191.1 ± 6.7
23	1	0	0	62.31 ± 3.07	214.8 ± 4.4
24	1	0	1	58.53 ± 3.45	222.5 ± 2.7
25	1	1	-1	72.49 ± 1.71	204.8 ± 4.3
26	1	1	0	66.88 ± 1.45	225.5 ± 2.7
27	1	1	1	62.85 ± 0.51	241.6 ± 3.1

*values are represented as mean ± s.d.

The results of ANOVA of the second order polynomial equation of PDE and PS are given in table 4.19 and 4.20 respectively. Since the calculated F value was less than the

Table 4.17 Model coefficients estimated by multiple regression analysis for PDE of ATZ loaded cPCL NPs.

Factor	Coefficients	t Stat	p-value
Intercept	55.92	83.798	< 0.0001*
X_1	6.23	20.165	< 0.0001*
X_2	4.34	14.042	< 0.0001*
X_3	-4.33	-13.863	< 0.0001*
X_1^2	0.70	1.306	0.2098
X_2^2	-0.32	-0.608	0.5519
X_3^2	0.25	0.469	0.6449
X_1X_2	-0.53	-1.408	0.1782
X_1X_3	0.04	0.089	0.9302
X_2X_3	-0.34	-0.892	0.3855
$X_1X_2X_3$	-0.44	-0.946	0.3580

* Significant at $p < 0.05$

Table 4.18 Model coefficients estimated by multiple regression analysis for PS of ATZ loaded cPCL NPs

Factor	Coefficients	t Stat	p-value
Intercept	192.82	115.068	< 0.0001*
X_1	17.29	22.293	< 0.0001*
X_2	16.31	21.025	< 0.0001*
X_3	17.69	22.547	< 0.0001*
X_1^2	1.03	0.769	0.453
X_2^2	2.02	1.501	0.153
X_3^2	-4.19	-3.118	0.0066*
X_1X_2	-0.7	-0.737	0.472
X_1X_3	0.32	0.305	0.764
X_2X_3	0.49	0.523	0.608
$X_1X_2X_3$	1.11	0.956	0.353

* Significant at $p < 0.05$

tabulated F value for PDE and for PS [Bolton 1997], it was concluded that the neglected terms did not significantly contribute in the prediction of PDE and PS. Hence, F-Statistic

of the results of ANOVA of full and reduced model justified the omission of non-significant terms of equation 9 and 10.

Table 4.19 ANOVA of full and reduced models for PDE of ATZ loaded cPCL NPs

		df	SS	MS	F	R	R^2	Adjusted R^2
Regression	FM	10	1385.7	138.6	80.7	0.9902	0.9805	0.9684
	RM	3	1375.4	458.5	279.3	0.9865	0.9733	0.9698
Residual	FM	16	27.5	1.71				
	RM	23	37.8	1.64				

SSE2 - SSE1 = 37.8 - 27.5 = 10.3

No. of parameters omitted = 7

MS of error (full model) = 1.71

F calculated = (SSE2 - SSE1 / No. of parameters omitted) / MS of error (FM)

= (10.3 / 7) / 1.71

= 0.8605

F tabulated = 2.6572

Table 4.20 ANOVA of full and reduced models for PS of ATZ loaded cPCL NPs

		df	SS	MS	F	R	R^2	Adjusted R^2
Regression	FM	10	15934.9	1593.5	147.1	0.9946	0.9892	0.9825
	RM	4	15884.3	3971.1	390.3	0.9930	0.9861	0.9836
Residual	FM	16	173.3	10.83				
	RM	22	223.9	10.18				

SSE2 - SSE1 = 223.9 - 173.3 = 50.6

No. of parameters omitted = 6

MS of error (full model) = 10.83

F calculated = (SSE2 - SSE1 / No. of parameters omitted) / MS of error (FM)

= (50.6 / 6) / 10.83

= 0.7787

F tabulated = 2.7413

When the coefficients of the three independent variables in equation 13 and 14 were compared, the value for the variable X_1 (b_1 = 6.23) for PDE and X_3 (b_3 = 17.69) for PS was considered to be a major contributing variable affecting the PDE and PS of the NPs. The Fisher F test with a very low probability value ($P_{model} > F = 0.000001$) demonstrated

a very high significance for the regression model. The goodness of fit of the model was checked by the determination coefficient (R^2). In this case, the values of the determination coefficients (R^2 = 0.9805 and 0.9892 for FM and 0.9733 and 0.9861 for RM for PDE and PS respectively) indicated that over 97% of the total variations were explained by the model. High R^2 values of FM as compared to RM were due to the large number of factors included. R^2 value is more if the number of factors are more [Montgomery 2004]. The values of adjusted R^2 (0.9684 and 0.9825 for FM and 0.9698 and 0.9836 for RM for PDE and PS respectively) were similar for FM and RM for both PDE and PS, indicating the suitability of reducing the model. Moreover, the high values of correlation coefficients (R = 0.9902 and 0.9946 for FM and 0.9865 and 0.9930 for RM for PDE and PS respectively) signifies an excellent correlation between the independent variables [Box et al. 1978]. All the above considerations indicated an excellent adequacy of the developed regression model [Adinarayana and Ellaiah 2002; Akhnazarova 1982; Box et al. 1978; Yee and Blanch 1993].

4.12.2.1 Contour plots

Contour plots were established between X_1 vs X_2, X_1 vs X_3 and X_2 vs X_3 at fixed level (-1) of third variable as shown in figure 4.14 and 4.15 for PDE and PS respectively. The plots showed that PDE was greatly dependent on drug:polymer ratio and polymer concentration (figure 4.14A). When both these variables were at their maximum levels, PDE was found to be maximum (>65%). However, the contour of drug:polymer ratio vs surfactant concentration (figure 4.14B) showed increase in PDE with increase in drug:polymer ratio and decrease in surfactant conc. PDE was found to increase linearly with increase in polymer concentration and simultaneous decrease in surfactant conc. (figure 4.14C). Also, the parallel lines in all the three contour plots implies the linear increase or decrease in PDE with change in any two independent variables at constant level of third variable. PS was found to increase with increase in both drug:polymer ratio and polymer conc. (figure 4.15A) and was maximum at +1 level of X_1 and X_2 at 0 level of X_3. Similar observations were observed when counter of drug:polymer ratio was plotted with surfactant conc. at fixed level (-1) of polymer conc. PS was found to increase with simultaneous increase in both the variables (figure 4.15B). Lowest PS of about 160 nm was observed at -1 level of polymer and surfactant concentration and 0 level of drug:polymer ratio (figure 4.15C). PS was found to be maximum at high level

(+1) of polymer conc. and high level of surfactant conc. It increased from 160 to 220 nm linearly with increase in both the variables i.e., polymer and surfactant concentration (figure 4.15C). It was concluded from the contours that NPs with smallest PS can be prepared at low levels (-1) of all the three variables.

4.12.2.2 Response surface plots

Three dimensional response surface plots are very helpful in learning about both the main and interaction effects of the independent variables. These were plotted between X_1 vs X_2, X_1 vs X_3 and X_2 vs X_3 at fixed level (-1) of third variable as shown in figure 4.16 and 4.17 for each PDE and PS respectively. PDE was not significantly affected when polymer conc. was varied alone, but was increased upon simultaneous increase in drug:polymer ratio with polymer concentration showing interactive effect between the two variables (figure 4.16A). However, PDE was found to increase with decrease in surfactant conc. and increase in drug:polymer ratio and found to be highest at -1 level of X_3 and +1 level of X_1 (figure 4.16B). Similar trend was observed in response surface plot of polymer conc. and surfactant conc. (figure 4.16C). It can be concluded from the response surface plots that increase in drug:polymer ratio and polymer conc. increases PDE, whereas increase in surfactant conc. causes decrease in PDE. Response surface plot of drug:polymer ratio vs polymer concentration showed increase in PS with increase in drug:polymer ratio and increase in polymer conc. possibly due to increased viscosity of organic phase with increase in polymer conc. (figure 4.17A). Response surface plot of drug:polymer ratio and surfactant conc. also showed similar trends and NPs of the PS more than 220 nm was formed at +1 level of both the variables at 0 level of polymer conc. (figure 4.17B). Interaction effect of polymer conc. and surfactant conc. showed increase in PS with increase in both the variables (figure 4.17C).

4.12.2.3 Desirability criteria

From the results, the optimum levels of independent variables were screened by multiple regression analysis. Since PDE and PS were taken into consideration simultaneously, the batch with smallest particle size of 138.2 ± 4.9 nm exhibited only 49.63 ± 1.15% PDE while that with highest PDE of 72.49 ± 1.71% produced particle size of 204.8 ± 4.3 nm (at X_1 = 1, X_2 = 0.6 to 1.0, X_3 = -0.4 to -1.0). Hence, desirability criteria obtained using Design Expert software (version 8.0.3) was used to find out optimized formulation parameters. Our criteria included maximum PDE and PS not more

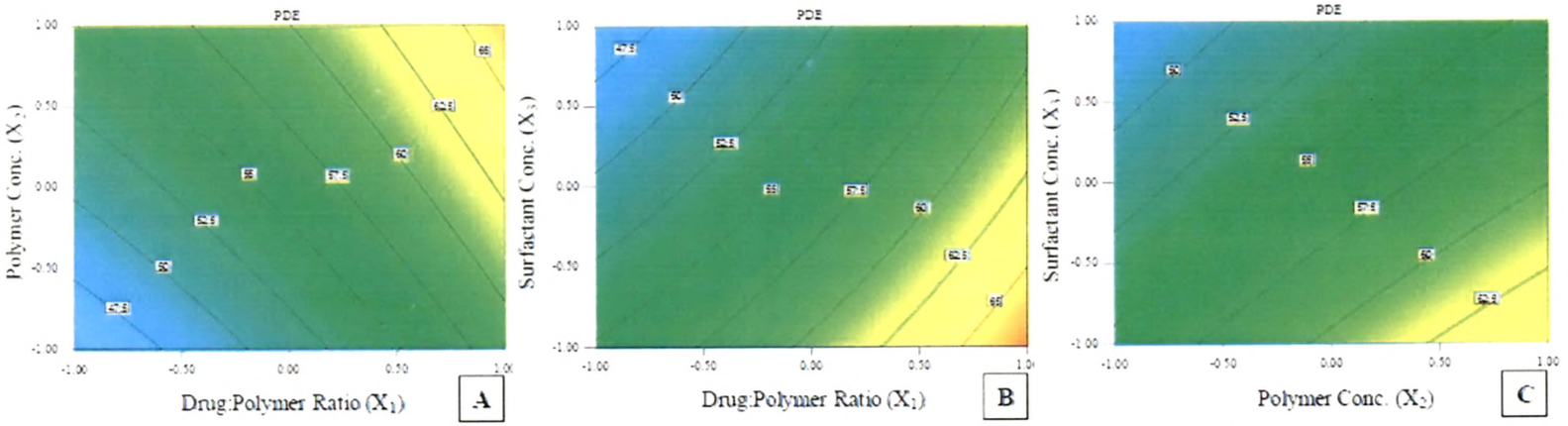

Figure 4.14 Contour plots showing effect of (A) X_1 vs X_2 (at -1 level of X_3), (B) X_1 vs X_3 (at -1 level of X_2) and (C) X_2 vs X_3 (at -1 level of X_1) on PDE of ATZ loaded cPCL NPs.

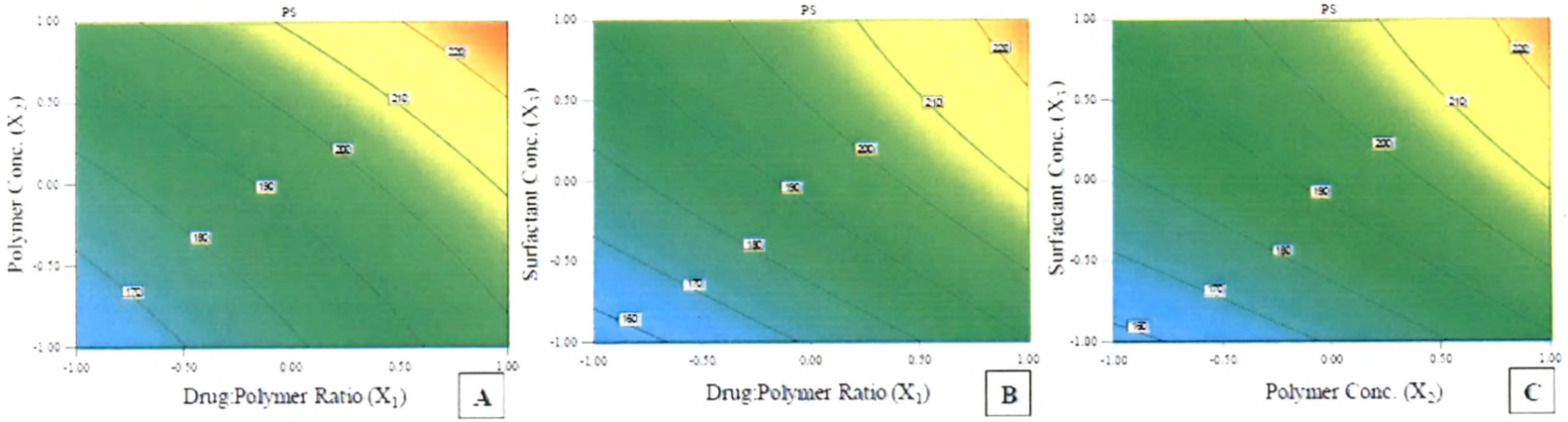

Figure 4.15 Contour plots showing effect of (A) X_1 vs X_2 (at -1 level of X_3), (B) X_1 vs X_3 (at -1 level of X_2) and (C) X_2 vs X_3 (at -1 level of X_1) on PS of ATZ loaded cPCL NPs.

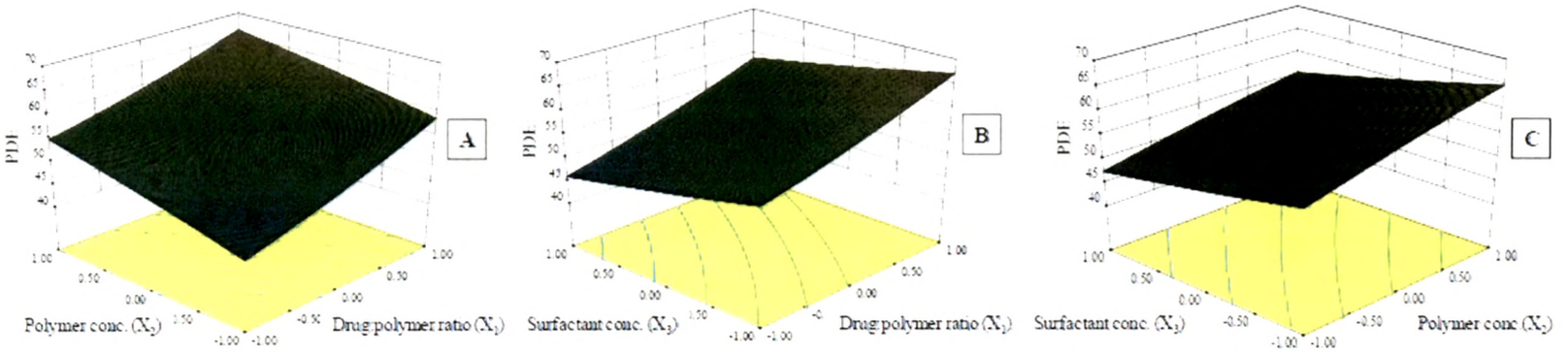

Figure 4.16 Response surface plot showing effect of (A) X_1 vs X_2 (at -1 level of X_3), (B) X_1 vs X_3 (at -1 level of X_2) and (C) X_2 vs X_3 (at -1 level of X_1) on PDE of ATZ loaded cPCL NPs.

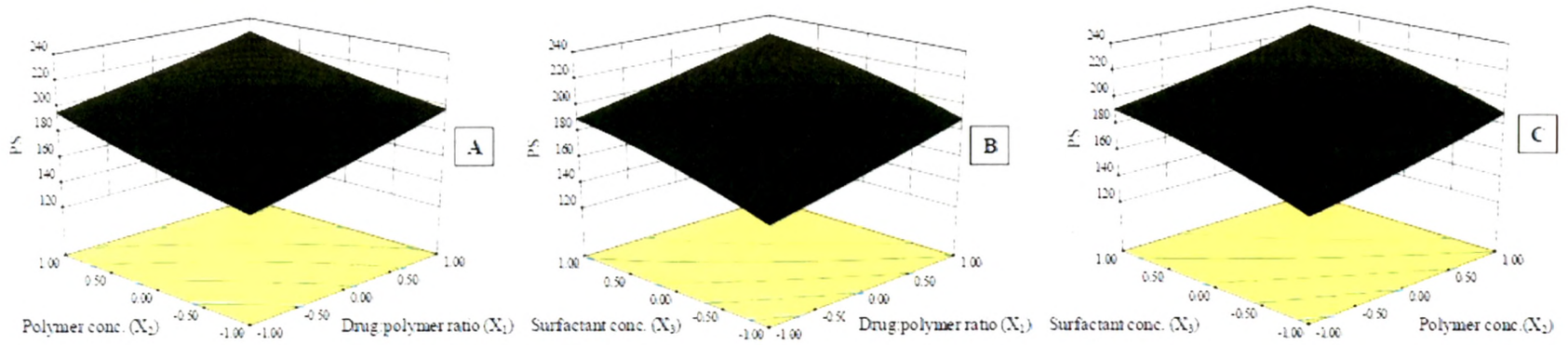

Figure 4.17 Response surface plot showing effect of (A) X_1 vs X_2 (at -1 level of X_3), (B) X_1 vs X_3 (at -1 level of X_2) and (C) X_2 vs X_3 (at -1 level of X_1) on PS of ATZ loaded cPCL NPs.

than 200 nm. The optimum formulation offered by the software based on desirability was found at 1.0, 0.69, and -1.0 level of X_1, X_2 and X_3 respectively. The results of dependent variables from the software were found to be 70.21% for PDE and 200 nm for PS (figure 4.18) at these levels which is as per our desired criteria. The calculated desirability factor for offered formulations was 0.965, which was near to 1 and indicates suitability of the designed factorial model.

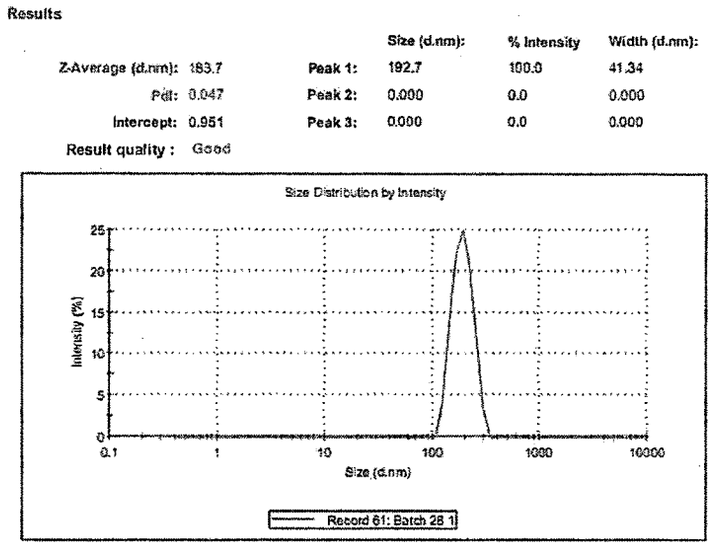

Figure 4.18 Particle size distribution of ATZ loaded cPCL NPs

4.12.2.4 Checkpoint analysis and normalized error

Table 4.21 Check point analysis, t test analysis and normalized error determination

Checkpoint batches with their predicted and measured values of PDE and PS							
Batch No.	X_1	X_2	X_3	PDE		PS	
				Observed (avg.)	Predicted	Observed (avg.)	Predicted
1	-1 (1:10)	-0.2 (92.5 mg)	0.1 (52.5 mg)	47.93	48.81	173.8	176.02
2	0 (1:15)	0.7 (55 mg)	-0.8 (70 mg)	63.51	62.84	192.9	189.47
3	1 (1:20)	-0.8 (67.5 mg)	-0.3 (37.5 mg)	59.58	60.39	195.4	193.43
		$t_{calculated}$		0.5681		0.024	
		$t_{tabulated}$		2.9199		2.9199	
		Normalized Error		0.0252		0.0431	

Three batches were prepared for check point analysis and results of both PDE and PS (table 4.21) indicated that the measured response was more accurately predicted by regression analysis which was proven by lower NE value of regression analysis (0.0252 for PDE and 0.0431 for PS). Data analysis using student's t test revealed that there was no statistically significant difference ($p<0.05$) between experimentally obtained values and predicted values by MRA.

4.12.3 Lyophilization and optimization of cryoprotectants

In this study, different cryoprotectants (trehalose, sucrose and mannitol) were used in different ratios (1:1, 1:2, 1:3, 1:4) and PS was recorded as shown in table 4.22. Initial PS of NPs was found to be 194.7 nm. The ratio of PS (after lyophilization, S_f and before lyophilization, S_i) was found to be lowest (1.24) for sucrose in 1:2 ratio. Trehalose also showed less increase in PS after re-dispersion (S_f/S_i ratio of 1.41). Batches prepared with trehalose and sucrose at 1:1 and 1:2 ratio showed good re-dispersibility with PDI less than 0.2. PDI is a measure of dispersion homogeneity and usually ranges from 0 to 1. Values close to 0 indicate a homogeneous dispersion while those greater than 0.3 indicate high heterogeneity [Ahlin et al. 2002].

Table 4.22 Effect of cryoprotectants and their concentration on PS of lyophilized NPs after re-dispersion in distilled water

Cryoprotectant	Ratio	Final Avg. PS (nm)	S_f/S_i
Trehalose	1:1	280.3	1.44*
	1:2	275.1	1.41*
	1:3	297.1	1.53
	1:4	342.1	1.76
Sucrose	1:1	254.9	1.31*
	1:2	241.5	1.24*
	1:3	272	1.40*
	1:4	302.3	1.55
Mannitol	1:1	282.9	1.45*
	1:2	326.1	1.67
	1:3	341.2	1.75
	1:4	332.8	1.71

*indicates good re-dispersibility

4.13 Formulation and optimization of EXE loaded PLGA NPs

4.13.1 Preliminary optimization of EXE loaded PLGA NPs

4.13.1.1 Selection of organic solvent

Three different organic solvents (acetone, acetonitrile and tetrahydrofuran) were used for preparation of PLGA NPs (table 4.23). NPs formulated using acetone showed PDE of 73.2 ± 2.0% with PS of 195.1 ± 3.6 nm while NPs formulated using acetonitrile were of low PDE and high PS. No significant change in PDE was observed when tetrahydrofuran was used as solvent with increase in PS. Hence, acetone was selected for further studies.

Table 4.23 Selection of organic phase in preliminary optimization of EXE loaded PLGA NPs

Solvents	PDE (%)	PS (nm)
Acetone	73.2 ± 2.0	195.1 ± 3.6
Acetonitrile	71.6 ± 1.3	211.3 ± 4.1
Tetra hydro furan	72.7 ± 1.1	245.7 ± 4.1

4.13.1.2 Selection of surfactant phase

Three different surfactants were initially used for formulation development namely Pluronic F-68® (P188), Pluronic F-127® (P127) and Poly vinyl alcohol (PVA) (table 4.24). Out of these, better one is selected based on resultant PDE and PS. With constant level of surfactant concentration (0.5%) for all three surfactants, no significant change in PDE was observed, but at the same time PS was found to be of larger size (229.8 ± 4.2 nm) using PVA as surfactant. No significant difference in PS was observed when P188 or P127 was used, but PDE was higher when P188 was used as surfactant. Hence, P188 was used in further studies.

Table 4.24 Selection of surfactant phase in preliminary optimization of EXE loaded PLGA NPs

Surfactant	PDE (%)	PS (nm)
P188	51.2 ± 2.0	203.7 ± 2.7
P127	50.7 ± 1.1	217.6 ± 5.4
PVA	51.6 ± 1.8	229.8 ± 4.2

4.13.1.3 Selection of surfactant concentration

Different concentrations (0.5, 1.0, 1.5%) of surfactant (P188) were used in aqueous phase and results are represented in table 4.25. It was observed that as the

concentration was increased, PS increases significantly with no major change in PDE (50.8 – 52.4%). This was possibly due to coating of surfactant on NPs after precipitation. Hence, 0.5% of P188 was selected as surfactant concentration.

Table 4.25 Selection of surfactant concentration in preliminary optimization of EXE loaded PLGA NPs

Surfactant concentration	PDE (%)	PS (nm)
0.5%	51.2 ± 2.0	203.7 ± 2.7
1.0%	50.8 ± 1.4	218.6 ± 4.1
1.5%	52.4 ± 1.5	240.1 ± 3.9

4.13.2 Optimization of EXE loaded PLGA NPs using BBD

Using BBD, thirteen batches of EXE loaded PLGA NPs were prepared with drug:polymer ratio (X_1), amount of polymer (X_2) and volume of organic phase (X_3) as three independent variables. Coded values and actual values of the three independent variables are represented in table 4.26. Batches prepared using BBD were evaluated for PDE and PS as the dependent variables and recorded in table 4.27.

Table 4.26 Coded values of the formulation parameters of EXE loaded PLGA NPs

Coded values	Actual values		
	X_1	X_2	X_3
-1	1 : 15	50 mg	6 ml
0	1 : 20	100 mg	8 ml
1	1 : 25	150 mg	10 ml

X_1 Drug:polymer ratio
X_2 Amount of polymer (mg)
X_3 Volume of organic phase

The obtained PDE and PS were subjected to multiple regression to yield second order polynomial equations (equation 17 and 18, for PDE and PS respectively). Linear coefficients (b_1, b_2 and b_3 of X_1, X_2 and X_3, respectively) represent extent of effect by changing individual variable. Positive or negative sign in equation against different coefficients indicate increase or decrease in individual dependent response. The value of coefficients against interactions terms (X_1X_2, X_1X_3 and X_2X_3) shows how the PDE and

Table 4.27 Box Behnken experimental design with measured responses for EXE loaded PLGA NPs

Sr. No.	Box Behnken experimental design with measured responses				
	X_1	X_2	X_3	Y_1* (PDE ± SD)	Y_2* (PS ± SD)
1	0	-1	-1	51.2 ± 2.0	203.7 ± 2.7
2	0	-1	1	66.7 ± 1.7	150.7 ± 4.9
3	0	1	-1	21.8 ± 2.5	239.7 ± 6.8
4	0	1	1	66.3 ± 0.8	187.5 ± 8.1
5	-1	0	-1	52.7 ± 0.1	258.9 ± 5.8
6	-1	0	1	58.8 ± 1.7	192.5 ± 2.7
7	1	0	-1	44.3 ± 2.1	293.3 ± 0.6
8	1	0	1	73.2 ± 2.0	195.1 ± 3.6
9	-1	-1	0	64.5 ± 0.6	169.1 ± 3.8
10	-1	1	0	49.9 ± 1.8	345.9 ± 22.1
11	1	-1	0	68.1 ± 2.2	214.4 ± 7.1
12	1	1	0	62.7 ± 0.9	384.1 ± 10.9
13	0	0	0	75.49	188.55
14	0	0	0	76.15	190.4
15	0	0	0	73.84	186.7

*values are represented as mean ± s.d.

$$Y_1 = 75.16 + 2.79\,X_1 - 6.22\,X_2 + 11.88\,X_3 + 2.28\,X_1X_2 + 5.69\,X_1X_3 + 7.25\,X_2X_3 - 4.06\,X_1^2 - 9.81\,X_2^2 - 13.87\,X_3^2 \quad (17)$$

$$Y_2 = 188.55 + 13.81\,X_1 + 52.4\,X_2 - 33.98\,X_3 - 1.78\,X_1X_2 - 8.46\,X_1X_3 + 0.2\,X_2X_3 + 64.39\,X_1^2 + 25.38\,X_2^2 - 18.51\,X_3^2 \quad (18)$$

$$Y_1 = 72.66 - 6.22\,X_2 + 11.88\,X_3 + 7.25\,X_2X_3 - 9.49\,X_2^2 - 13.56\,X_3^2 \quad (19)$$

$$Y_2 = 192.48 + 52.4\,X_2 + 63.9\,X_1^2 \quad (20)$$

PS changes when two variables were simultaneously changed. The values of all the 13 batches showed wide variation of 21.8 ± 2.5 to 76.2 ± 1.2% and 150.7 ± 4.9 to 384.1 ± 10.9 nm for PDE and PS, respectively as shown in table 4.27. This variation is reflected by the wide range of coefficients of the terms representing the individual and combined variables.

Table 4.28 Model coefficients estimated by multiple regression analysis for PDE of EXE loaded PLGA NPs

Factor	Coefficients	t Stat	P-value
Intercept	75.16	28.21	1.05E-06*
X_1	2.79	1.71	0.1477
X_2	-6.22	-3.81	0.0125*
X_3	11.88	7.28	0.0008*
X_1X_2	2.28	0.99	0.3687
X_1X_3	7.25	2.46	0.0569
X_2X_3	5.69	3.14	0.0256*
X_1^2	-4.06	-1.69	0.1519
X_2^2	-9.81	-4.08	0.0095*
X_3^2	-13.87	-5.77	0.0021*

* Significant at $p < 0.05$

Table 4.29 Model coefficients estimated by multiple regression analysis for PS of EXE loaded PLGA NPs

Factor	Coefficients	t Stat	P-value
Intercept	188.55	7.25	0.0008*
X_1	14.81	0.93	0.3952
X_2	52.40	3.29	0.0217*
X_3	-33.98	-2.13	0.0860
X_1X_2	-1.78	-0.08	0.9402
X_1X_3	-8.46	-0.38	0.7225
X_2X_3	0.20	0.01	0.9933
X_1^2	64.39	2.75	0.0405*
X_2^2	25.38	1.08	0.3283
X_3^2	-18.51	-0.79	0.4656

* Significant at $p < 0.05$

The significance of each coefficient of equations 17 and 18 were determined by student's 't' test and p-value, which are listed in table 4.28 and 4.29 respectively. The larger the magnitude of the 't' value and the smaller the p-value, the more significant is the corresponding coefficient [Adinarayana and Ellaiah 2002; Akhnazarova 1982]. Small

values of the coefficients of the terms X_1, X_1X_2, X_1X_3 and X_1^2 in equation 17 and X_1, X_3, X_1X_2, X_1X_3, X_2X_3, X_2^2 and X_3^2 in equation 18 implied that all these terms were least contributing in the preparation of EXE loaded PLGA NPs. These small values of coefficients had $p>0.05$. Hence, these terms were neglected from the FM considering non-significance and reduced polynomial equations (equation 19 and 20, for PDE and PS respectively) were obtained following regression analysis of PDE and PS. From RM, it was evident that drug:polymer ratio did not affect any of the dependent variables significantly ($p>0.05$). For PDE, the quadratic effect of drug:polymer ratio and interaction effects of X_1X_2 and X_1X_3 were found to be non-significant ($p>0.05$). For PS, all factors other than linear effect of amount of polymer and quadratic effect of drug:polymer ratio were found to be non-significant ($p>0.05$) (table 4.28 and 4.29).

The results of ANOVA of the second order polynomial equation of PDE and PS are given in table 4.30 and 4.31 respectively. Since the calculated F value (3.2077) is less than the tabulated F value (5.1922) ($\alpha = 0.05$, $V_1 = 4$ and $V_2 = 5$) [Bolton 1997] for PDE, and calculated F value (1.0719) is less than the tabulated F value (4.8759) ($\alpha = 0.05$, $V_1 = 7$ and $V_2 = 5$) [Bolton 1997] for PS, it was concluded that the neglected terms did not significantly contribute in the prediction of PDE and PS. Thus, the results of ANOVA of full and reduced model justified the omission of non-significant terms of equation 17 and 18. When the coefficients of the three independent variables in equation 17 and 18 were compared, the values for the variables X_3 (11.88) for PDE and X_2 (52.4) for PS were

Table 4.30 ANOVA of full and reduced models for PDE of EXE loaded PLGA NPs

		df	SS	MS	F	R	R^2	Adjusted R^2
Regression	FM	10	2876.2	287.6	15.01	0.9820	0.9643	0.7000
	RM	6	2602.9	433.8	12.34	0.9342	0.8727	0.6908
Residual	FM	5	106.5	21.3				
	RM	9	379.8	42.2				

SSE2 - SSE1 = 379.8 – 106.5 = 273.3

No. of parameters omitted = 4

MS of error (full model) = 21.3

F calculated = (SSE2 - SSE1 / No. of parameters omitted) / MS of error (FM)

= (273.3 / 4) / 21.3

= 3.2077

found to be maximum and hence these variables were considered to be major contributing variables affecting the PDE and PS of the NPs. The Fisher F test with a very low probability value ($P_{model} > F = 0.000001$) demonstrated a very high significance for the derived regression model.

Table 4.31 ANOVA of full and reduced models for PS of EXE loaded PLGA NPs

		df	SS	MS	F	R	R^2	Adjusted R^2
Regression	FM	10	52435.4	5243.5	2.87	0.9154	0.8379	0.3461
	RM	3	37211.3	12403.8	8.80	0.7711	0.5946	0.4437
Residual	FM	5	10144.3	2028.9				
	RM	12	25368.4	2114.0				

SSE2 - SSE1 = 25368.4 – 10144.3 = 15224.1

No. of parameters omitted = 7

MS of error (full model) = 2028.9

F calculated = (SSE2 - SSE1 / No. of parameters omitted) / MS of error (FM)

= (15224.1 / 7) / 2028.9

= 1.0719

4.13.2.1 Contour plots

Values of X_1, X_2 and X_3 were computed for PDE and PS and contour plots were established between X_1 vs X_2, X_1 vs X_3 and X_2 vs X_3 at fixed level (+1) of third variable as shown in figure 4.19 and 4.20 for each PDE and PS respectively. Contour plots showed that PDE was greatly dependent on drug:polymer ratio and amount of polymer (figure 4.19A). PDE was found to be more than 75% in the range of -0.25 to +0.75 for X_1 and -0.7 to 0 level of X_2 at +1 level of X_3. Contour plot of drug:polymer ratio vs volume of organic phase showed maximum PDE of more than 75% at -0.4 to +1.0 value of X_1 and 0.0 to +1.0 value of X_3 at +1 level of X_2 (figure 4.19B). PDE was found to be below 55% when formulations prepared at any level of X_1 (-1.0 to +1.0) and -0.75 to -1 level of X_3 at +1 level of X_2. Contour plot of amount of polymer vs volume of organic phase at +1 level of drug:polymer ratio indicated PDE of more than 75% when X_2 varied from -0.75 to 0.25 level and X_3 from 0 to +0.75 level (figure 4.19C). Lowest PS of about 180 nm was observed at -0.7 to 0.4 level of drug:polymer ratio, -0.4 to -1.0 level of amount of polymer and at +1 level of volume of organic phase (figure 4.20A). When drug:polymer ratio was varied with volume of organic phase, PS was first found to decrease and then

it increases as drug:polymer ratio increases. PS of less than 160 nm can be obtained at -0.5 to 0.5 level of X_1, 0.7 to 1.0 level of X_3 and 1.0 level of X_2 (figure 4.20B). From figure 4.20C, it can be concluded that PS increases as amount of polymer increases (from -1.0 to 1.0) and volume of organic solvent decreases. It was concluded from the contours that mid level of drug:polymer ratio, low amount of polymer and highest volume of organic phase are required for preparation of EXE NPs with highest PDE and lowest PS.

4.13.2.2 Response surface plots

Response surface plot is a very important tool when interaction effects of independent variables needs to be evaluated. Response surface plots were plotted between X_1 vs X_2, X_1 vs X_3 and X_2 vs X_3 at fixed level (+1) of third variable as shown in figure 4.21 and 4.22 for PDE and PS respectively. PDE was found to first increase with decrease in amount of polymer, and further decrease caused decrease in PDE (figure 4.21A). Drug:polymer ratio does not have significant effect on PDE, with increase in drug:polymer ratio, PDE first increases marginally and then decreases. No increase or decrease in PDE was observed when both the variables varied simultaneously. In response surface plot of drug:polymer ratio vs volume of organic phase, PDE increases with increase in volume of organic phase from -1.0 to 0.5 level and then decreases. Simultaneous increase in both the variable results into increase in PDE and was found to be maximum at 0.5 level of X_3 and 1.0 level of X_1 (figure 4.21B). In response surface plot of volume of organic phase vs amount of polymer, PDE was found to increase with increase in volume of organic phase and found to be maximum at mid level (0) of X_2 and 1.0 level of X_3 (figure 4.21C). Response surface plot of drug:polymer ratio vs amount of polymer showed increase in PS with increase in X_2. PS first decreases upto 0 level of $X_1$and then increases. Smallest particles were formed at 0 level of X_1 and -1 level of X_2 (figure 4.22A). In response surface plot of drug:polymer ratio vs volume of organic phase, PS was found to be maximum at high level of X_1 and low level of X_3 (figure 4.22B). Response surface plot of amount of polymer vs volume of organic phase depicts that as volume of organic phase increases and amount of polymer decreases, PS increases. Both the variables together showed interactive effect with decreases in PS as X_3 increases and X_2 decreases (figure 4.22C).

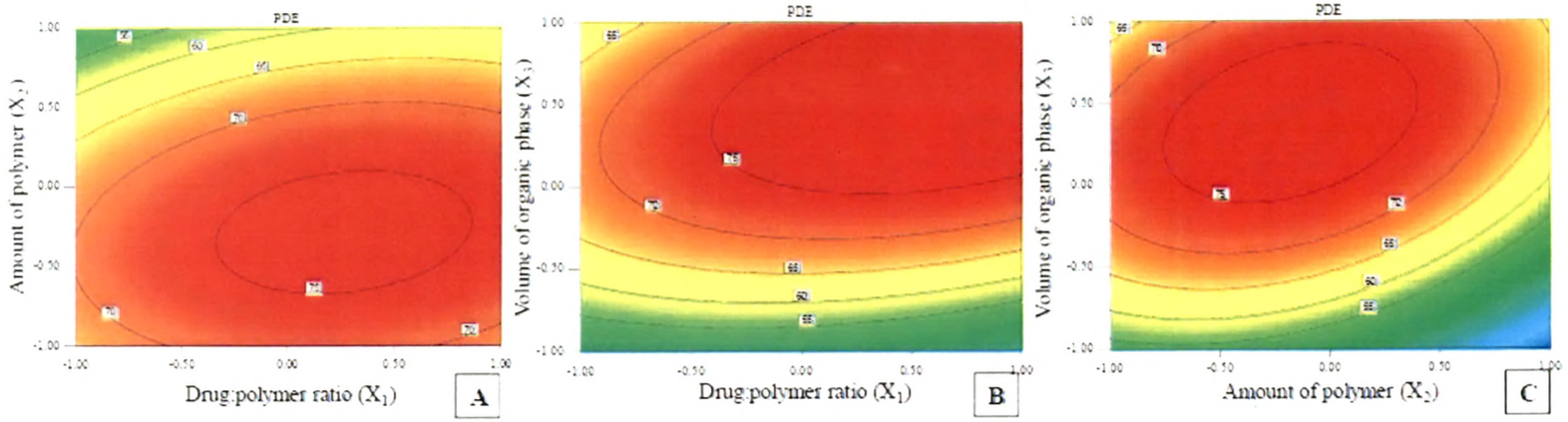

Figure 4.19 Contour plots showing effect of (A) X_1 vs X_2 (at -1 level of X_3), (B) X_1 vs X_3 (at -1 level of X_2) and (C) X_2 vs X_3 (at -1 level of X_1) on PDE of EXE loaded PLGA NPs.

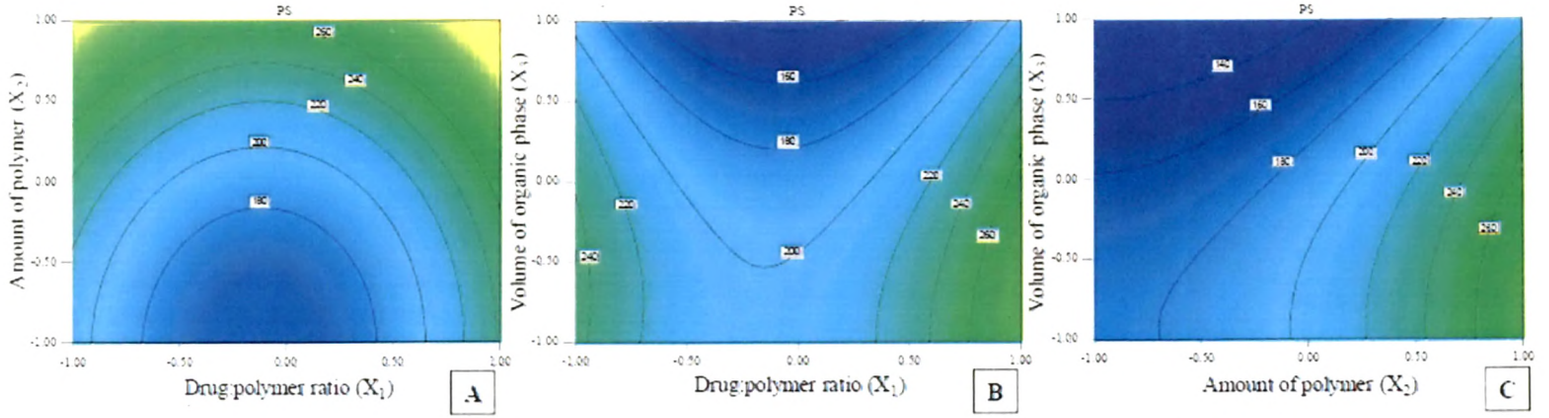

Figure 4.20 Contour plots showing effect of (A) X_1 vs X_2 (at -1 level of X_3), (B) X_1 vs X_3 (at -1 level of X_2) and (C) X_2 vs X_3 (at -1 level of X_1) on PS of EXE loaded PLGA NPs.

4.13.2.3 Desirability criteria

From the results of experiments performed as per Box-Behnken design, the optimum levels of independent variables were screened out by regression analysis. Formulation was optimized on the basis of PDE and PS and as both these dependent variables were taken into consideration simultaneously, the results were unable to attend both the dependent variables at a time. The batch with smallest particle size of 150.7 ± 4.9 nm exhibited only about 66.7 ± 1.7% while that with highest PDE of 73.2 ± 2.0% had particle size close to 200 nm. Hence, desirability criteria were used to find out formula with desired parameters. The desirability criteria were obtained using Design Expert software (version 8.0.3). Our criteria included maximum PDE and PS not more than 200 nm. The optimum formulation offered by the Design Expert 8.0.3 software based on desirability was found at 0.41, -0.09 and 0.75 levels of X_1, X_2 and X_3 respectively. The calculated desirability factor for offered formulations was 1, which indicated suitability of the designed factorial model. The results of dependent variables from the software were found to yield 78.37% PDE and 162.28 nm PS (figure 4.23) at these levels.

4.13.2.4 Checkpoint analysis and normalized error

Check point analysis was performed to check the predictability of the results from the generated algorithm. Three batches with random levels were prepared for check point analysis and evaluated for PDE and PS as shown in table 4.32. Results indicated that the measured response was more accurately predicted by reduced model of regression analysis which was proved by lower normalized error value of regression analysis

Table 4.32 Check point analysis, t test analysis and normalized error determination

Batch No.	X_1	X_2	X_3	PDE		PS	
				Observed	Predicted	Observed	Predicted
1	-1 (1:15)	- 0.3 (85 mg)	0.5 (9 ml)	56.91	57.53	305.2	298.3
2	0 (1:20)	0.2 (110 mg)	- 0.8 (6.4 ml)	75.26	74.62	204.1	199.76
3	1 (1:25)	- 0.7 (65 mg)	0.8 (9.6 ml)	52.72	53.46	242	239.51
$t_{calculated}$				0.6411		0.0699	
$t_{tabulated}$				2.9199		2.9199	
Normalized Error				0.0197		0.0327	

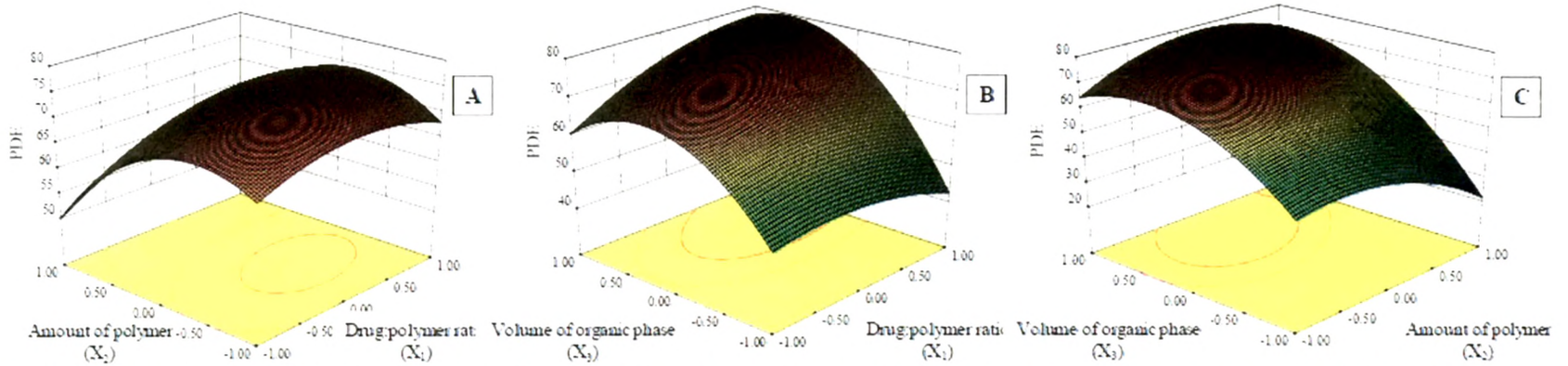

Figure 4.21 Response surface plot showing effect of (A) X_1 vs X_2 (at -1 level of X_3), (B) X_1 vs X_3 (at -1 level of X_2) and (C) X_2 vs X_3 (at -1 level of X_1) on PDE of EXE loaded PLGA NPs.

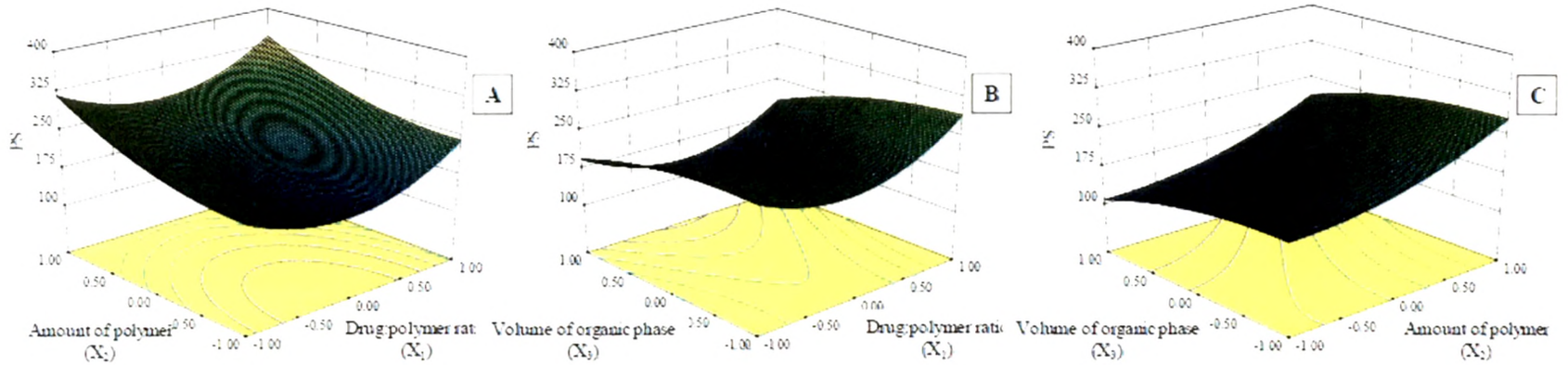

Figure 4.22 Response surface plot showing effect of (A) X_1 vs X_2 (at -1 level of X_3), (B) X_1 vs X_3 (at -1 level of X_2) and (C) X_2 vs X_3 (at -1 level of X_1) on PS of EXE loaded PLGA NPs.

(0.0197 for PDE and 0.0327 for PS). Data analysis using student's 't' test was performed to check the difference in the observed and predicted responses. Calculated t value ($t_{calculated}$) for PDE and PS was found to be 0.6411 and 0.0699, respectively which was less than the tabulated 't' value of 2.9199 which indicates that there was no statistically significant difference ($p<0.05$) between experimentally obtained values and predicted values by regression analysis and hence confirms the utility of the established contour plots and reduced polynomial equations in the preparation of NPs.

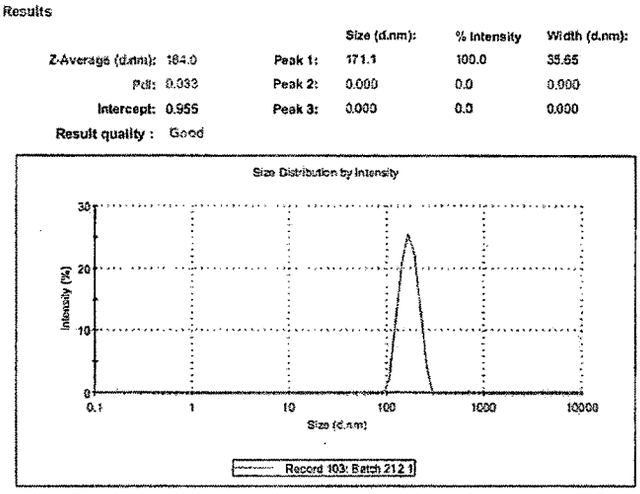

Figure 4.23 Particle size of EXE loaded PLGA NPs

4.13.3 Lyophilization and optimization of cryoprotectants

In this study, different cryoprotectants (trehalose, sucrose and mannitol) were used in different ratios (1:1, 1:2, 1:3, 1:4) and PS was recorded as shown in table 4.33. Initial PS of NPs was found to be 174.8 nm. The ratio of PS (after lyophilization, S_f and before lyophilization, S_i) was found to be lowest (1.25) for sucrose in 1:2 ratio. Trehalose also showed less increase in PS after re-dispersion (S_f/S_i ratio of 1.39). Trehalose at 1:2 and sucrose 1:1 and 1:2 ratio showed less S_f/S_i ratio indicating good re-dispersibility with PDI less than 0.2. PDI is a measure of dispersion homogeneity and usually ranges from 0 to 1. Values close to 0 indicate a homogeneous dispersion while those greater than 0.3 indicate high heterogeneity [Ahlin et al. 2002].

Table 4.33 Effect of cryoprotectants and their concentration on PS of lyophilized NPs after re-dispersion in distilled water

Cryoprotectant	Ratio	Final Avg. PS (nm)	S_f/S_i
Trehalose	1:1	252.5	1.44
	1:2	237.3	1.36*
	1:3	281.3	1.61
	1:4	324.3	1.86
Sucrose	1:1	229.6	1.31*
	1:2	218.2	1.25*
	1:3	260.2	1.49
	1:4	304.3	1.74
Mannitol	1:1	264.9	1.52
	1:2	289.9	1.66
	1:3	320.2	1.83
	1:4	332.8	1.90

*indicates good re-dispersibility

4.14Formulation and optimization of EXE loaded cPCL NPs

4.14.1 Preliminary optimization of EXE loaded cPCL NPs

4.14.1.1 Selection of organic solvent

Three different organic solvents (acetone, acetonitrile and tetrahydrofuran) were used for preparation of cPCL NPs (table 4.34). NPs formulated using acetone showed PDE of 82.0 ± 1.1% with PS of 212.4 ± 3.1 nm while NPs formulated using acetonitrile were of low PDE and high PS. No significant change in PDE was observed when tetrahydrofuran was used as solvent with significant increase in PS. Hence, acetone was selected for further studies.

Table 4.34 Selection of organic phase in preliminary optimization of EXE loaded cPCL NPs

Solvents	PDE (%)	PS (nm)
Acetone	82.0 ± 1.1	212.4 ± 3.1
Acetonitrile	80.6 ± 2.3	227.6 ± 5.2
Tetra hydro furan	82.3 ± 1.7	255.1 ± 4.7

4.14.1.2 Selection of surfactant

Three different surfactants were initially used for formulation development namely Pluronic F-68® (P188), Pluronic F-127® (P127) and Poly vinyl alcohol (PVA) (table 4.35). Out of these, better one is selected based on resultant PDE and PS. With constant level of surfactant concentration (0.5%) for all three surfactants, no significant change in PDE was observed, but at the same time PS was found to be of larger size (251.1 ± 5.3 nm) using PVA as surfactant. No significant difference in PS was observed when P188 or P127 was used, but PDE was higher when P188 was used as surfactant. Hence, P188 was used in further studies.

Table 4.35 Selection of surfactant in preliminary optimization of EXE loaded cPCL NPs

Surfactant	PDE (%)	PS (nm)
P188	56.32 ± 1.74	224.1 ± 7.2
P127	55.98 ± 2.12	214.6 ± 3.7
PVA	56.67 ± 1.89	251.1 ± 5.3

4.14.1.3 Selection of surfactant concentration

Different concentrations (0.5, 1.0, 1.5%) of surfactant (P188) were used in aqueous phase and results are represented in table 4.36. It was observed that as the concentration was increased, PS increases significantly with no major change in PDE (55.86 – 56.97%). This was possibly due to coating of surfactant on NPs after precipitation. Hence, 0.5% of P188 was selected as surfactant concentration.

Table 4.36 Selection of surfactant concentration in preliminary optimization of EXE loaded cPCL NPs

Surfactant concentration	PDE (%)	PS (nm)
0.5%	56.32 ± 1.74	224.1 ± 7.2
1.0%	55.86 ± 1.41	232.5 ± 2.9
1.5%	56.97 ± 1.64	258.1 ± 4.6

4.14.2 Optimization of EXE loaded cPCL NPs using BBD

Thirteen batches of EXE loaded cPCL NPs were prepared as per BBD changing three independent variables, drug:polymer ratio (X_1), amount of polymer (X_2) and volume of organic phase (X_3). Coded values and actual values of the three independent variables,

drug:polymer ratio (X_1), surfactant concentration (X_2) and volume of organic phase (X_3) are represented in table 4.37. Batches prepared using BBD were evaluated for PDE and PS as the dependent variables and recorded in table 4.38.

Table 4.37 Coded values of the formulation parameters of EXE loaded cPCL NPs

Coded Values	Actual values		
	X_1	X_2	X_3
-1	1 : 15	50 mg	6 ml
0	1 : 20	100 mg	8 ml
1	1 : 25	150 mg	10 ml

X_1 Drug:polymer ratio
X_2 Amount of polymer (mg)
X_3 Volume of organic phase (ml)

Table 4.38 Box Behnken experimental design with measured responses for EXE loaded cPCL NPs

Sr. No.	X_1	X_2	X_3	Y_1 (PDE, mean ± S.D.)	Y_2 (PS, mean ± S.D.)
1	0	-1	-1	56.32 ± 1.74	224.1 ± 7.2
2	0	-1	1	73.36 ± 2.08	115.0 ± 3.6
3	0	1	-1	23.94 ± 1.25	263.7 ± 4.5
4	0	1	1	72.89 ± 1.44	256.3 ± 5.4
5	-1	0	-1	57.93 ± 1.73	284.8 ± 4.9
6	-1	0	1	64.68 ± 1.92	185.0 ± 4.4
7	1	0	-1	48.71 ± 0.71	302.6 ± 2.9
8	1	0	1	82.00 ± 1.10	212.4 ± 3.1
9	-1	-1	0	70.91 ± 1.79	185.9 ± 3.5
10	-1	1	0	54.94 ± 1.81	340.4 ± 8.3
11	1	-1	0	74.89 ± 2.64	235.8 ± 6.8
12	1	1	0	68.95 ± 3.21	350.0 ± 7.2
13	0	0	0	82.67 ± 1.31	207.4 ± 2.0

*values are represented as mean ± s.d.

$Y_1 = 82.68 + 3.26\ X_1 - 6.84\ X_2 + 13.25\ X_3 + 2.51\ X_1X_2 + 6.63\ X_1X_3 + 7.98\ X_2X_3 - 4.27\ X_1^2 - 10.98\ X_2^2 - 15.07\ X_3^2$ (21)

$Y_2 = 207.41 + 13.08\ X_1 + 56.19\ X_2 - 38.32\ X_3 - 10.06\ X_1X_2 + 2.38\ X_1X_3 + 25.42\ X_2X_3 + 51.04\ X_1^2 + 19.61\ X_2^2 - 12.25\ X_3^2$ (22)

$Y_1 = 77.79 - 6.84\ X_2 + 13.25\ X_3 + 7.98\ X_2X_3 - 9.14\ X_2^2 - 13.23\ X_3^2$ (23)

$Y_2 = 213.29 + 56.19\ X_2 - 38.32\ X_3 + 25.42\ X_2X_3 + 48.83\ X_1^2$ (24)

The obtained PDE and PS were subjected to multiple regression to yield second order polynomial equations (equation 21 and 22, for PDE and PS respectively). Linear coefficients (b_1, b_2 and b_3 of X_1, X_2 and X_3, respectively) represents extent of effect by changing individual variable. Positive or negative sign in equation against different coefficients indicate increase or decrease in individual dependent response. The value of coefficients against interactions terms (X_1X_2, X_1X_3 and X_2X_3) shows how the PDE and PS changes when two variables were simultaneously changed. The values of all the 13 batches showed wide variation of 23.94 ± 1.25 to 82.68 ± 1.31% and 115.03 ± 3.60 to 350.03 ± 7.21 nm for PDE and PS, respectively as shown in table 4.38. This variation is reflected by the wide range of coefficients of the terms representing the individual and combined variables. The significance of each coefficient of equations 21 and 22 were determined by student's 't' test and p-value, which are listed in table 4.39 and 4.40 respectively. The larger the magnitude of the 't' value and the smaller the p-value, the more significant is the corresponding coefficient [Adinarayana and Ellaiah 2002; Akhnazarova 1982]. Small values of the coefficients of the terms X_1, X_1X_2, X_1X_3 and X_1^2 in equation 21 and X_1, X_1X_2, X_1X_3, X_2^2 and X_3^2 in equation 22 implied that all these terms were least contributing in the preparation of EXE loaded cPCL NPs. These small values of coefficients had $p>0.05$. Hence, these terms were neglected from the full model considering non-significance and reduced polynomial equations (equation 23 and 24, for PDE and PS respectively) were obtained following regression analysis of PDE and PS. From reduced model, it was evident that drug:polymer ratio did not affect any of the dependent variables significantly ($p>0.05$). The interaction effects of X_1X_2 and X_1X_3 was also found to be non-significant ($p>0.05$) for both PDE and PS. For PDE, the quadratic effect of drug:polymer ratio, while for PS the quadratic effect of amount of polymer and volume of organic phase were insignificant (table 4.39 and 4.40).

Table 4.39 Model coefficients estimated by multiple regression analysis for PDE of EXE loaded cPCL NPs

Factor	Coefficients	t Stat	P-value
Intercept	82.67	13.5711	0.0009*
X_1	3.2596	1.5135	0.2274
X_2	-6.8440	-3.1777	0.0482*
X_3	13.2531	6.1536	0.0086*
X_1X_2	2.5067	0.8230	0.4708
X_1X_3	6.6334	2.1779	0.1176
X_2X_3	7.9769	2.6190	0.0491*
X_1^2	-4.2709	-1.0600	0.3669
X_2^2	-10.9755	-2.7240	0.0423*
X_3^2	-15.0662	-3.7392	0.0334*

* Significant at $p < 0.05$

Table 4.40 Model coefficients estimated by multiple regression analysis for PS of EXE loaded cPCL NPs

Factor	Coefficients	t Stat	P-value
Intercept	207.4	8.7941	0.0031*
X_1	13.0775	1.5684	0.2148
X_2	56.1863	6.7384	0.0067*
X_3	-38.3225	-4.5960	0.0194*
X_1X_2	-10.0588	-0.8530	0.4563
X_1X_3	2.3788	0.2017	0.8530
X_2X_3	25.4188	2.1556	0.0301*
X_1^2	51.0381	3.2718	0.0467*
X_2^2	19.6131	1.2573	0.2976
X_3^2	-12.2444	-0.7849	0.4898

* Significant at $p < 0.05$

The results of ANOVA of the second order polynomial equation of PDE and PS are given in table 4.41 and 4.42 respectively. Since the calculated F value (1.3911) is less than the tabulated F value (9.0135) ($\alpha = 0.05$, $V_1 = 5$ and $V_2 = 3$) [Bolton 1997] for PDE, and calculated F value (2.2086) is less than the tabulated F value (9.1172) ($\alpha = 0.05$, $V_1 = 4$

and V_2 = 3) [Bolton 1997] for PS, it was concluded that the neglected terms did not significantly contribute in the prediction of PDE and PS. Thus, the results of ANOVA of full and reduced model justified the omission of non-significant terms of equation 21 and 22. When the coefficients of the three independent variables in equation 23 and 24 were compared, the values for the variables X_3 (13.25) for PDE and X_2 (56.19) for PS were found to be maximum and hence these variables were considered to be major contributing variables affecting the PDE and PS of the NPs. The Fisher F test with a very low probability value ($P_{model} > F = 0.000001$) demonstrated a very high significance for the derived regression model.

Table 4.41 ANOVA of full and reduced models for PDE of EXE loaded cPCL NPs

		df	SS	MS	F	R	R^2	Adjusted R^2
Regression	FM	9	50793.0	5643.7	10.1466	0.9839	0.9681	0.8727
	RM	4	46924.3	11731.1	16.9481	0.9457	0.8944	0.8416
Residual	FM	3	1668.6	556.2				
	RM	8	5537.4	692.2				

SSE2 - SSE1 =5537.387 – 1668.632 = 3868.755

No. of parameters omitted = 5

MS of error (full model) = 556.2107

F calculated = (SSE2 - SSE1 / No. of parameters omitted) / MS of error (FM)

= (3868.755 / 5) / 556.2107

= 1.3911

Table 4.42 ANOVA of full and reduced models for PS of EXE loaded cPCL NPs

		df	SS	MS	F	R	R^2	Adjusted R^2
Regression	FM	9	2935.15	326.13	8.7886	0.9815	0.9634	0.8538
	RM	5	2607.32	521.46	8.3118	0.9251	0.8558	0.7528
Residual	FM	3	111.32	37.11				
	RM	7	439.16	62.74				

SSE2 - SSE1 = 439.1605 - 111.3241 = 327.8364

No. of parameters omitted = 4

MS of error (full model) = 37.1080

F calculated = (SSE2 - SSE1 / No. of parameters omitted) / MS of error (FM)

= (327.8364 / 4) / 37.1080

= 2.2086

The goodness of fit of the model was checked by the determination coefficient (R^2). In this case, the values of the determination coefficients (R^2 = 0.9681 and 0.9634 for PDE and PS, respectively) indicated that over 96% of the total variations were explained by the model. After reducing the equation, the values of the determination coefficients (R^2 = 0.8944 and 0.8558 for PDE and PS, respectively) indicated that over 85% of the total variations were explained by the model. High R^2 values of full model as compared to reduced model is possibly due to the number of factors included. More the number of factors, more is the R^2 value, even if the factors are not significant [Montgomery 2004]. The values of adjusted determination coefficients (adj R^2 = 0.8727 and 0.8538 for PDE and PS respectively) were also very high (>85%) indicating high significance of the model. Moreover, the high values of correlation coefficients (R = 0.9839 and 0.9815 for PDE and PS, respectively) signify an excellent correlation between the independent variables [Box et al. 1978]. All the above considerations indicate an excellent adequacy of the derived regression model [Adinarayana and Ellaiah 2002; Akhnazarova 1982; Box et al. 1978; Yee and Blanch 1993].

4.14.2.1 Contour plots

Values of X_1, X_2 and X_3 were computed for PDE and PS and contour plots were established between X_1 vs X_2, X_1 vs X_3 and X_2vs X_3 at fixed level (+1) of third variable as shown in figure 4.24 and 4.25 for each PDE and PS respectively. Contour plots showed that PDE was greatly dependent on drug:polymer ratio and amount of polymer (figure 4.24A). PDE was found to be maximum at high level of X_1 and mid to high level of X_2. PDE was found to be more than 60% in the whole range of -1 to +1 for both X_1 and X_2 at +1 level of X_3. Contour plot of drug:polymer ratio vs volume of organic phase showed maximum PDE of more than 70% at 0 to +1 value of X_1 and +0.1 to +1.0 value of X_3 at +1 level of X_2 (figure 4.24B). PDE remained to be less than 80% in the whole range (-1 to +1) of both variables. Contour plot of amount of polymer vs volume of organic phase at +1 level of drug:polymer ratio indicated PDE of more than 80% when X_2 varied from -0.5 to 0.9 level and X_3 from 0 to +1.0 level (figure 4.24C). Lowest PS of about 175 nm was observed at -0.5 to 0 level of drug:polymer ratio, -0.8 to -1.0 level of amount of polymer at +1 level of volume of organic phase (figure 4.25A). When drug:polymer ratio was varied with volume of organic phase, PS was less than 275 nm at -0.5 to 0.5 level of X_1 and 0.5 to 1.0 level of X_3 at +1 level of X_2 (figure 4.25B). From figure 4.25C, it is

evident that at highest level of drug:polymer ratio (+1.0), PS increased as the amount of polymer increased (-1.0 to +1.0) and volume of organic phase decreased (+1.0 to -1.0), PS increases. It was concluded from the contours that high drug:polymer ratio, low amount of polymer and highest volume of organic phase were required for preparation of EXE NPs with highest PDE and lowest PS.

4.14.2.2 Response surface plots

Response surface plots are very important tools in learning both the main and interaction effects of the independent variables. Response surface plots were plotted between X_1 vs X_2, X_1 vs X_3 and X_2 vs X_3 at fixed level (+1) of third variable as shown in figure 4.26 and 4.27 for PDE and PS respectively. PDE was found to first increase with increase in amount of polymer, and further increase caused decrease in PDE. PDE was maximum at highest level of drug:polymer ratio and mid level of amount of polymer (figure 4.26A). The volume of organic phase had more significant effect on the outcome of PDE. PDE decreased sharply with decrease in volume of organic phase. However, PDE was not found to be much influenced by changing the drug:polymer ratio (figure 4.26B). PDE was found to decrease with increase in amount of polymer. Decrease in volume of organic phase and increase in amount of polymer resulted in overall decrease in PDE (figure 4.26C). Response surface plot of drug:polymer ratio vs amount of polymer showed non-linear behavior. With decrease in drug:polymer ratio, no significant change in PS was observed. Simultaneous increase in both drug:polymer ratio as well as polymer concentration showed increased PS. Increase in PS was more influenced by change in amount of polymer than drug:polymer ratio (figure 4.27A). Response surface plot between drug:polymer ratio and volume of organic phase showed no significant change in PS (figure 4.27B). Plot between amount of polymer and volume of organic phase showed increase in PS when amount of polymer increased and volume of organic phase decreased at the same time (figure 4.27C).

4.14.2.3 Desirability criteria

From the results, the optimum levels of independent variables were screened out by regression analysis. Since PDE and PS were taken into consideration simultaneously, the results were unable to attend both the dependent variables at a time. The batch with smallest particle size of less than 175 nm exhibited only about 69-71% PDE (at X_1 = -0.5 to 0, X_2 = -0.8 to -1.0, X_3 = +1.0) while that with highest PDE of more than 80% had

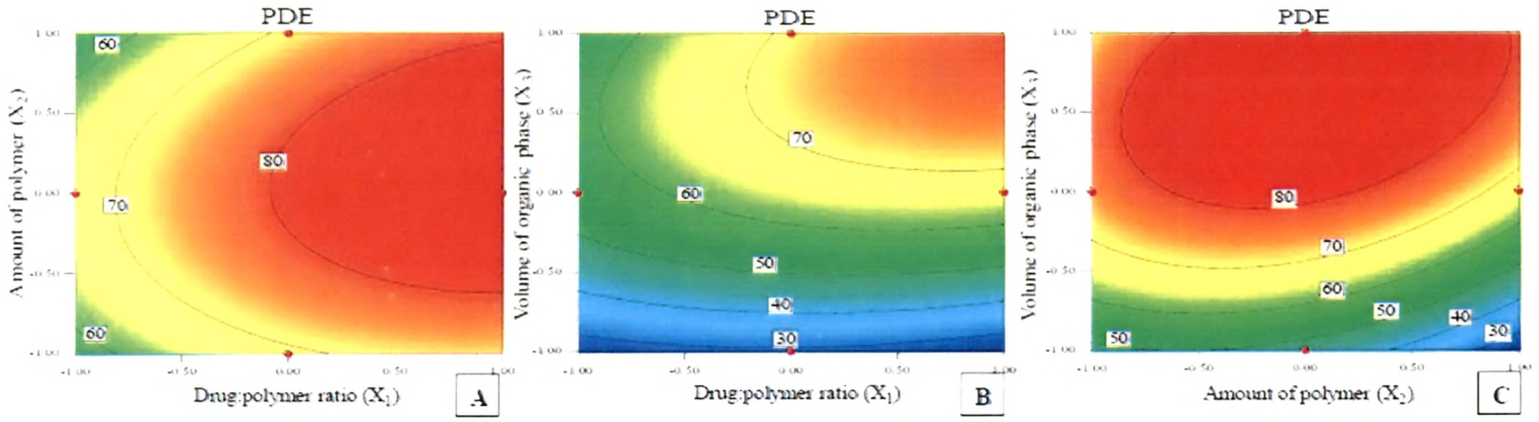

Figure 4.24 Contour plots showing effect of (A) X_1 vs X_2 (at -1 level of X_3), (B) X_1 vs X_3 (at -1 level of X_2) and (C) X_2 vs X_3 (at -1 level of X_1) on PDE of EXE loaded cPCL NPs.

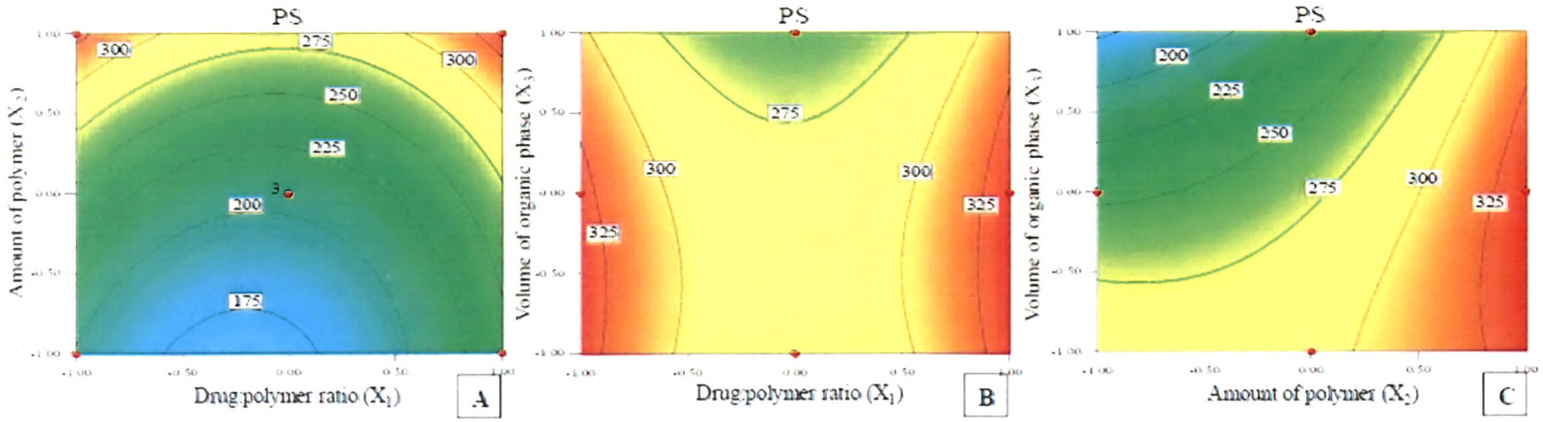

Figure 4.25 Contour plots showing effect of (A) X_1 vs X_2 (at -1 level of X_3), (B) X_1 vs X_3 (at -1 level of X_2) and (C) X_2 vs X_3 (at -1 level of X_1) on PS of EXE loaded cPCL NPs.

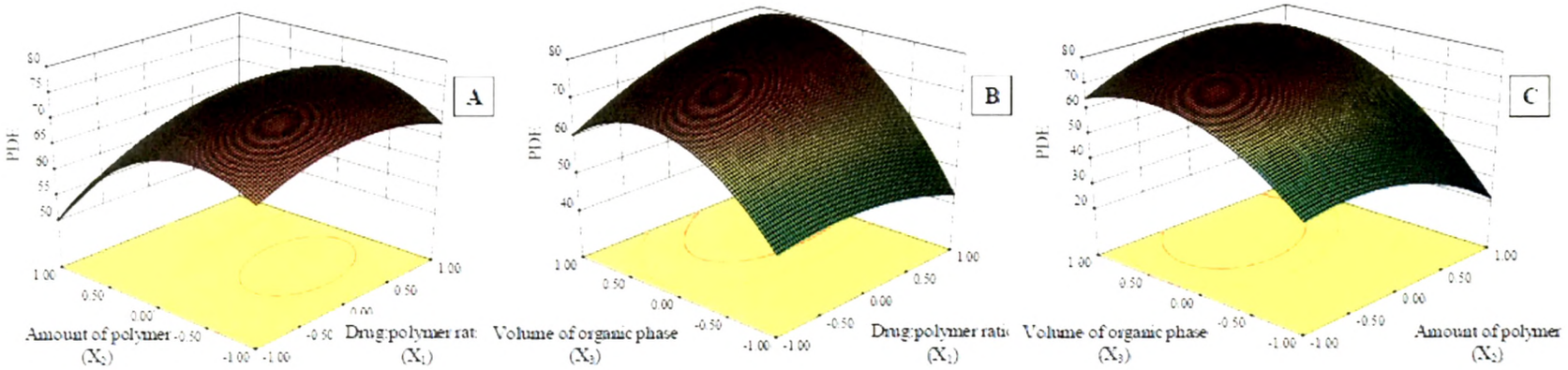

Figure 4.26 Response surface plot showing effect of (A) X_1 vs X_2 (at -1 level of X_3), (B) X_1 vs X_3 (at -1 level of X_2) and (C) X_2 vs X_3 (at -1 level of X_1) on PDE of EXE loaded cPCL NPs.

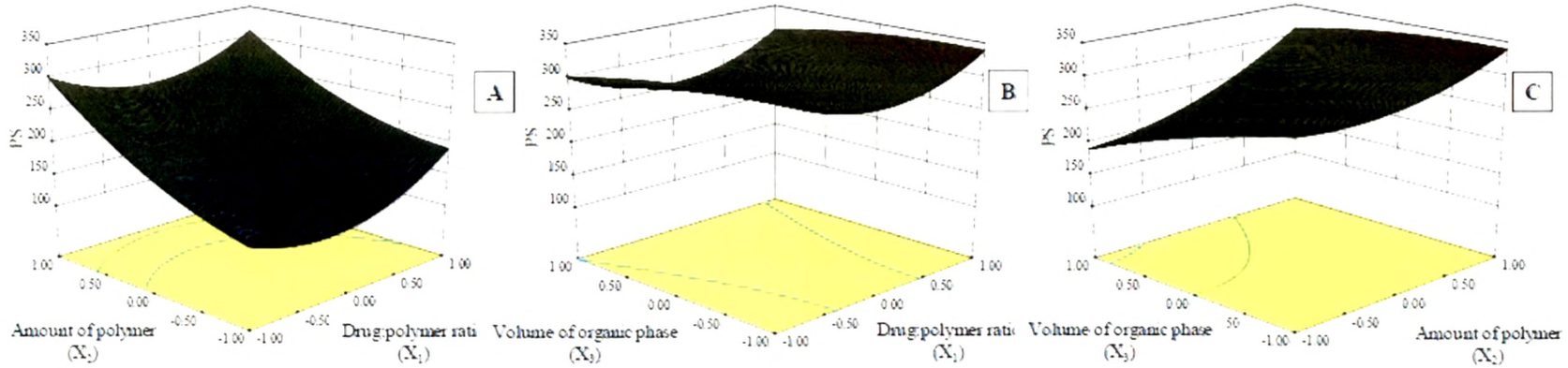

Figure 4.27 Response surface plot showing effect of (A) X_1 vs X_2 (at -1 level of X_3), (B) X_1 vs X_3 (at -1 level of X_2) and (C) X_2 vs X_3 (at -1 level of X_1) on PS of EXE loaded cPCL NPs.

PS of 210 to 300 nm (at X_1 = +1, X_2 = -0.5 to 0.9, X_3 = 0 to +1.0) (figure 4.23 and 4.24). Hence, desirability criteria were used to find out optimized formulation parameters. The desirability criteria were obtained using Design Expert software (version 8.0.3). Our criteria included maximum PDE and PS not more than 200 nm. The optimum formulation offered by the Design Expert 8.0.3 software based on desirability was found at 0.43, -0.68, and 0.27 level of X_1, X_2 and X_3 respectively. The calculated desirability factor for offered formulations was 1, which indicated suitability of the designed factorial model. The results of dependent variables from the software were found to yield 83.96% PDE and 180.51 nm PS (figure 4.28) at these levels.

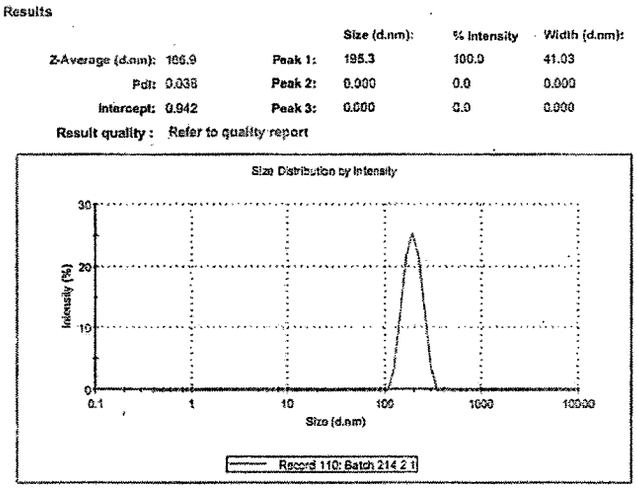

Figure 4.28 Particle size distribution of EXE loaded cPCL NPs

4.14.2.4 Checkpoint analysis and Normalized error

Three batches were prepared for check point analysis and evaluated for PDE and PS as shown in table 4.43. Results indicated that the measured response was more accurately predicted by regression analysis which was proved by lower normalized error value of regression analysis (0.04167 for PDE and 0.02591 for PS). Data analysis using student's 't' test revealed that there was no statistically significant difference ($p<0.05$) between experimentally obtained values and predicted values by regression analysis and hence, it confirms the utility of the established contour plots and reduced polynomial equation in the preparation of NPs.

Table 4.43 Check point analysis, t test analysis and normalized error determination

Batch No.	X_1	X_2	X_3	PDE		PS	
				Observed (avg.)	Predicted	Observed (avg.)	Predicted
1	-1 (1:15)	- 0.3 (85 mg)	0.5 (9 ml)	84.14	85.93	225.6	222.29
2	0 (1:20)	0.2 (110 mg)	- 0.8 (6.4 ml)	58.63	57.08	256.4	251.12
3	1 (1:25)	- 0.7 (65 mg)	0.8 (9.6 ml)	65.72	64.13	176.9	177.9
$t_{calculated}$				0.7267		0.3057	
$t_{tabulated}$				2.9199		2.9199	
Normalized Error				0.04167		0.02591	

4.14.3 Lyophilization and optimization of cryoprotectants

In this study, different cryoprotectants (trehalose, sucrose and mannitol) were used in different ratios (1:1, 1:2, 1:3, 1:4) and PS was recorded as shown in table 4.44. Initial PS of NPs was found to be 180.5 nm. The ratio of PS (after lyophilization, S_f and before

Table 4.44 Effect of cryoprotectants and their concentration on PS of lyophilized NPs after re-dispersion in distilled water

Cryoprotectant	Ratio	Final Avg. PS (nm)	S_f/S_i
Trehalose	1:1	254.0	1.41*
	1:2	250.6	1.39*
	1:3	288.4	1.60*
	1:4	315.9	1.75
Sucrose	1:1	232.4	1.29*
	1:2	220.7	1.22*
	1:3	273.5	1.52*
	1:4	298.1	1.65
Mannitol	1:1	275.9	1.53
	1:2	290.2	1.61
	1:3	318.0	1.76
	1:4	348.5	1.93

*indicates good re-dispersibility

lyophilization, S_i) was found to be lowest (1.22) for sucrose in 1:2 ratio. Trehalose also showed less increase in PS after re-dispersion (S_f/S_i ratio of 1.39). Trehalose and sucrose at 1:1, 1:2 and 1:3 ratio showed less S_f/S_i ratio indicating good re-dispersibility with PDI less than 0.2. PDI is a measure of dispersion homogeneity and usually ranges from 0 to 1. Values close to 0 indicate a homogeneous dispersion while those greater than 0.3 indicate high heterogeneity [Ahlin et al. 2002].

4.15 Characterization of ATZ loaded PLGA NPs

4.15.1 Zeta potential

Zeta potential gives information to predict the storage stability of colloidal dispersions [Thode et al. 2000]. The zeta potential values ranged between -21.5 to -34.4 mV for all 27 formulations. Highly negative values of the zeta potential indicate that the electrostatic repulsion between particles will prevent their aggregation and thereby stabilize the nanoparticulate dispersion [Feng and Huang 2001; Joshi et al. 2010]. The surfactant concentration affected the charge on the particle. It was seen that as the surfactant concentration was increased from 0.25 to 0.75%, there was a decrease in the zeta potential value. This is possibly because the surfactant is non- ionic and with increase in its concentration, total charge on the particle decreases due to increased surfactant coating which also results in increased PS [Redhead et al. 2001].

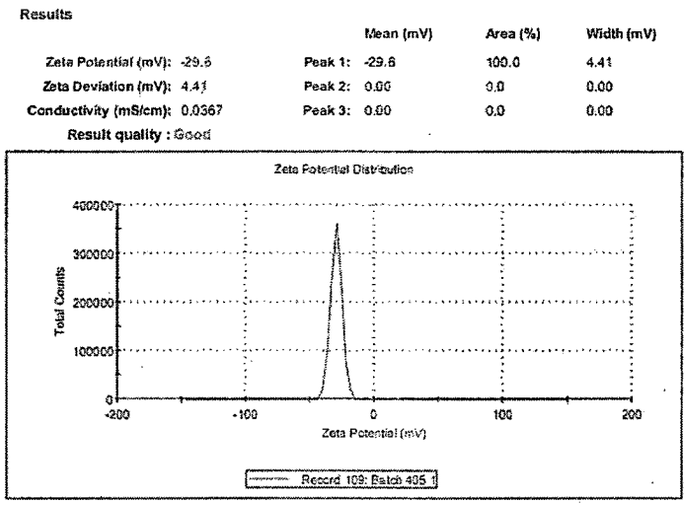

Figure 4.29 Zeta potential of ATZ loaded PLGA NPs

4.15.2 Transmission electron microscopy (TEM)

TEM image of ATZ loaded PLGA NPs is shown in figure 4.30 which reveals discrete, round and uniformly shaped NPs. The mean diameters of NPs were in the range of 80 - 100 nm. The higher hydrodynamic diameter of NPs achieved by DLS analysis as compared to the size obtained by TEM analysis may be contributed by the hydration of the surface associated Poloxamer [Das and Sahoo 2012; Misra and Sahoo 2010].

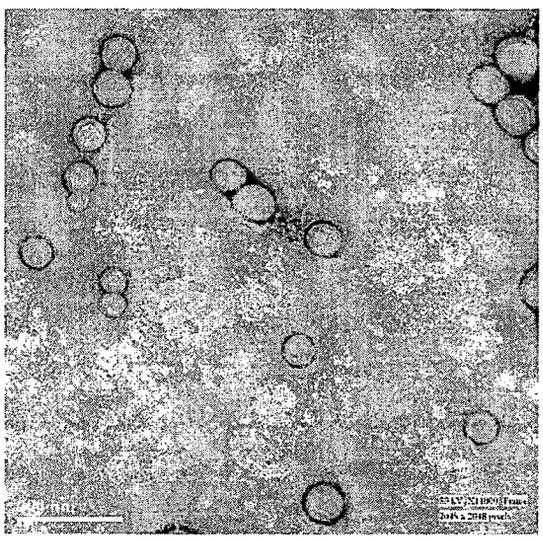

Figure 4.30 TEM image of ATZ loaded PLGA NPs

4.15.3 Differential scanning calorimetry (DSC)

In the absence of any interaction, the thermogram of a formulation will show patterns corresponding to those of the individual components. In the event that an interaction occurs, there may be disappearance of one or more peaks, the appearance of one or more new peaks corresponding to those of the components [Nanjwade et al. 2009] or shift in peaks [Jain and Ram 2011]. DSC thermograms of pure ATZ (A), PLGA polymer (B) and ATZ loaded PLGA NPs (C) are shown in figure 4.31. Pure ATZ showed an endothermic melting peak at 84.7 °C indicating its crystalline nature while PLGA showed endothermic peak at 51.99 °C corresponding to its glass transition temperature [Montgomery] [Chaudhari et al. 2010; Lacoulonche et al. 1999]. There was no peak of ATZ in the thermogram of NPs indicating that ATZ may be in an amorphous phase in the polymer matrix [Kashi et al. 2012].

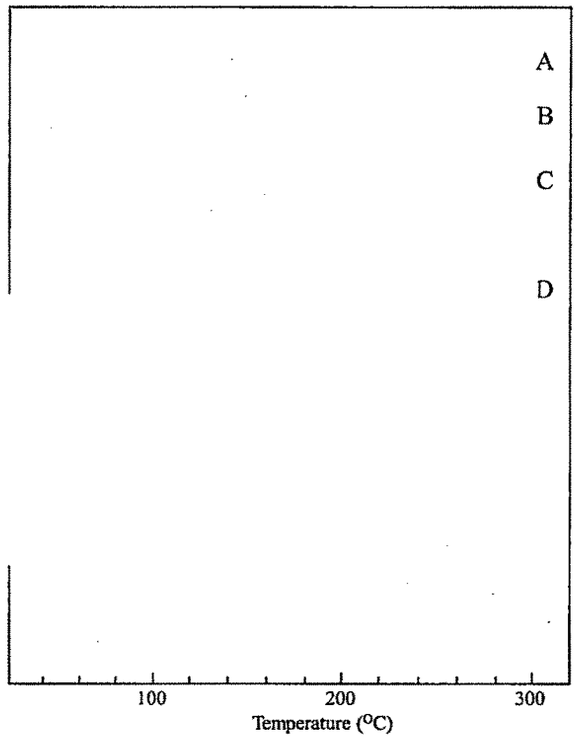

Figure 4.31 DSC thermogram of ATZ (A), ATZ loaded PLGA NPs (B), Sucrose (C), PLGA (D) and Physical mixture (E).

4.15.4 In vitro drug release studies

The in vitro drug release studies from different nanoparticulate formulations were performed in PBS pH 7.4. Pegylated NPs showed faster release as compared with non-pegylated NPs. In vitro release of ATZ from drug suspension and NPs is shown in figure 4.32. Within 3 h, 82.56 ± 0.623% drug release occurred from plain drug suspension, whereas only 24.14 ± 0.316% and 28.90 ± 1.03% drug released from PLGA and pegylated PLGA NPs, reaching 48.02 ± 0.566% and 60.29 ± 0.85% after 120 h and 64.9 ± 0.249% and 83.04 ± 0.55% after 240 h from PLGA and pegylated PLGA NPs, respectively indicative of sustained release. The drug release from NPs followed biphasic release model with an initial burst release for about 3 h followed by sustained release for more than 240 h. This biphasic release may be attributed to the drug molecules entrapped near particle surface causing initial burst release [Seju et al. 2011]. This initial fast release may also have been mediated by the presence of the surfactant molecules which are known to facilitate drug release. Also, particles of nano size range leads to a shorter

average diffusion path for the matrix entrapped drug molecules, thereby causing faster diffusion [Mainardes and Evangelista 2005; Shah et al. 2009]. After initial burst release, the release rate decreased, reflecting the release of drug entrapped in the strong polymer matrix. The release rate in the second phase is assumed to be controlled by diffusion rate of drug across the polymer matrix [Corrigan and Li 2009]. Pegylated PLGA NPs showed faster release of drug when compared to PLGA NPs as reported by Derakhshandeh et al. [Derakhshandeh et al. 2010].

The regression coefficient of the plot of log M_t/M_∞ versus log t for PLGA and pegylated PLGA NPs was found to be 0.948 and 0.956 with value of release exponent (n) as 0.255 and 0.264, respectively. The n value is the release exponent which characterizes the transport mechanism and if its value is less than 0.5, it indicates Fickian release. Hence, it can be concluded that the release of ATZ from NPs was by Fickian diffusion.

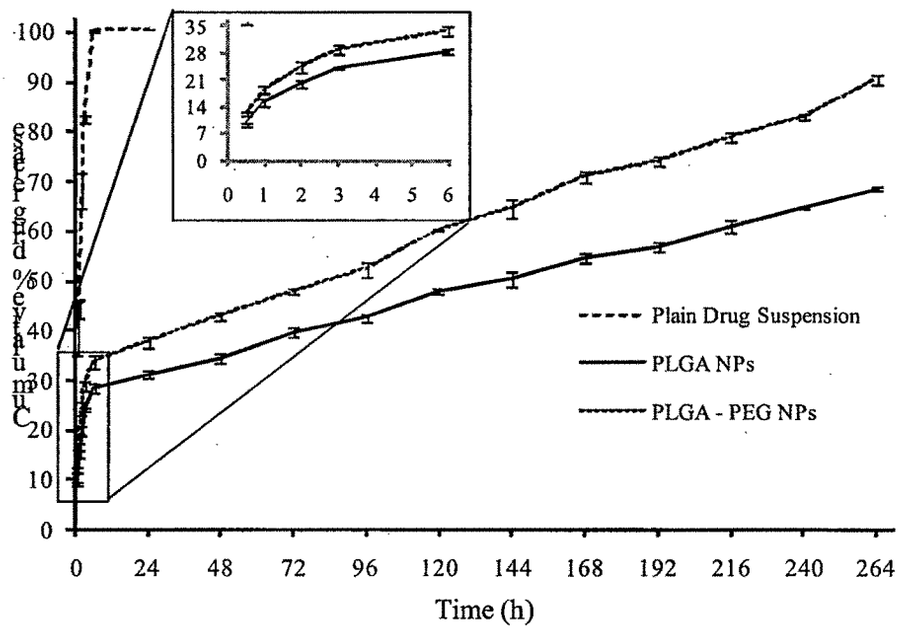

Figure 4.32 Drug release profile of ATZ from plain drug suspension, PLGA NPs and pegylated PLGA NPs across semi-permeable membrane using the dialysis bag diffusion technique in phosphate buffered saline (pH 7.4). The values represent mean ± S.D. of three batches.

4.15.5 Stability studies

Total drug content after different time intervals showed change in case of the NPs stored at room temperature to that of the NPs stored at refrigerator temperature. After different time intervals, increase in PS was observed for NPs stored at room temperature as compared to NPs stored at refrigerator temperature, which may attributed to the aggregation of polymeric particles (table 4.45). Also, drug content was found to decrease with increase in time as well as storage temperature (figure 4.33). Thus, it was concluded that the optimum temperature condition for storage of the ATZ loaded PLGA NPs would be refrigerated condition (2-8 °C).

Table 4.45 Stability data of ATZ loaded PLGA NPs stored at different temperature conditions

Storage time	% Drug content		Particle size (nm)	
	Room temp.	Refrigerator temp. (2–8 °C)	Room temp.	Refrigerator temp. (2–8 °C)
Initial	100	100	157.8 ± 2.3	157.8 ± 2.3
1 month	99.78 ± 0.29	99.85 ± 0.34	160.2 ± 1.4	159.7 ± 1.1
2 months	99.41 ± 0.58	99.57 ± 0.41	165.7 ± 2.9	160.2 ± 2.7
3 months	98.79 ± 0.61	99.14 ± 0.43	171.6 ± 3.8	165.9 ± 4.2

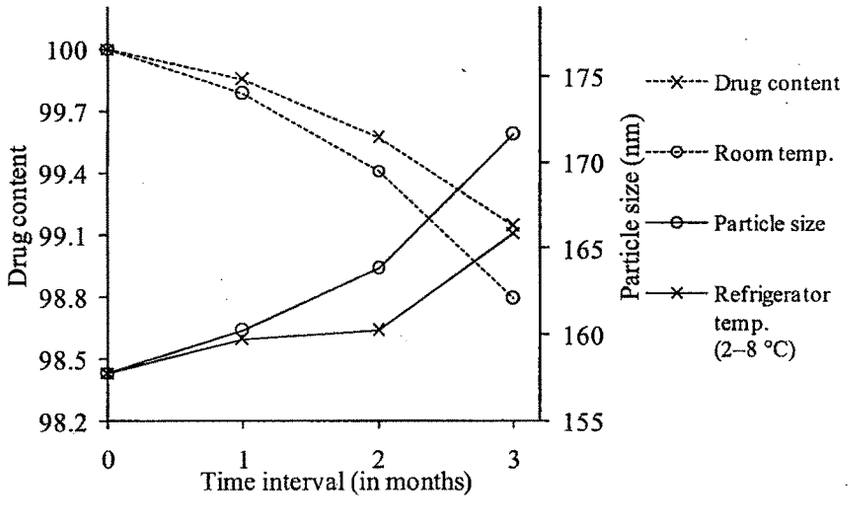

Figure 4.33 Effect of different storage conditions on drug content and PS of ATZ loaded PLGA NPs.

4.16 Characterization of ATZ loaded cPCL NPs

4.16.1 Zeta potential

Zeta potential gives information to predict the storage stability of colloidal dispersions [Thode et al. 2000]. The zeta potential values ranged between -23.7 to -35.1 mV for all 27 formulations. Highly negative values of the zeta potential indicate that the electrostatic repulsion between particles will prevent their aggregation and thereby stabilize the nanoparticulate dispersion [Feng and Huang 2001; Joshi et al. 2010]. Zeta potential was found to be affected by surfactant concentration, as the surfactant concentration was increased from 0.25 to 0.75%, the decrease in the zeta potential values were observed which is possibly because with increase in concentration of non-ionic surfactant, total charge on the particle decreases due to increased surfactant coating which also resulted into increased particle size [Redhead et al. 2001]. Polymer concentration had no significant effect on zeta potential values. The optimized batch of ATZ loaded cPCL NPs was found to have zeta potential of -32.1 ± 1.1 mV (figure 4.34). Zeta potential values in the -15 to -30 mV are common for well stabilized NPs [Musumeci et al. 2006]. Hence it was concluded that the NPs would remain physically stable.

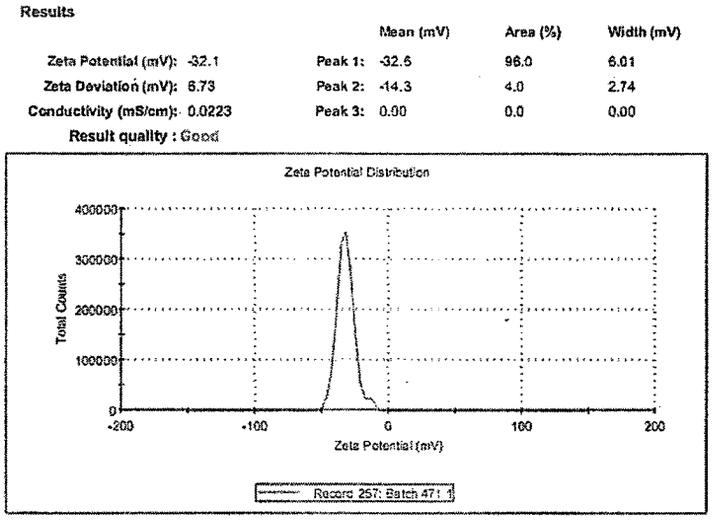

Figure 4.34 Zeta potential of ATZ loaded cPCL NPs

4.16.2 Transmission electron microscopy (TEM)

TEM image of ATZ loaded cPCL NPs is shown in figure 4.35 which reveals discrete, round and uniformly shaped NPs. The NPs were found with mean diameters in the range of 80 - 100 nm. The higher hydrodynamic diameter of NPs observed by DLS

analysis as compared to the size obtained by TEM analysis is possible due to the hydration of the surface associated Poloxamer [Das and Sahoo 2012; Misra and Sahoo 2010].

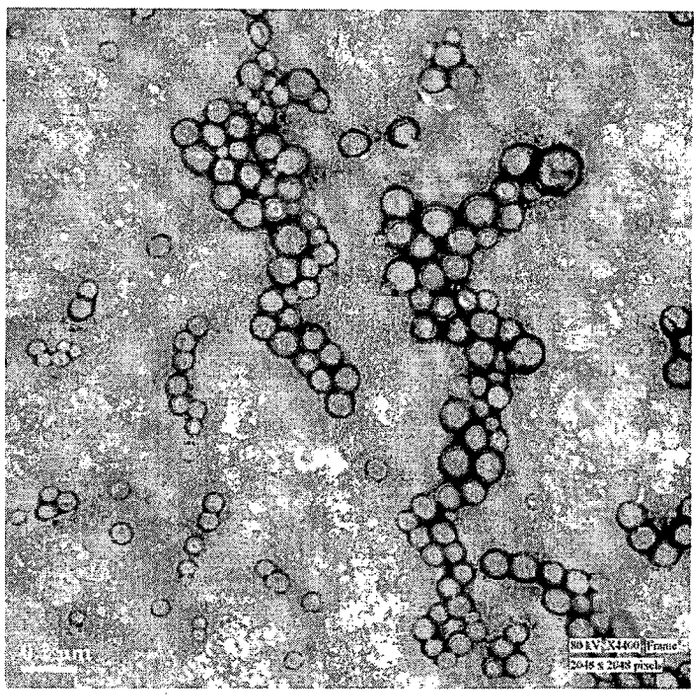

Figure 4.35 TEM image of ATZ loaded cPCL NPs

4.16.3 Differential scanning calorimetry (DSC)

In the absence of any interaction, the thermogram of a formulation will show patterns corresponding to those of the individual components. In the event that an interaction occurs, there may be disappearance of one or more peaks, the appearance of one or more new peaks corresponding to those of the components [Nanjwade et al. 2009] or shift in peaks [Jain and Ram 2011]. DSC thermograms of pure ATZ (A), cPCL polymer (B) and ATZ loaded cPCL NPs (C) are shown in figure 4.36. Pure ATZ showed an endothermic melting peak at 84.7 °C indicating its crystalline nature while cPCL showed endothermic peak at 47.65 °C corresponding to its melting temperature [Chaudhari et al. 2010; Lacoulonche et al. 1999]. There was no peak of ATZ in the thermogram of NPs indicating that ATZ may be in an amorphous phase in the polymer matrix [Kashi et al. 2012].

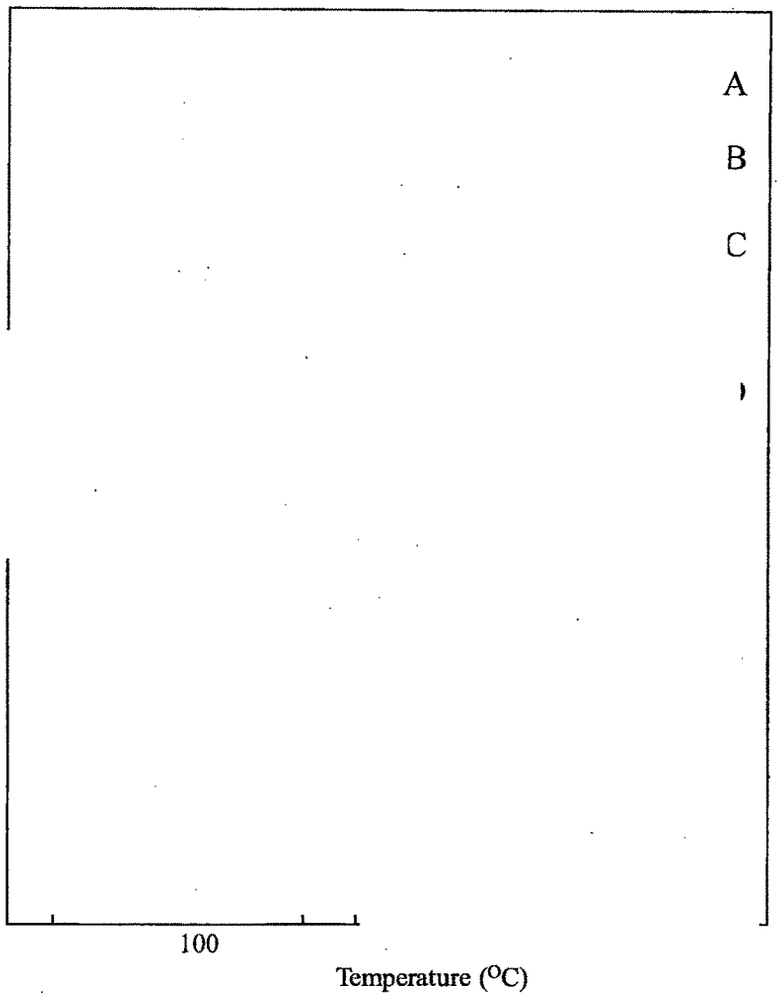

Figure 4.36 DSC thermogram of ATZ (A), ATZ loaded cPCL NPs (B), Sucrose (C), cPCL (D) and Physical mixture (E).

4.16.4 In vitro drug release studies

In vitro release of ATZ from plain drug suspension and NPs is shown in figure 4.37. In 3 h, 82.56 ± 0.62% drug released from plain drug suspension, whereas only 21.36 ± 0.41% and 26.57 ± 1.81% drug release occurred from cPCL NPs and pegylated PCL NPs, reaching 44.14 ± 0.69% and 56.71± 0.67% after 120 h and 58.22 ± 0.99% and 82.21 ± 0.74% after 240 h from cPCL and pegylated PCL NPs, respectively indicative of sustained release. The drug release from NPs followed biphasic release model with an initial burst

4.16.5 Stability studies

Total drug content after different time intervals showed change in case of the NPs stored at room temperature to that of the NPs stored at refrigerator temperature. After different time intervals, increase in PS was observed for NPs stored at room temperature as compared to NPs stored at refrigerator temperature, which may attributed to the aggregation of polymeric particles (table 4.46). Also, drug content was found to decrease with increase in time as well as storage temperature (figure 4.38). Thus, it was concluded that the optimum temperature condition for storage of the ATZ loaded cPCL NPs would be refrigerated condition (2-8 °C).

Table 4.46 Stability data of ATZ loaded cPCL NPs stored at different temperature conditions

Storage time	% Drug content		Particle size (nm)	
	Room temp.	Refrigerator temp. (2–8 °C)	Room temp.	Refrigerator temp. (2–8 °C)
Initial	100	100	198.4 ± 3.7	198.4 ± 3.7
1 month	99.81 ± 0.25	99.91 ± 0.21	200.5 ± 2.2	200.1 ± 1.8
2 months	99.38 ± 0.64	99.62 ± 0.18	207.1 ± 4.1	204.5 ± 2.5
3 months	99.01 ± 0.49	99.24 ± 0.37	215.0 ± 3.8	211.2 ± 3.1

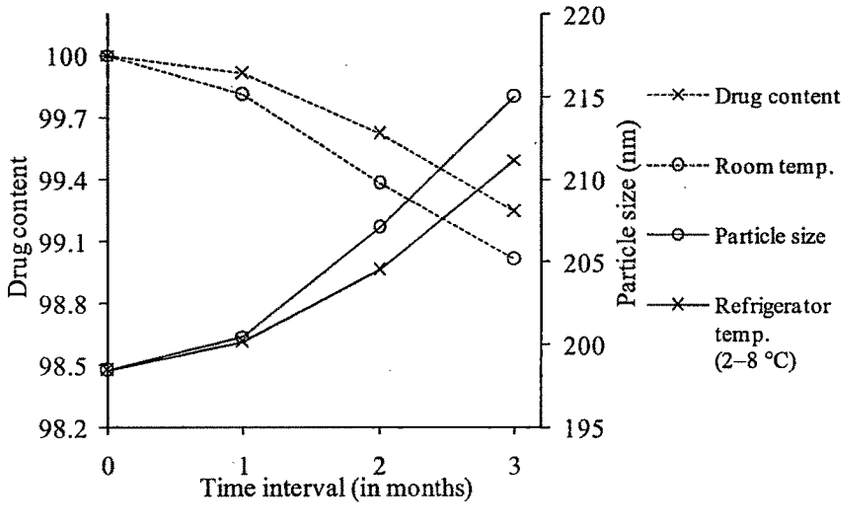

Figure 4.38 Effect of different storage conditions on drug content and PS of ATZ loaded cPCL NPs.

4.17 Characterization of EXE loaded PLGA NPs

4.17.1 Zeta potential

The zeta potential values ranged between -21.2 to -31.9 mV for all 13 formulations. The surfactant concentration affected the charge on the particle. It was seen that as the surfactant concentration was increased from 0.25 to 0.75%, there was a decrease in the zeta potential value. This is possibly because with increase in concentration of non-ionic surfactant, total charge on the particle decreases due to increased amount of surfactant coating which also resulted in increased particle size [Redhead et al. 2001]. However, change in polymer concentration had no effect on zeta potential values. The optimized batch of EXE loaded cPCL NPs was found to have zeta potential of -29.5 ± 1.4 mV (figure 4.39). Zeta potential values in the -15 mV to -30 mV are common for well stabilized NPs [Musumeci et al. 2006]. Hence it was concluded that the NPs would remain physically stable.

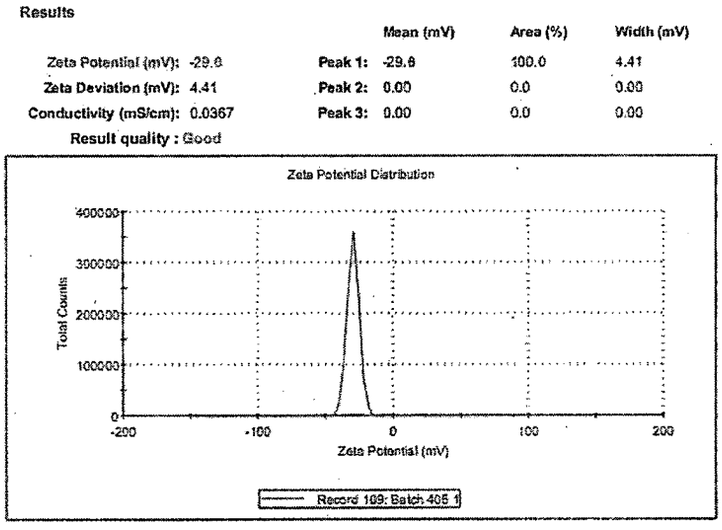

Figure 4.39 Zeta potential of EXE loaded PLGA NPs

4.17.2 Transmission electron microscopy (TEM)

TEM image of EXE loaded PLGA NPs is shown in figure 4.40. The image reveals that the particles were discrete, round and uniform in shape with diameters in the range of 80–100 nm. The higher hydrodynamic diameter of NPs achieved by DLS analysis as

compared to the size obtained by TEM analysis may be contributed by the hydration of the surface associated Poloxamer [Das and Sahoo 2012; Misra and Sahoo 2010].

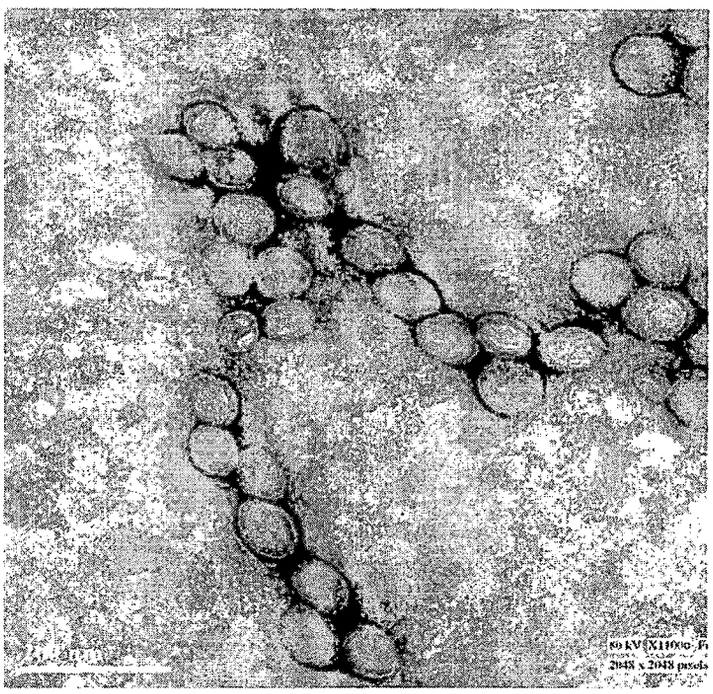

Figure 4.40 TEM image of EXE loaded PLGA NPs

4.17.3 Differential scanning calorimetry (DSC)

DSC thermograms of pure EXE, PLGA polymer, sucrose, physical mixture and EXE loaded PLGA NPs are shown in figure 4.41. Pure EXE showed an endothermic melting peak at 182.56 °C indicating its crystalline nature while PLGA showed endothermic peak at 51.9 °C corresponding to its glass transition temperature [Chaudhari et al. 2010; Lacoulonche et al. 1999]. In the absence of any interaction, the thermogram of a formulation will show patterns corresponding to those of the individual components. In the event that an interaction occurs, there may be disappearance of one or more peaks, the appearance of one or more new peaks corresponding to those of the components [Nanjwade et al. 2009] or shift in peaks [Jain and Ram 2011]. There was no peak of EXE in the thermogram of NPs indicating that EXE may be in an amorphous phase in the polymer matrix [Kashi et al. 2012].

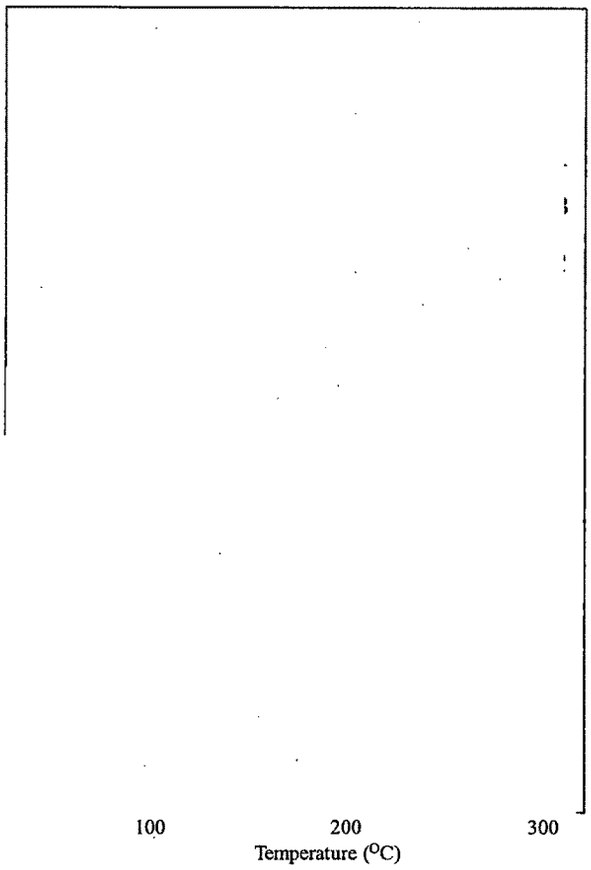

Figure 4.41 DSC thermogram of EXE loaded PLGA NPs (A), EXE (B), Sucrose (C), PLGA (D) and Physical mixture (E).

4.17.4 In vitro drug release studies

The in vitro drug release studies from different nanoparticulate formulations were performed in PBS pH 7.4. Pegylated PLGA NPs showed faster release as compared with non-pegylated NPs. In vitro release of EXE from drug suspension and NPs is shown in figure 4.42. Within 3 h, 71.36 ± 1.23% drug release occurred from plain drug suspension, whereas only 25.18 ± 0.56% and 20.21 ± 0.23% drug released from PLGA and pegylated PLGA NPs, reaching 48.05 ± 0.94% and 54.25 ± 0.23% after 120 h and 71.4 ± 1.23% and 73.9 ±0.86% after 240 h from PLGA and pegylated PLGA NPs, respectively indicative of sustained release. The drug release from NPs followed biphasic release model with an initial burst release for about 3 h followed by sustained release for more than 240 h. Pegylated PLGA NPs showed faster release when compared to PLGA NPs as reported by Derakhshandeh et al. [Derakhshandeh et al. 2010]. The

burst release may be attributed to the drug molecules associated near particle surface [Seju et al. 2011]. Also, particles of nano size range lead to a shorter average diffusion path for the matrix entrapped drug molecules, thereby causing faster diffusion [Mainardes and Evangelista 2005; Shah et al. 2009]. After initial burst release, the release rate decreased, reflecting the release of drug entrapped in the polymer matrix. The release rate in the second phase was assumed to be controlled by diffusion rate of drug across the polymer matrix [Corrigan and Li 2009]. The data obtained from *in vitro* drug release studies was fitted to Korsmeyer - Peppas model.

The regression coefficient of the plot of log M_t/M_∞ versus log t for PLGA and pegylated PLGA NPs was found to be 0.935 and 0.984 with value of release exponent (n) as 0.271 and 0.312, respectively. The n value is the release exponent which characterizes the transport mechanism and if its value is less than 0.5, it indicates Fickian release. Hence, it can be concluded that the release of EXE from NPs was by Fickian diffusion.

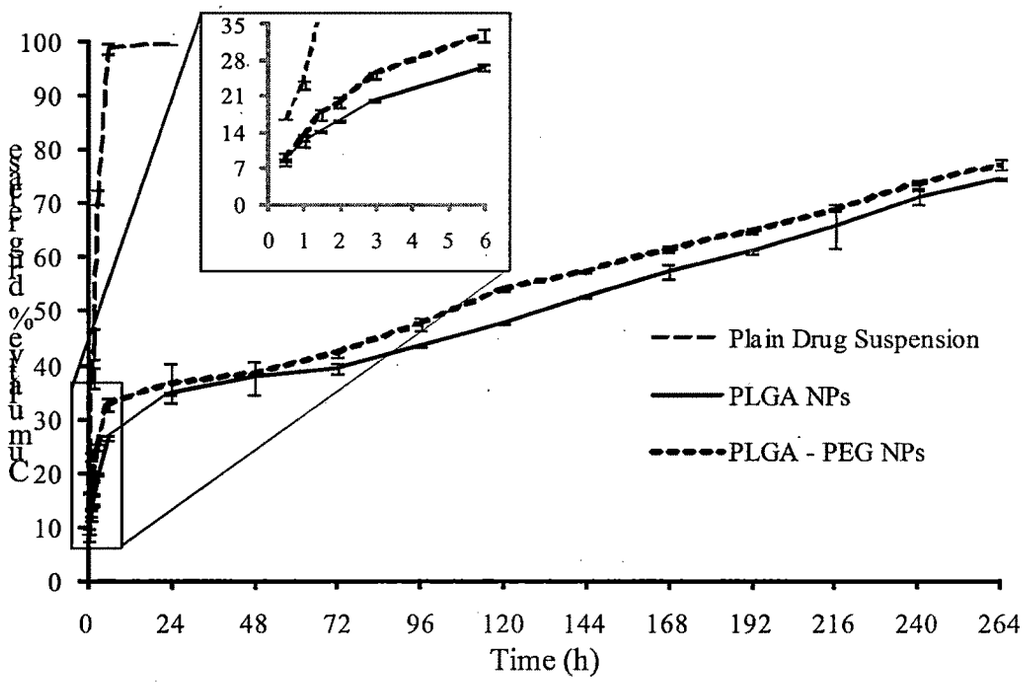

Figure 4.42 Drug release profile of EXE from plain drug suspension, PLGA NPs and pegylated PLGA NPs across semi-permeable membrane using the dialysis bag diffusion technique in phosphate buffered saline (pH 7.4). The values represent mean ± S.D. of three batches.

4.17.5 Stability studies

Total drug content after different time intervals showed change in case of the NPs stored at room temperature to that of the NPs stored at refrigerator temperature. After different time intervals, increase in PS was observed for NPs stored at room temperature as compared to NPs stored at refrigerator temperature, which may attributed to the aggregation of polymeric particles (table 4.47). Also, drug content was found to decrease with increase in time as well as storage temperature (figure 4.43). Thus, it was concluded that the optimum temperature condition for storage of the EXE loaded PLGA NPs would be refrigerated condition (2-8 °C).

Table 4.47 Stability data of EXE loaded PLGA NPs stored at different temperature conditions

Storage time	% Drug content		Particle size (nm)	
	Room temp.	Refrigerator temp. (2–8 °C)	Room temp.	Refrigerator temp. (2–8 °C)
Initial	100	100	179.8 ± 2.8	179.8 ± 2.8
1 month	99.54 ± 0.52	99.67 ± 0.38	181.3 ± 2.4	180.1 ± 3.4
2 months	99.09 ± 0.64	99.24 ± 0.41	186.7 ± 2.9	186.4 ± 1.7
3 months	98.79 ± 0.75	98.96 ± 0.66	195.4 ± 4.1	188.6 ± 2.3

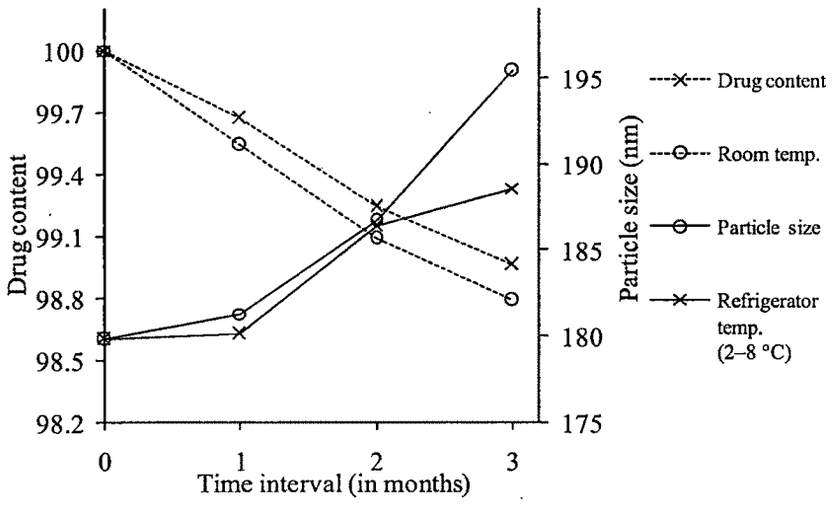

Figure 4.43 Effect of different storage conditions on drug content and PS of EXE loaded PLGA NPs.

4.18 Characterization of EXE loaded cPCL NPs

4.18.1 Zeta potential

The zeta potential values ranged between -19.6 to -34.0 mV for all 13 formulations. The surfactant concentration affected the charge on the particle. It was seen that as the surfactant concentration was increased from 0.25 to 0.75%, there was a decrease in the zeta potential value. This is possibly because with increase in concentration of non-ionic surfactant, total charge on the particle decreases due to increased amount of surfactant coating which also resulted in increased particle size [Redhead et al. 2001]. However, change in polymer concentration had no effect on zeta potential values. The optimized batch of EXE loaded cPCL NPs was found to have zeta potential of -33.8 ± 2.1 mV (figure 4.44). Zeta potential values in the -15 mV to -30 mV are common for well stabilized NPs [Musumeci et al. 2006]. Hence it was concluded that the NPs would remain physically stable.

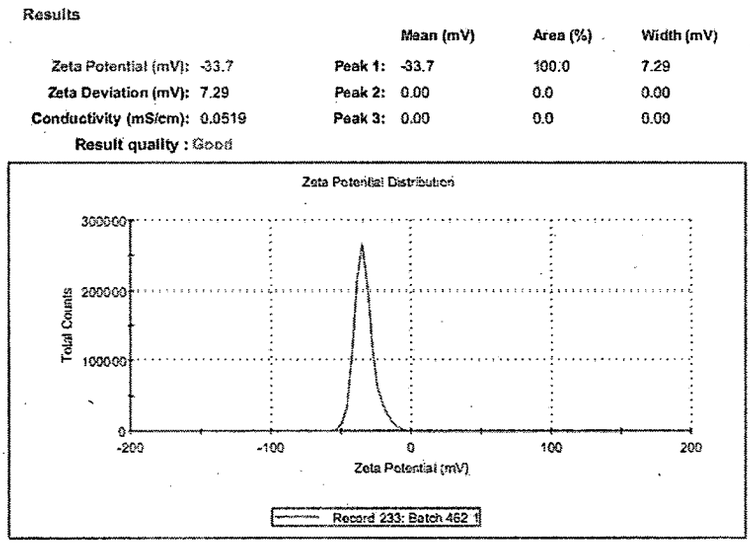

Figure 4.44 Zeta potential of EXE loaded cPCL NPs

4.18.2 Transmission electron microscopy (TEM)

TEM image of EXE loaded cPCL NPs is shown in figure 4.45. The image reveals that the particles were discrete, round and uniform in shape with diameters in the range of 80–100 nm. The higher hydrodynamic diameter of NPs achieved by DLS analysis as compared to the size obtained by TEM analysis may be contributed by the hydration of the surface associated Poloxamer [Das and Sahoo 2012; Misra and Sahoo 2010].

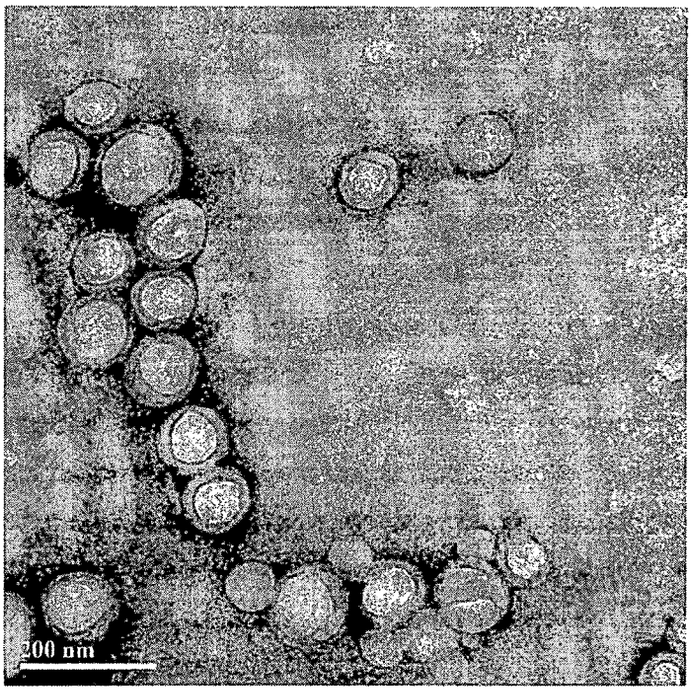

Figure 4.45 TEM image of EXE loaded cPCL NPs

4.18.3 Differential scanning calorimetry (DSC)

DSC thermograms of pure EXE, cPCL polymer, sucrose, physical mixture and EXE loaded cPCL NPs are shown in figure 4.46. Pure EXE showed an endothermic melting peak at 182.56 °C indicating its crystalline nature. cPCL showed endothermic peak at 47.65 °C, which was lower than the reported melting point of PCL (60 °C). It has been reported that modifications in polymer or polymer structure will change its melting point (Orozco-Castellanos et al. 2011). Thus, the lowering of melting point of PCL in cPCL can be taken as an indication of its carboxylation, which was also confirmed by FTIR and GPC. There was no peak of EXE in the thermogram of NPs indicating that EXE may be existing as a molecular dispersion or in an amorphous phase in the polymer matrix [Kashi et al. 2012]. It is reported that no detectable endotherm will be observed if the drug is present in a molecular dispersion or solid solution state in the polymeric NPs [Dubernet 1995]. However, as the drug is crystalline, total disappearance of its peak in the thermogram of the NPs indicate towards its existence as a molecular dispersion rather than amorphous form.

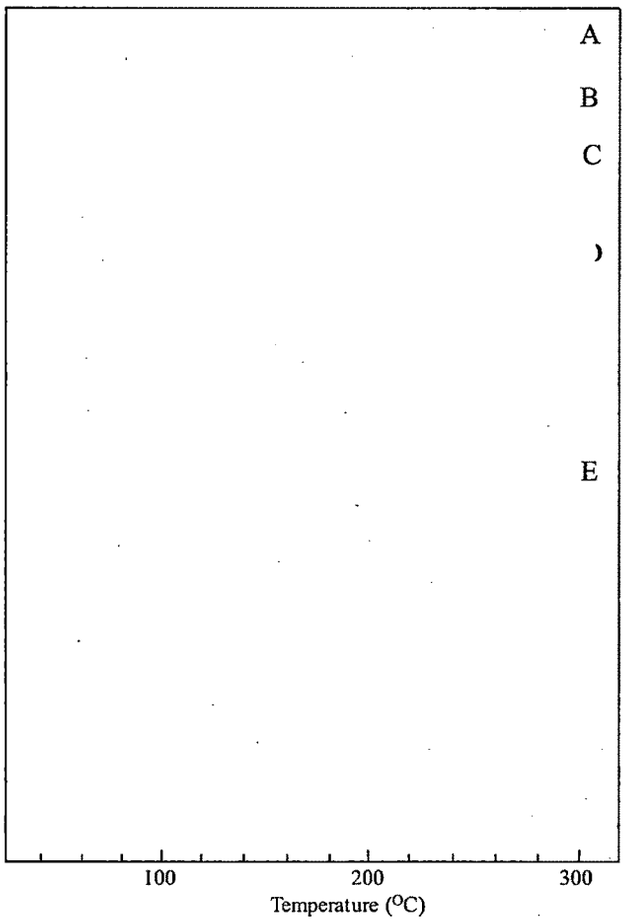

Figure 4.46 DSC thermogram of EXE loaded cPCL NPs (A), EXE (B), cPCL (C), Sucrose (D) and Physical mixture (E).

4.18.4 In vitro drug release studies

The in vitro drug release studies from different nanoparticulate formulations were performed in PBS pH 7.4. Pegylated PCL NPs showed faster release as compared with non-pegylated NPs. In vitro release of EXE from drug suspension and NPs is shown in figure 4.47. Within 3 h, 71.36 ± 1.23% drug release occurred from plain drug suspension, whereas only 20.06 ± 1.31% and 24.88 ± 1.13% drug released from cPCL and pegylated PCL NPs, reaching 44.89 ± 1.3% and 52.22 ± 3.1% after 120 h and 70.67 ± 1.76% and 83.26 ± 0.85% after 240 h from cPCL and pegylated PCL NPs, respectively indicative of sustained release. The drug release from NPs followed biphasic release model with an initial burst release for about 3 h followed by sustained release for more than 240 h. Pegylated PCL NPs showed faster release when compared to cPCL NPs as reported by Derakhshandeh et al. [Derakhshandeh et al. 2010]. The burst release may

be attributed to the drug molecules associated near particle surface [Seju et al. 2011]. Also, particles of nano size range lead to a shorter average diffusion path for the matrix entrapped drug molecules, thereby causing faster diffusion [Mainardes and Evangelista 2005; Shah et al. 2009]. After initial burst release, the release rate decreased, reflecting the release of drug entrapped in the polymer matrix. The release rate in the second phase was assumed to be controlled by diffusion rate of drug across the polymer matrix [Corrigan and Li 2009]. The data obtained from *in vitro* drug release studies was fitted to Korsmeyer - Peppas model. The regression coefficient of the plot of log M_t/M_∞ versus log t for cPCL and pegylated PCL NPs was found to be 0.942 and 0.952 with value of release exponent (n) as 0.303 and 0.306, respectively. The n value is the release exponent which characterizes the transport mechanism and if its value is less than 0.5, it indicates Fickian release. Hence, it can be concluded that the release of EXE from NPs was by Fickian diffusion.

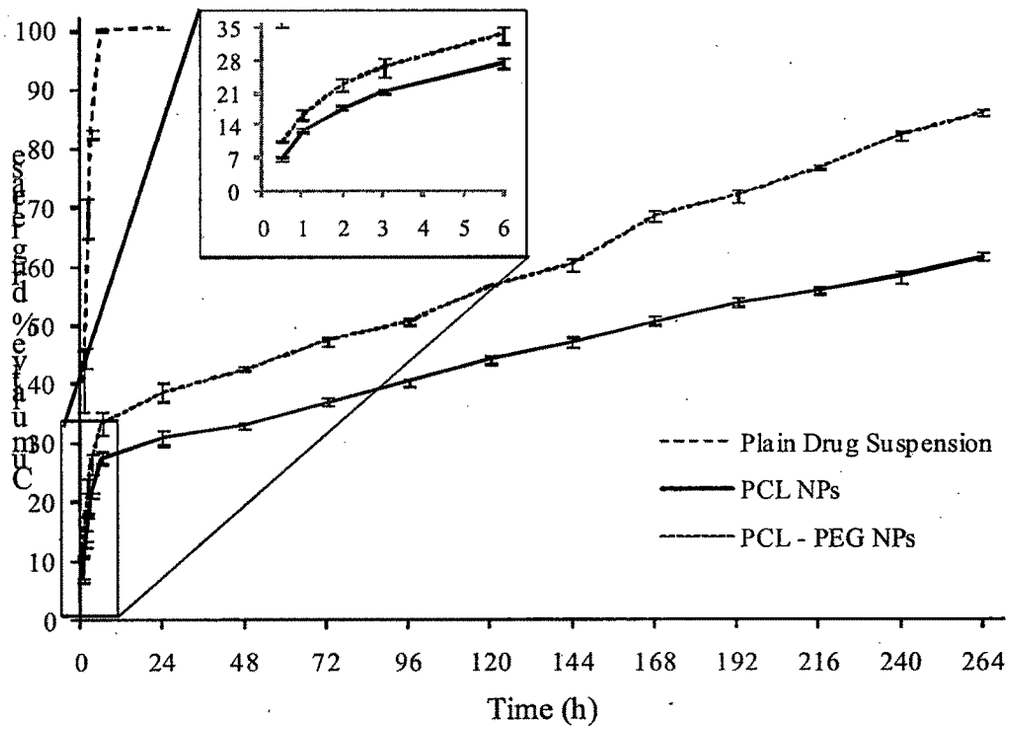

Figure 4.47 Drug release profile of EXE from plain drug suspension, cPCL NPs and pegylated PCL NPs across semi-permeable membrane using the dialysis bag diffusion technique in phosphate buffered saline (pH 7.4). The values represent mean ± S.D. of three batches.

4.18.5 Stability studies

Total drug content after different time intervals showed change in case of the NPs stored at room temperature to that of the NPs stored at refrigerator temperature. After different time intervals, increase in PS was observed for NPs stored at room temperature as compared to NPs stored at refrigerator temperature, which may attributed to the aggregation of polymeric particles (table 4.48). Also, drug content was found to decrease with increase in time as well as storage temperature (figure 4.48). Thus, it was concluded that the optimum temperature condition for storage of the EXE loaded cPCL NPs would be refrigerated condition (2-8 °C).

Table 4.48 Stability data of EXE loaded cPCL NPs stored at different temperature conditions

Storage time	% Drug content		Particle size (nm)	
	Room temp.	Refrigerator temp. (2–8 °C)	Room temp.	Refrigerator temp. (2–8 °C)
Initial	100	100	182.6 ± 2.9	182.6 ± 2.9
1 month	99.50 ± 0.53	99.71 ± 0.27	185.1 ± 1.9	184.5 ± 2.4
2 months	99.11 ± 0.28	99.32 ± 0.41	192.7 ± 3.8	189.4 ± 1.7
3 months	98.87 ± 0.33	99.04 ± 0.19	200.4 ± 5.4	196.4 ± 3.8

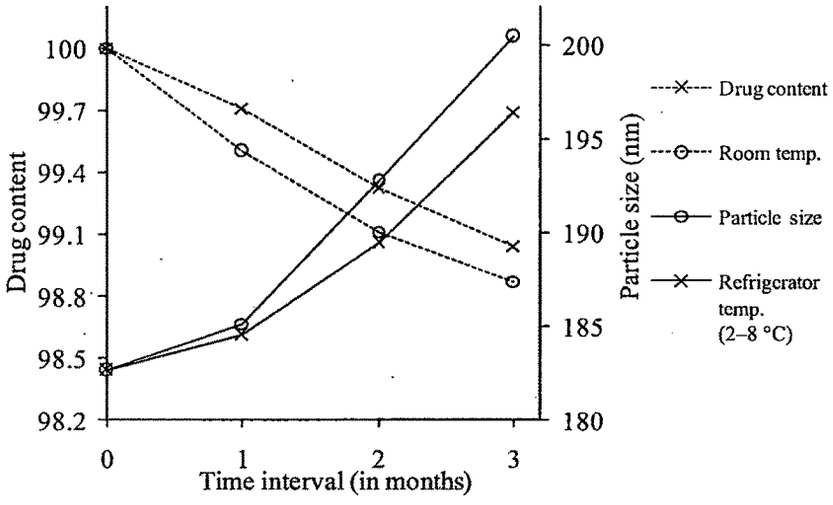

Figure 4.48 Effect of different storage conditions on drug content and PS of EXE loaded cPCL NPs.

4.19 References

Abdelwahed W, Degobert G, Stainmesse S, Fessi H. 2006. Freeze-drying of nanoparticles: formulation, process and storage considerations. Adv. Drug. Deliv. Rev. 58(15):1688-1713.

Abdul M, Ramlal S, Hoosein N. 2008. Ryanodine receptor expression correlates with tumor grade in breast cancer. Pathol. Oncol. Res. 14(2):157-160.

Aberturas MR, Hernan Perez de la Ossa D, Gil ME, Ligresti A, De Petrocellis L, Torres AI, Di Marzo V, Molpeceres J. 2011. Anandamide-loaded nanoparticles: preparation and characterization. J. Microencapsul. 28(3):200-210.

Acharya S, Dilnawaz F, Sahoo SK. 2009. Targeted epidermal growth factor receptor nanoparticle bioconjugates for breast cancer therapy. Biomaterials 30(29):5737-5750.

Adinarayana K, Ellaiah P. 2002. Response surface optimization of the critical medium components for the production of alkaline protease by a newly isolated Bacillus sp. J. Pharm. Pharm. Sci. 5(3):272-278.

Ahlin P, Kristl J, Kristl A, Vrečer F. 2002. Investigation of polymeric nanoparticles as carriers of enalaprilat for oral administration. Int. J. Pharm. 239(1–2):113-120.

Akhnazarova S. 1982. Experiment optimization in chemistry and chemical engineering. Moscow: Mir Publications.

Armstrong AN, James KC. 1996. Pharmaceutical experimental design and interpretation. Bristol, USA: Taylor and Francis Publishers.

Avgoustakis K, Beletsi A, Panagi Z, Klepetsanis P, Livaniou E, Evangelatos G, Ithakissios DS. 2003. Effect of copolymer composition on the physicochemical characteristics, in vitro stability, and biodistribution of PLGA–mPEG nanoparticles. Int. J. Pharm. 259(1–2):115-127.

Bae S, Shoda M. 2005. Statistical optimization of culture conditions for bacterial cellulose production using Box-Behnken design. Biotechnol. Bioeng. 90(1):20-28.

Barichello JM, Morishita M, Takayama K, Nagai T. 1999. Encapsulation of hydrophilic and lipophilic drugs in PLGA nanoparticles by the nanoprecipitation method. Drug Dev. Ind. Pharm. 25(4):471-476.

Behan N, Birkinshaw C, Clarke N. 2001. Poly n-butyl cyanoacrylate nanoparticles: a mechanistic study of polymerisation and particle formation. Biomaterials 22(11):1335-1344.

Bolton S, Bon C. 1997. Pharmaceutical statistics: practical and clinical applications. New York: Marcel Dekker Inc.

Box GEP, Hunter WG, Hunter WS. 1978. Statistics for experimenters: An introduction to design, data analysis, and model building. New York: John Wiley and Sons.

Box GEP, Wilson KB. 1951. On the experimental attainment of optimum conditions. J. Roy. Stat. Soc. 13:1-45.

Breda M, Pianezzola E, Benedetti MS. 1993. Determination of exemestane, a new aromatase inhibitor, in plasma by high-performance liquid chromatography with ultraviolet detection. J. Chromato. 620(2):225-231.

Causes of death in India Srs. 2009. Registrar general of India and centre for global health research. New Delhi: Government of India.

Chacon M, Molpeceres J, Berges L, Guzman M, Aberturas MR. 1999. Stability and freeze-drying of cyclosporine loaded poly(D,L lactide-glycolide) carriers. Eur. J. Pharm. Sci. 8(2):99-107.

Chaudhari KR, Kumar A, Khandelwal V, Ukawala M, Manjappa AS, Mishra AK, Monkkonen J, Murthy RSR. 2012. Bone metastasis targeting: A novel approach to reach bone using Zoledronate anchored PLGA nanoparticle as carrier system loaded with Docetaxel. J. Controlled Rel. 158(3):470-478.

Chaudhari KR, Shah N, Patel H, Murthy R. 2010. Preparation of porous PLGA microspheres with thermoreversible gel to modulate drug release profile of water-soluble drug: bleomycin sulphate. J. Microencapsul. 27(4):303-313.

Chowdhury S, Ellis PA. 2005. Recent advances in the use of aromatase inhibitors for women with postmenopausal breast cancer. J. Br. Menopause Soc. 11(3):96-102.

Clemett D, Lamb HM. 2000. Exemestane: a review of its use in postmenopausal women with advanced breast cancer. Drugs 59(6):1279-1296.

Corrigan OI, Li X. 2009. Quantifying drug release from PLGA nanoparticulates. Eur. J. Pharm. Sci. 37(3-4):477-485.

Darbandy SM, Bakhtiary A, Taheri H. 2011. Novel and efficient catalyst for the synthesis of caprolactone. 2nd International Conference on Chemical Engineering and Applications. Maldives: IACSIT Press, Singapore. 125-129.

Das M, Sahoo SK. 2012. Folate decorated dual drug loaded nanoparticle: role of curcumin in enhancing therapeutic potential of nutlin-3a by reversing multidrug resistance. Plos One 7(3):e32920.

De Jong WH, Borm PJ. 2008. Drug delivery and nanoparticles:applications and hazards. Int. J. Nanomedicine 3(2):133-149.

Derakhshandeh K, Soheili M, Dadashzadeh S, Saghiri R. 2010. Preparation and in vitro characterization of 9-nitrocamptothecin-loaded long circulating nanoparticles for delivery in cancer patients. Int. J. Nanomed. 5:463-471.

Derringer G, Suich R. 1980. Simultaneous optimization of several response variables. J. Quality Technol. 12(4):214-219.

Dowsett M. 1998. Theoretical considerations for the ideal aromatase inhibitor. Breast Cancer Res. Treat. 49 Suppl 1:S39-44; discussion S73-S77.

Dubernet C. 1995. Thermoanalysis of microspheres. Thermochimica Acta 248(0):259-269.

Feng S, Huang G. 2001. Effects of emulsifiers on the controlled release of paclitaxel (Taxol) from nanospheres of biodegradable polymers. J. Controlled Rel. 71(1):53-69.

Fessi H, Puisieux F, Devissaguet JP, Ammoury N, Benita S. 1989. Nanocapsule formation by interfacial polymer deposition following solvent displacement. Int. J. Pharm. 55(1):R1-R4.

Fonseca C, Simoes S, Gaspar R. 2002. Paclitaxel-loaded PLGA nanoparticles: preparation, physicochemical characterization and in vitro anti-tumoral activity. J. Controlled Rel. 83(2):273-286.

George Box DB. 1960. Some new three level designs for the study of quantitative variables. Technometrics 2:455-475.

Henderson IC, Canellos GP. 1980. Cancer of the breast: the past decade (first of two parts). N. Engl. J. Med. 302(1):17-30.

Jain NK, Ram A. 2011. Development and characterization of nanostructured lipid carriers of oral hypoglycemic agent: selection of surfactants. Int. J. Pharm. Sci. Rev. and Res. 7(2):125-130.

Johannessen DC, Engan T, Di Salle E, Zurlo MG, Paolini J, Ornati G, Piscitelli G, Kvinnsland S, Lonning PE. 1997. Endocrine and clinical effects of exemestane (PNU 155971), a novel steroidal aromatase inhibitor, in postmenopausal breast cancer patients: a phase I study. Clin. Cancer Res. 3(7):1101-1108.

Joshi SA, Chavhan SS, Sawant KK. 2010. Rivastigmine-loaded PLGA and PBCA nanoparticles: preparation, optimization, characterization, in vitro and pharmacodynamic studies. Eur. J. Pharm. Biopharm. 76(2):189-199.

Kashi TS, Eskandarion S, Esfandyari-Manesh M, Marashi SM, Samadi N, Fatemi SM, Atyabi F, Eshraghi S, Dinarvand R. 2012. Improved drug loading and antibacterial activity of minocycline-loaded PLGA nanoparticles prepared by solid/oil/water ion pairing method. Int. J. Nanomed. 7:221-234.

Kenneth WY, Mak MGSY, Wah Koon Teo. 1995. Formulation and optimization of two culture media for the production of tumour necrosis factor-β in Escherichia coli. J. Chem. Technol. Biotechnol. 62(3):289-294.

Kumar A, Sawant K. 2013. Encapsulation of exemestane in polycaprolactone nanoparticles: optimization, characterization, and release kinetics. Cancer Nano. 4(4-5):57-71.

Kwon HY, Lee JY, Choi SW, Jang Y, Kim JH. 2001. Preparation of PLGA nanoparticles containing estrogen by emulsification–diffusion method. Coll. Surf. A: Physicochemical and Engineering Aspects 182(1–3):123-130.

Lacoulonche F, Gamisans F, Chauvet A, Garcia ML, Espina M, Egea MA. 1999. Stability and in vitro drug release of flurbiprofen-loaded poly-epsilon-caprolactone nanospheres. Drug Dev. Ind. Pharm. 25(9):983-993.

Lam CX, Savalani MM, Teoh SH, Hutmacher DW. 2008. Dynamics of in vitro polymer degradation of polycaprolactone-based scaffolds: accelerated versus simulated physiological conditions. Biomed. Mater. 3(3):034108.

Levison KK, Takayama K, Isowa K, Okabe K, Nagai T. 1994. Formulation optimization of indomethacin gels containing a combination of three kinds of cyclic

monoterpenes as percutaneous penetration enhancers. J. Pharm. Sci. 83(9):1367-1372.

Lonning PE. 1998. Pharmacological profiles of exemestane and formestane, steroidal aromatase inhibitors used for treatment of postmenopausal breast cancer. Breast Cancer Res. Treat. 49 Suppl 1:S45-52; discussion S73-S77.

Mainardes RM, Evangelista RC. 2005. Praziquantel-loaded PLGA nanoparticles: preparation and characterization. J. Microencapsul. 22(1):13-24.

Mak KWY, Yap MGS, Teo WK. 1995. Formulation and optimization of two culture media for the production of tumour necrosis factor-β in Escherichia coli. J. Chem. Technol. Biotechnol. 62(3):289-294.

McPherson K, Steel CM, Dixon JM. 2000. ABC of breast diseases. Breast cancer-epidemiology, risk factors, and genetics. BMJ 321(7261):624-628.

Mehta AK, Yadav KS, Sawant KK. 2007. Nimodipine loaded PLGA nanoparticles: formulation optimization using factorial design, characterization and in vitro evaluation. Curr. Drug Deliv. 4(3):185-193.

Mendes GD, Hamamoto D, Ilha J, Pereira Ados S, De Nucci G. 2007. Anastrozole quantification in human plasma by high-performance liquid chromatography coupled to photospray tandem mass spectrometry applied to pharmacokinetic studies. J. Chromato. 850(1-2):553-559.

Miller AJ. 1984. Selection of subsets of regression variables. J. R. Stat. Soc. Ser. A. 147:389-425.

Misra R, Sahoo SK. 2010. Intracellular trafficking of nuclear localization signal conjugated nanoparticles for cancer therapy. Eur. J. Pharm. Sci. 39(1-3):152-63.

Montgomery DC. 2004. Introduction to factorial designs. New York: John Wiley and Sons. 392-426 p.

Moraes CM, de Matos AP, de Paula E, Rosa AH, Fraceto LF. 2009. Benzocaine loaded biodegradable poly-(d,l-lactide-co-glycolide) nanocapsules: factorial design and characterization. Mater. Sci. Eng.: B 165(3):243-246.

Musumeci T, Ventura CA, Giannone I, Ruozi B, Montenegro L, Pignatello R, Puglisi G. 2006. PLA/PLGA nanoparticles for sustained release of docetaxel. Int. J. Pharm. 325(1-2):172-179.

Myer RH, Khuri AI, Carter WH. 1989. Response surface methodology: 1966-1988. Technometrics 31:137-157.

Myer RH, Montogomery DC. 2002. Response Surface Methodology: Process and product optimization using designed experiment. New York: John Wiley and Sons.

Nanjwade BK, Manjappa AS, Murthy RSR, Pol YD. 2009. A novel pH-triggered in situ gel for sustained ophthalmic delivery of ketorolac tromethamine. Asian J. Pharm. Sci. 4(3):189 - 199.

Paolicelli P, Prego C, Sanchez A, Alonso MJ. 2010. Surface-modified PLGA-based nanoparticles that can efficiently associate and deliver virus-like particles. Nanomedicine 5(6):843-853.

Peppas NA. 1985. Analysis of Fickian and non-Fickian drug release from polymers. Pharm Acta Helv 60(4):110-111.

Quintanar-Guerrero D, Allemann E, Fessi H, Doelker E. 1998. Preparation techniques and mechanisms of formation of biodegradable nanoparticles from preformed polymers. Drug Dev. Ind. Pharm. 24(12):1113-1128.

Rahman Z, Zidan AS, Khan MA. 2010. Non-destructive methods of characterization of risperidone solid lipid nanoparticles. Eur J. Pharm. Biopharm. 76(1):127-137.

Ray S. 2006. RSM: a statistical tool for process optimization. Ind. Tex. J. 117:24-30.

Ray S, Lalman JA, Biswas N. 2009. Using the Box-Benkhen technique to statistically model phenol photocatalytic degradation by titanium dioxide nanoparticles. Chem. Eng. J. 150(1):15-24.

Redhead HM, Davis SS, Illum L. 2001. Drug delivery in poly(lactide-co-glycolide) nanoparticles surface modified with poloxamer 407 and poloxamine 908: in vitro characterisation and in vivo evaluation. J. Controlled Rel. 70(3):353-363.

Sarkar K, Yang H. 2008. Encapsulation and extended release of anti-cancer anastrozole by stealth nanoparticles. Drug Deliv. 15(5):343-346.

Scott LJ, Wiseman LR. 1999. Exemestane. Drugs 58(4):675-682

Seju U, Kumar A, Sawant KK. 2011. Development and evaluation of olanzapine-loaded PLGA nanoparticles for nose-to-brain delivery: In vitro and in vivo studies. Acta Biomater 7(12):4169-4176.

Seth AK, Misra A. 2002. Mathematical modelling of preparation of acyclovir liposomes: reverse phase evaporation method. J. Pharm. Pharm. Sci. 5(3):285-291.

Shah N, Chaudhari K, Dantuluri P, Murthy RS, Das S. 2009. Paclitaxel-loaded PLGA nanoparticles surface modified with transferrin and Pluronic®P85, an in vitro cell line and in vivo biodistribution studies on rat model. J. Drug Target. 17(7):533-542.

Shi K, Cui F, Yamamoto H, Kawashima Y. 2009. Optimized formulation of high-payload PLGA nanoparticles containing insulin-lauryl sulfate complex. Drug Dev. Ind. Pharm. 35(2):177-184.

Shirakura O, Yamada M, Hashimoto M, Ishimaru S, Takayama K, Nagai T. 1991. Particle-size design using computer optimization technique. Drug Dev. Ind. Pharm. 17(4):471-483.

Snehalatha M, Venugopal K, Saha RN, Babbar AK, Sharma RK. 2008. Etoposide loaded PLGA and PCL nanoparticles II: biodistribution and pharmacokinetics after radiolabeling with Tc-99m. Drug Deliv. 15(5):277-287.

Song Z, Feng R, Sun M, Guo C, Gao Y, Li L, Zhai G. 2011. Curcumin-loaded PLGA-PEG-PLGA triblock copolymeric micelles: Preparation, pharmacokinetics and distribution in vivo. J. Colloid Interface Sci. 354(1):116-23.

Strassmer-Weippl K, Goss PE. 2003. Prevention of breast cancer using SERMs and aromatase inhibitors. J. Mammary Gland Biol. Neoplasia 8(1):5-18.

Theobald AJ. 2000. Management of advanced breast cancer with endocrine therapy: the role of the primary healthcare team. Int. J. Clin. Pract. 54(10):665-669.

Thode K, Muller RH, Kresse M. 2000. Two-time window and multiangle photon correlation spectroscopy size and zeta potential analysis--highly sensitive rapid assay for dispersion stability. J. Pharm. Sci. 89(10):1317-1324.

Tuncay M, Calis S, Kas HS, Ercan MT, Peksoy I, Hincal AA. 2000. Diclofenac sodium incorporated PLGA (50:50) microspheres: formulation considerations and in vitro/in vivo evaluation. Int. J. Pharm. 195(1-2):179-188.

von Pawel J, Gatz emeier U, Pujol JL, Moreau L, Bildat S, Ranson M, Richardson G, Steppert C, Rivière A, Camlett I. 2001. Phase II comparator study of oral versus intravenous topotecan in patients with chemosensitive small-cell lung cancer. J. Clin. Oncol. 19:1743-1749.

Wagner JM, Shimshak DG. 2007. Stepwise selection of variables in data envelopment analysis: Procedures and managerial perspectives. Eur. J. Oper. Res. 180(1):57-67.

Yadav KS, Sawant KK. 2010. Modified nanoprecipitation method for preparation of cytarabine-loaded PLGA nanoparticles. AAPS Pharmscitech 11(3):1456-1465.

Yallapu MM, Gupta BK, Jaggi M, Chauhan SC. 2010. Fabrication of curcumin encapsulated PLGA nanoparticles for improved therapeutic effects in metastatic cancer cells. J. Colloid Interface Sci. 351(1):19-29.

Yang SC, Lu LF, Cai Y, Zhu JB, Liang BW, Yang CZ. 1999. Body distribution in mice of intravenously injected camptothecin solid lipid nanoparticles and targeting effect on brain. J. Controlled Rel. 59(3):299-307.

Yee L, Blanch HW. 1993. Defined media optimization for growth of recombinant Escherichia coli X90. Biotechnol. Bioeng. 41(2):221-230.

Zhang Q, Xu W, Wang Z. 1994. Synthesis of polycaprolactone with two carboxy end groups. J. Mater. Sci. Technol. 10:351-354.